Cell-compatible multi-functional crosslinker-based hydrogels for tissue engineering

By

Lianlian Yu

A Thesis submitted to the Faculty of Graduate Studies of

The University of Manitoba

In partial fulfillment of the requirements of the degree of

MASTER OF SCIENCE

Department of Textile Sciences

University of Manitoba

Winnipeg

Abstract

This thesis includes two parts related to cell-compatible multi-functional crosslinker-based hydrogels for tissue engineering.

Firstly, a linear functional poly (amidoamine) (PAA) crosslinker is synthesized via Michael-addition polymerization of agmatine to N, N'-Methylene bis (acrylamide). The linear crossllinker is applied to poly (ethylene glycol) (PEG) hydrogel, 1H NMR and FTIR characterizations show the successful synthesis of the crosslinker and the hybrid hydrogel. Mechanical tests show that the stiffness of the hydrogel can be controlled by tuning the mass ratio of the PAA crosslinker. The engineered hydrogel shows remarkable swelling ratios and in vitro degradability. Cell viability and cell morphology tests also demonstrate the hydrogel's biocompatibility. This agmatine-containing PAA crosslinker is promising for tissue engineering applications. This linear PAA crossllinker is also applied to N-Isopropylacrylamide (NIPAM) to form a thermo-sensitive hydrogel. A rat depressed defects model is set up to conduct the in vivo experiment. CCK-8 assay and SEM images confirm that Adipose-derived Stem Cells (ASCs) can attach to the hydrogel containing the PAA crosslinker. Then four fillers 1) the hydrogel-ASCs mixture, 2) the hydrogel only, 3) hyaluronic acid (HA), 4) Phosphate-Buffered Saline (PBS) was injected to the four depressed defect sites

randomly. *In vivo* results show that the thermo sensitive hydrogel was injectable and fixed well onto the defects. After 4 weeks, gross and histological analysis showed defects in hydrogel, hydrogel-ASCs, and HA groups recovered significantly and there were no significant differences among them. Most importantly, after 6 months, defects in hydrogel group and hydrogel-ASCs group remained recovery significantly, but HA group became depressed again, like PBS group. H&E staining images showed that regenerated tissue can be found in the depressed area of the defects. Immunohistochemical study of s-100 protein distribution revealed the regenerated cells was immature adipocytes. Green Fluorescent Protein (GFP) Immunofluorescence implied the hydrogel repaired defects by recruiting host-derived mesenchymal stromal cells to defect sites. Such cell attachable thermo sensitive hydrogel is demonstrated to be a promising filling material which has persistent effect for small depressed defect. And ultimately might become a new material in plastic and reconstructive surgery in the clinic.

Another novel photo-stimulated self-healing hydrogel system is developed. A coumarin methacrylate crosslinker (CMA) is synthesized and used to modify the polyacrylamide-based hydrogel. The coumarin-contained hydrogel exhibits high self-healing property at wavelengths longer than 310nm due to the [2+2] cycloaddition of a couple of coumarin moieties. A hyperbranched poly (amidoamine) (PAA) crosslinker is also synthesized to improve the cell compatibility of the hydrogel.

Changes in light exposure times and wavelengths of irradiation significantly alter the self-healing property of the hydrogel. Finally, the hydrogel is seeded with bone marrow-derived mesenchymal stem cells and their relative mRNA expressions are recorded to examine their osteogenic differentiation.

Acknowledgments

I would like to appreciate Dr Wen Zhong (my supervisor) and Dr Malcolm Xing (my co-supervisor), for their giving me the motivation to investigate on new biomaterials and their encouragement of independent thinking. I'd like to thank other members of my committee as well for helping me improving the research, and sparing time on attending my final defense.

My heartful acknowledgement also goes to Xiaolian Xiao, who has been performing animal experiments and providing results analyses for me. I am grateful to all my colleagues for being the surrogate family during the two years I stayed in Winnipeg and for their continued love and support.

My final words go to my family. I want to thank my family, whose love and guidance is with me in whatever I pursue. On a different note, many people have been a part of my graduate education and I am highly grateful to all of them.

List of Figures

Chapter 1. Introduction

1.1 General Overview

According to recent reports, approximately a quarter of patients die when they are waiting for suitable organ donors for transplantation in US [1,2]. The supply of donor organs and tissues for transplantation has long been falling far short of demand, and such shortage in supply will remain in the near future [1,3]. Cell transplantation and tissue engineering has been recently introduced to provide an alternative way to fulfill the goal of organ transplantation [4-6]. In such procedures, to avoid allograft rejections, tissues from a donor are usually harvested and dissociated into individual cells [7]. Such individual cells are attached to and cultured on a suitable substrate known as a scaffold. Finally the scaffold will be implanted into the desired site to develop into a functioning tissue [7].

Therefore, tissue engineering has become an important interdisciplinary field involving biomedical engineering, tissues harvesting, implants and prostheses [8]. Artificial extracellular scaffolds with high porosity are critical to accommodate stem cells, guide their growth and regenerate tissues in a 3D structure [8].

Multitudinous strategies have been applied to develop scaffolds for tissue engineering.

These scaffolds act as an extracellular matrix (ECM) to organize cells into a 3D structure and to deliver nutrients as well as signal molecules which regulate the tissue's growth and regeneration [7]. The requirements for scaffold materials and their properties differ dramatically according to their specific applications. Most scaffold materials, such as poly (lactide-co-glycolide) (PLG), are hydrolytically degradable polymers [9,10]. However, they are usually hydrophobic and should be processed under a quite strict condition, making it difficult for growth factor incorporation and cell entrapment.

Hydrogels generally have high water content and stretchable properties similar to those of the native tissues, therefore are attractive materials for scaffolds [11]. With a architecture similar to that of the ECM of many tissues, hydrogels can help to promote cell proliferation and functioning. Therefore, hydrogels have been commonly used in drug and growth factor delivery, tissues regeneration, and various biomedical applications [12].

Polymers derived from natural materials such as collagen, HA, chitosan and alginate are frequently used in tissue engineering, because they generally have low toxicity and similar macromolecular components to the natural ECM. However, the applications of many natural polymers are limited by the difficulty to obtain materials with a narrow range of molecular weights and by their unsatisfied mechanical performance, including

elastic property, compressibility, viscoelasticity, tensile strength, and strain deformation [13].

Using synthetic hydrogels is another appealing choice for tissue engineering applications because of their governable chemical and physical properties. Synthetic polymers can be designed to have certain molecular weights, desirable structures, degradable linkages, and crosslinking modes in a reproducible way. These aspects decide the gel formation dynamics, crosslinking density, and mechanical and degradable properties [12]. For example, PEG is a hydrophilic polymer and is one of the most commonly used synthetic hydrogel polymers which have been approved by FDA.

1.2 Problem Definition

Existing 3D scaffolds for tissue engineering are rarely ideal for their applications [8] in terms of their mechanical stiffness, degradability and biocompatibility [14].

One critical issue for synthetic hydrogels is their poor cellular adhesion, proliferation and differentiation, even though these hydrogels are nontoxic and do not elicit any severe immunogenic response [12]. For example, without collagen, a natural ECM protein in mammals, majority of cells do not own receptors for hydrogels, so they are

hard to attach to the gel surface or grow inside [15]. It is also difficult for ECM proteins (e.g., laminin, fibronectin, and vitronectin) to be absorbed to the surface of the gel due to the hydrophilic nature of gel [16].

The phenomenon of self-healing exists widely in living organisms, from micro blood clotting to macro skin repairs. This special biological process allows living organisms to restore their integrity and prolong their lifespan [17]. To mimic such a natural healing feature, materials with the capacity to repair by themselves after damage are highly desirable with the increasing concerns on environmental and energy issues. A variety of smart materials have been developed based on various strategies [18-25]. Photo stimulated self-healing materials composed of polymers with macromolecular networks constructed by coumarin complementarity are still rarely reported. Moreover, it is still a great challenge to fabricate self-healing macromolecular materials that are cell-compatible and suitable for medical uses [26-28].

1.3 Objective

In order to ameliorate the properties of hydrogels, the overall objective of this thesis was to design hydrogels based on cell-compatible multi-functional crosslinkers. To achieve this, the following tasks are to be performed:

1. To prepare cell compatible linear and hyperbranched Polyamidoamines (PAA)

crosslinkers via Michael-addition polymerization of amines to bis-acrylamides [29,30]; To incorporate Polyamidoamines (PAA) crosslinkers into PEG hydrogels to form cell compatible hydrogels with tunable stiffness by adjusting the proportion of PAA crosslinkers; To incorporate Polyamidoamines (PAA) crosslinkers into NIPAM to form a cell compatible thermo-sensitive injectable hydrogel, and to apply it in a rat depressed defects model.

2. To synthesize a coumarin methacrylate crosslinkers (CMA) and use it in polyacrylamide-based hydrogels to develop a novel photo-stimulated self-healing hydrogel system. In addition, the hyperbranched Polyamidoamine (PAA) crosslinker is also incorporated to improve the cell compatibility of self-healing hydrogel.

1.4 Summary of Experimental Methods and Major Findings

1.4.1 Summary of Experimental Methods

In this work, two kinds of cell-compatible multi-functional crosslinkers were developed and incorporated into hydrogels for tissue engineering.

A linear agmatine-contained Polyamidoamines (PAA) crosslinker was synthesized to improve cell attachment. This novel functional PAA crosslinker was then

copolymerized with poly (ethylene glycol) (PEG) to form a 3D hydrogel scaffolds with tunable stiffness. Then the linear PAA crosslinker was applied to Poly (N-isopropylacrylamide) (NIPAM) to form a thermo-sensitive injectable 3D hydrogel scaffold. Rat depressed defects model was set up for the vivo experiment. CCK-8 assay and SEM were used to confirm that ASCs can attach to the gel containing PAA crosslinker. *In vivo*, H&E staining images, immunohistochemical study for s100 and Green Fluorescent Protein (GFP) immunofluorescence were recorded after 4 weeks and 6 months.

A novel photo-stimulated self-healing hydrogel system was developed. Coumarin methacrylate crosslinker (CMA) was synthesized and used to modify the polyacrylamide-based hydrogels. A hyperbranched Poly (amidoamine) (PAA) crosslinker was also synthesized to improve the cell compatibility of hydrogels. Tensile tests were conducted to investigate the self-healing properties of the hydrogels that went through different times of light exposure and wavelengths of irradiation. Finally, the gels were seeded with bone marrow derived mesenchymal stem cells and their relative mRNA expressions were recorded to monitor osteogenic differentiation.

1.4.2 Summary of Major Findings

According to the preliminary evaluation of the novel biodegradable and biocompatible agmatine-contained PAA crosslinker, PEG hydrogels fabricated by this crosslinker

have controllable stiffness and excellence cell adhesion. Results show that, by changing the mass ratio of crosslinker, a hydrogel with ideal stiffness that is close to nature ECM can be obtained to support cell growth. In vitro tests also demonstrate that PAA crosslinked hydrogels can successfully provide a 3D structure to allow the cells adhere and grow. Hereby PAA-containing hydrogels are promising for implantable scaffolds for tissue regeneration.

The novel multifunctional poly (amidoamine) crosslinker-contained injectable and biocompatible NIPAM hydrogel, for the first time, was employed as filler for pitting defects in a rat model. The data reported in this article are preliminary but clearly support that such hydrogel is promising in many important respects, such as biodegradability, biocompatibility, as confirmed by in vitro and in vivo tests. In conclusion, such cell attachable thermo-sensitive hydrogel definitely warrant its potential as a filling material for small pitting defects and maybe a new material in plastic surgery.

A novel macro gels with self-healing capability and biocompatibility was successfully developed. Coumarin derivatives are successively introduced to construct into polyacrylamide-based hydrogels. The reversible photodimerization and photocleavage reactivity of coumarin has been imparted to the polymer. The resultant functional gels show noticeable self-healing property after exposure to 365nm UV irradiation, ascribed

to the intramolecular [2+2] photocycloaddition reactions of coumarins. The self-healing gels also possess high mechanical strength after healing for 60min with stress intensity of $2x10^5$ Pa and the elongation at break over 96%. More interestingly, cell attachment property was significantly improved by adding hyperbranched PAA crosslinker. The interesting development of method and materials in this work provides a new insight into the fabrication of novel biocompatible self-healing materials for extensive applications.

1.5 Thesis Layout

This thesis contains six chapters. The organization is as follows,

- Chapter 1 includes a brief introduction of background, problem definition, objectives, methodology and major findings;

- Chapter 2 contains a general literature review on tissue engineering, materials for cell compatible crosslinkers, self-healing polymers, and hydrogels, preparation and characterization methods of hydrogels;

- Chapter 3 provides detailed experimental procedures, results and discussion for hydrogel based on cell compatible crosslinkers;

- Chapter 4 provides detailed experimental procedures, results and discussion for cell-compatible photo-reversible self-healing hydrogel;

- Chapter 5 summarizes the major findings and conclusions of the research;

- Chapter 6 provides suggestions for future work.

Chapter 2. Literature Review

2.1 Background

2.1.1 Tissue Engineering

According to the recent reports, approximately a quarter of patients die when they are waiting for a suitable organ donor for transplants in US [1,2]. The current supply of transplant organs and tissues falls far short of demand, and this number is continually rising, as the demand is increasing [1,3]. Cell transplantation has been recently proposed as an alternative way to fulfill the goal of whole organ transplantation [4-6]. In order to avoid allograft rejection and to create an autologous implant, tissue from the donor is harvested and dissociated into individual cells [7]. Such individual cells are attached and cultured onto a suitable substrate known as a scaffold. Finally the scaffold will be implanted at the desired site of the functioning tissue [7].

In order to meet the tremendous need for organs and tissues, tissue engineering has been developed [4,31-33] to fabricate living replaceable parts for the body [34]. Therefore, tissue engineering becomes an important crossing field in biomedical engineering, tissues harvest, implants and prostheses [8]. An artificial extracellular scaffold with high porosity is very important to accommodate stem cells, to guide their growth and to regenerate tissues in a 3D structure [8].

2.1.2 Hydrogels in Tissue Engineering

Scaffolds play the role of extra cellular matrix (ECM) to organize cells into a 3D structure and to deliver stimuli, which regulate the tissue's growth and regeneration [7]. Polymer scaffolds provide various functions in tissue engineering for specific applications. For example, they act as vehicles to deliver bioactive molecules, as 3D structures to accommodate cells and as media to present stimuli to the tissues [12]. An ideal scaffold should comprise materials that combine both appropriate physical properties and biological design variables. Hydrogel has been an appealing scaffold material since it has a very similar structure to the extracellular matrix of tissues in human body. Most hydrogels can be processed under a mild condition, and may be applied in a relatively gentle way on living organism. Thus, hydrogels have been widely used as scaffold materials for tissue regeneration, drug and growth factor delivery, and a variety of other applications [12].

2.1.3 Cell Attachable Crosslinkers

Hydrogels, due to their high water content, may exhibit integral properties similar to soft tissues in organism, which have biocompatibility, nutrient permeability, tunable elasticity, and low interfacial tension [35]. Attention has been recently focused on natural (e.g., agarose, hyaluronic acid, or chitosan based) or synthetic (e.g., PEG-based) hydrogels as scaffolds for tissue regeneration. However, their properties, such as

permeability, biological degradability, and mechanical properties, are not yet satisfactory [14].

Polyamidoamines (PAAs) are one of the highly hydrophilic ionic polymers which can be easily synthesized and designed to be biodegradable and cell compatible in a living body. In general, linear PAAs are water soluble. Crosslinked PAAs can be obtained by several methods to form hydrogels containing large amount of water. Some of these hydrogels can be potentiality used as scaffolds for both *in vitro* and *in vivo* applications in tissue engineering. PAAs can be designed into highly biocompatible and biodegradable, nontoxic and self-buffered products that do not induce inflammation [29].

PAAs are synthetic polymers prepared by Michael-type polyaddition of amines to bis-acrylamides [30,36]. Cross-linked PAAs were obtained in the past by using multifunctional amines as cross-linkers, and they swell in water to turn into soft hydrogels. Amphoteric PAAs can be prepared using carboxylated bis-acrylamides as monomers. Their acid-base properties, that is, their isoelectric points, are tunable over a wide range [37]. Recently, Amphoteric PAA hydrogels have been developed and studied. For example, a PAA hydrogel that is prevailingly anionic at pH 7.4, was tested as scaffolds *in vitro* and was found to be highly biocompatible and degradable to non-toxic products, but unfortunately, poor in cell-adhesion properties [38].

2.1.4 Self-healing Polymers

The phenomenon of self-healing exists widely in living organisms, from blood clotting to skin repair. This special biological process helps living organisms restore their integrity and prolongs their lifespan [39]. To mimic such natural healing feature, materials with the capacity to repair by themselves after damage are highly desirable. A variety of smart materials have been developed based on various strategies [18,19,21,23-25,40,41].

Ceylan et al. [18] developed a peptide nanofiber which is inspired by the mussel curing strategy, they established iron cross-link points in self-assembled peptide networks. Their results showed that the mussel-inspired iron coordination into the supramolecular networks of peptides can improve mechanical properties without affecting the self-assembly process. Barthel et al.[19] demonstrated a well-defined poly (furfuryl glycidyl ether) (PFGE) homopolymer and poly (ethylene oxide)-b-poly (furfuryl glycidyl ether) (PEO-b-PFGE) block copolymers synthesized by living anionic polymerization as self-healing materials. Results showed that such materials have the capacity of healing complex scratch patterns for multiple times. A novel Lewis acid-catalysed self-healing system was investigated for implementation into epoxy-based fiber reinforced polymer (FRP) composite materials by the Coope's group [21]. Park & Braun[23] designed self-healing polymer coatings formed by

electrospinning. Capsules filled with healing agents were applied onto a substrate followed by infilling of a polymer matrix. Ghosh& Urban [24] reported the development of polyurethane networks that exhibit self-repairing property when exposure to UV light.

Other materials which are self-healing were also investigated, Tee et al.[40] created a composite material composed of a supramolecular organic polymer, which was embedded in nickel nanostructured microparticles. Such materials are designed to mimic the repeatable self-healing capability of the native skin. Optically healable supramolecular polymers were designed by Burnworth et al. [41]. They presented metallo supramolecular polymers that can be modified through exposure to light. When the materials were exposure to UV light, the metal–ligand motifs in the polymer chains are electronically excited and the absorbed energy is converted into heat. Such reaction induces temporary disengagement of the metal–ligand motifs. At the same time, there is a reversible decrease in the polymers' molecular mass and viscosity, thereby allowing quick and efficient defect healing.

Generally, among the reported non-covalent interactions, π-π stacking [42,43], hydrogen bond [44,45], electrostatic interaction [46,47] and hydrophobic interactions [48,49] are useful methods to produce self-healing functionalized materials. A recent report in 2008 by Leibler et al. showed that it is possible to use non-covalent

supramolecular interactions to produce materials with healing properties [50]. Supramolecular materials are usually composed of low molecular oligomers containing receptor units, so that they are able to assemble into higher ordered structure via dynamic, reversible, non-covalent interactions [51-53]. The resulting supermolecular materials usually present some physical properties similar to high molecular weight covalent polymers, such as high solution viscosity and mechanical strength [54-56].

Recent advances in polymer and materials chemistry have led to the development of materials that exhibit the ability to undergo spontaneous repair. Depending on the materials' structures and chemical compositions, the healing process may occur either with or without exposure to external stimuli, for just once or multiple times [25]. Polymeric systems with healing capabilities usually have a common property—reversibility, which may exhibit in the polymerization process or in the cross-linking process [57]. Photo stimulated self-healing polymers are promising [26,57], because they allow the self-healing process to occur upon exposure to light without any manual intervention.

Recently, several groups have got excellent achievements in this area. Chung et al. developed a photo-cross-linkable cinnamate monomer, 1, 1, 1-tris-(cinnamoyloxymethyl) ethane (TCE) with three optically active moieties [58]. It can be crosslinked to form an extremely hard solid via [2+2] photocycloaddition upon

ultraviolet (UV) irradiation at λ>280 nm. The sample of TCE was first given a microcrack manually, which result in a cleavage of cyclobutane ring due to its low bond strength. Then after irradiation with UV light at a specific wavelength, the crosslinked networks of materials began to recover as expected. The Healing efficiencies calculated from the flexural strength can reach 14 and 26%, respectively, upon exposure to UV stimulus or a combination of UV light and heating (100℃).

Froimowicz et al. reported that the anthracene can be a photosensitive part when introduced into dendritic macromonomers to create a photo-reversible material. It was proven that the formed networks can maintain a reversible self-healing property under continuous UV irradiations at 254 and 366 nm[59].

Burnworth et al. proposed optically healable metallo supramolecular polymers based on macromolecules with pyridine derivative termini and Zn^{2+} ions complexes [60]. The photo-dissociation of Zn^{2+} patterns results in the liquefaction of polymers, subsequently, the self-healing property was provided by re-complex.

Lately, photosensitive biopolymers have received increased attention in biological materials and processes [61,62]. The biological activity of poly (coumarin ethylene) s has been studied by Patel et al. They synthesized poly (3-substituted coumarin ethylene) by reacting salicylaldehyde-1, 2-dichloroethane resin (Mn=1530 g/mol) with various

carbethoxytriphenyl alkylidine phosphoranes under Wittig, Knoevenagel, and Perkin reaction conditions [63]. Fungal growth measurements were conducted to test the polymers' toxicity. The results showed all of the polymers displayed less than 50% inhibition on the growth of Aspergillus Niger and insignificant inhibition on the growth of Antrodiella. It was suggested that the polymers exhibit no considerable toxic effect on fungal growth.

Novel polyurethane was synthesized by Zhang et al.[64] The polyurethane was composed of isophorone diisocyanate, polyethylene glycol and photo-reversible moiety 5, 7-bis (2-hydroxyethoxy)-4-methylcoumarin. By taking advantage of reversible photodimerization and photocleavage habit of coumarin, the polyurethane can be repeatedly crosslinked and de-crosslinked under successive UV irradiations at 350 and 254 nm. Therefore the polyurethane exhibited self-healing properties and can be ideal for making UV stimulated self-healing products.

In this context, biomimetic self-healing might be available based on the photo-responsive behavior in nature. However, so far, most previous work only focuses into this aspect on the reaction mechanism, and there are only a few studies have applied into photo-controlled drug release with solvent [65,66] and photo-alignment of liquid crystalline polymers [67,68]. Nevertheless, photo-stimulated self-healing polymers with supermolecular networks constructed by photosensitive moieties are

still rarely reported [69-71]. Meanwhile, work on the biological application of coumarin and coumarin derivatives in self-healing macro hydrogels has also been rarely reported based on feature of reversible photo-crosslinking.

2.1.5 Thermo-sensitive Hydrogel

Recent years, environmentally sensitive hydrogels have attracted various applications. Some environmental variables, such as elevated temperatures, are found in the body. Therefore, thermo−sensitive hydrogels can be used in site-specific controlled medical applications [72]. The practical applications of hydrogels require significant improvements in the hydrogel properties [73].

Much attention has been focused on fabrication of thermo sensitive hydrogels. Linear and cross-linked polymer networks with a specific temperature-dependent solubility or swelling behavior have been developed for this purpose [74-79]. In these systems, variations in temperature, such as body temperature, soil and ambient temperature, can trigger alteration of polymer configurations. Thus, considerable research efforts are now being made to thermally control the release of drugs [74-79], agricultural agents [80] or other agents [81].

Solubility of most polymers increases with an increasing surrounding temperature.

However, for polymers with lower critical solution temperature (LCST), their water solubility decreases when the temperature increases. Hydrogels made of LCST polymers shrink when the temperature increases above the LCST. Swelling behavior like this is called negative temperature dependence. The negative temperature dependent hydrogels are made of polymers containing balanced amount of hydrophobic groups by mixing hydrophilic and hydrophobic segments properly [73].

At lower temperatures, the hydrogen bonding between the hydrophilic parts of the polymer chains and water molecules are dominates, resulting in enhanced dissolution in water. When the temperature increases, hydrophobic interactions among hydrophobic segments become strengthened, while hydrogen bonding becomes weaker. Such reverse change leads to the shrink of the hydrogels [73]. Hydrogel's LCST can be adjusted by changing the ratio of hydrophilic and hydrophobic segments of the polymer. One method is to synthesize copolymers from hydrophobic [e.g. poly (N-isopropylacrylamide) (NIPAM)] and hydrophilic (e.g. acrylic acid) monomers [76,82-84].

The continuous phase transition of PNIPAM can be changed to a discontinuous one by incorporating a small amount of ionogenic groups into the network of hydrogels [85,86] or by changing solvent composition[87]. By copolymerizing of NIPAM with different types of monomers, hydrogels with more versatile properties can be obtained, for

example, with faster rates of shrinking when being heated through the LCST[88], or with sensitivities to additional stimuli.

PNIPAM can precipitate upon heating above its LCST [76,89,90]. Precipitation of a polymer from solution upon heating is a common feature of polymers in both strongly interacting solvents (e.g., water) and weakly interacting organic solvents. Protein denaturation is a common example of the former process. Phase separation of such polymers as polystyrene from toluene above its boiling point or of poly(isobutylene) from pentane at 75 °C are examples of the latter process [91,92]. PNIPAM is like a protein in that it precipitates below the boiling point of the solvent. Moreover, copolymerization of NIPAM with other monomers of various hydrophilicity results in copolymers that precipitate at different temperatures. Unlike a protein, PNIPAM redissolves upon cooling. Thus, PNIPAM is a material that can be used to design "smart" or recoverable catalysts and substrates [76,90].

PNIPAM and its supported substrates are soluble in low temperature but insoluble in high temperature. As a result, PNIPAM based materials can be separated and recovered from aqueous solutions by simple heating and then reused after adding fresh cold water. This heating-induced insolubility also leads to "smart" thermo responsive behavior for materials which can be used as scaffolds in tissue engineering [93].

2.2 Preparation and Characterization of Hydrogels

2.2.1 Fabrication of Cell Compatible Crosslinkers

Hydrogels are water insoluble 3D networks of crosslinked natural or synthetic polymer chains. They present such properties as permeability to oxygen, metabolites and water, making them strategic candidates as scaffolds for regenerative medicine [94]. Biocompatible amphoteric poly(amidoamine) (PAA) hydrogels are particularly useful since they can be functionalized with biomolecules, made to be responsive to such external condition changes as pH and osmotic pressure, and tailored to have specific mechanical and chemical properties [95]. They are optically transparent, non-immunogenic, biodegradable materials with low toxicity, despite of their polycationic nature [95]. Poly (amidoamine) s are a group of synthetic polymers containing amido and tertiary amino groups, which usually appear along their polymer chain [30,95,96]. Most of them are synthesized via Michael-type polyaddition of primary or secondary amines to bis-acrylamides. Successfully synthesized PAAs normally exist as a side functional groups, such as additional tertiary amino groups, allyl groups, carboxyl groups, and hydroxyl groups [97], which can be easily obtained using suitably functionalized monomers, like aminocarbohydrate derivatives [98].

Despite of their very promising properties, synthetic hydrogels are characterized by poor cell adhesion, thus numerous chemical or physical modifications have been

proposed in order to overcome this problem [94]. In order to increase cell biocompatibility of PAAs hydrogels, functional comonomers, such as 4-aminobutyl guanidine or agmatine, have been imported to build a functional repeating unit which has amphoteric property and similar function to the tripeptide arginin-glycin-aspartic acid (RGD), which presents in several extra cellular matrix (ECM) proteins [98]. PAAs hydrogels incorporating agmatine group have shown a superior cell adhesion capability when compared to plain amphoteric PAAs [99].

Shi et al.[100] reported a multi-functional cationic poly (amidoamine) crosslinker synthesized through Michael addition of peptide mimetic agmatine to N, N'-bis (acryloyl) cystamine (CBA). Polyethylene glycol diacrylate (PEGDA) was added as the base of hydrogel. The hybrid hydrogel showed significant cell attaching capability, biodegradability and biocompatibility. The stiffness of gel can also be tuned. Morphology of the hydrogels indicated a 3D structure. RT-PCR demonstrated that the tunable stiffness of such hydrogels can regulate the osteogenic differentiation of MSCs (mesenchymal stem cells).

Magnaghi et al. [93] studied on the *in vivo* performance of a PAA hydrogel implant as scaffold for tissue engineering. An amphoteric agmatine-derived PAA hydrogel was shaped into a small tubing via radical polymerization of a soluble functional oligomeric precursor. They used this tubing as a conduit for nerve regeneration in a rat sciatic

nerve cut model. This amphoteric PAA based hydrogel was first employed as conduit for the regeneration of sciatic nerve in rats, and demonstrate potential as conduits for the regeneration of injured peripheral nerves in cases of traumatic or metabolic neuropathies, and more generally as implantable scaffolds for tissue regeneration.

Ekenseair et al. [101] developed a novel injectable NIPAM based hydrogel through synthesis and combination of thermo gelling macromer and a hydrophilic and degradable polyamidoamine cross-linking macromer. This injectable hydrogels become more like solid with the elevation of temperature to 37 ˚C. PNIPAM based polymer chain contained pendant epoxy rings and a hydrolytically degradable polyamidoamine-based diamine crosslinker. Network can be formed by the epoxy cross-linking reaction. The reaction is rapid and mild. This study introduces a promisingly injectable hydrogels that can be formed in situ.

2.2.2 Photosensitive Crosslinker

Recently, several groups get excellent achievements in this area. Chung et al. developed a photo-cross-linkable cinnamate monomer, 1, 1, 1-tris- (cinnamoyloxymethyl) ethane (TCE) with three optically active moieties [58]. It can be crosslinked to form an extreme hard solid via [2+2] photocycloaddition upon ultraviolet (UV) irradiation at λ>280 nm. The sample of TCE was first given a microcrack manually, which result in a cleavage of cyclobutane ring due to its low bond strength. Then after irradiation with

UV light at a specific wavelength, the crosslinked networks of materials began to recover as expected. The Healing efficiencies calculated from the flexural strength can reach 14 and 26%, respectively, upon exposure to UV stimulus or a combination of UV light and heating (100°C).

Urban and Ghosh synthesized a heterogeneous polyurethane network containing an oxetane-substituted derivative of chitosan (OXE-CHI) [102].The four-membered oxetane rings were opened to create two reactive ends when mechanical damage was applied to the materials. Upon exposure to UV light, chitosan chain scission occurred, generating crosslinks with the reactive oxetane ends, resulting in a one-way healing property.

Amamoto et al. introduced repeatable photo-induced self-healing of covalently crosslinked polymer through reshuffling of trithiocarbonate units. The damaged parts such as dynamic covalent reshuffling of trithiocarbonate was swollen in acetonitrile and healing process was completed upon exposure to UV light under nitrogen atmosphere with catalysis of catalysis of 2, 2'-azobis (isobutyronitrile)[103].

Froimowicz et al. reported that the anthracene can be a photosensitive part when introduced into dendritic macromonomer creating a photo-reversible material. It was proven that the formed networks can maintain a reversible self-healing property under

continuous UV irradiations at 254 and 366 nm[59].

Burnworth et al. proposed optically healable metallo supramolecular polymers based on macromolecules with pyridine derivative termini and Zn^{2+} ions complexes [60]. The photo-dissociation of Zn^{2+} patterns results in the liquefaction of polymers, subsequently, the self-healing property was provided by re-complex.

Coumarins are a class of molecules including several hundred derivatives. These molecules are naturally present in many plants and have also been synthesized via different routes [104,105]. They are used in various applications, including fragrances, medicines, drug delivery, and liquid crystalline polymers. Their photosensitivity was discovered one century ago[106].

Coumarin-containing polymers have also been well studied and widely applied in many fields, including biochemical, organic–inorganic hybrid materials, liquid crystalline materials, electro-optical materials, and light harvesting/energy transferring materials[107-114]. In addition, their photo-cleavage behavior and reversible photo crosslinking property have been widely investigated for the application of photo reversible materials [115-118]. The [2+2] cycloaddition of a couple of coumarin moieties leads to a cyclobutane ring under the irradiation of UVA wave band (320nm-400nm). While after irradiation of UVC lights (200–280 nm), the coumarin

photodimers can be cleaved and regenerate the original coumarin moieties. Thus, polymers containing coumarin structural parts exhibit fast photo-responsibility and effective photo-reversible property with alternative irradiation of UV light at different wavelengths.

Lately, photosensitive biopolymers have received increased attention in biological materials and processes [61,62]. The biological activity of poly (coumarin ethylene) s has been studied by Patel et al. They synthesized poly (3-substituted coumarin ethylene) by reacting salicylaldehyde-1, 2-dichloroethane resin (Mn=1530 g/mol) with various carbethoxytriphenyl alkylidine phosphoranes under Wittig, Knoevenagel, and Perkin reaction conditions [63]. Fungal growth measurements were conducted to test the polymers' toxicity. The results showed all of the polymers displayed less than 50% inhibition on the growth of Aspergillus Niger and insignificant inhibition on the growth of Antrodiella. It was suggested that the polymers exhibit no considerable toxic effect on fungal growth.

Coumarin fluoroprobes have also been developed in the application of fluorescent ligand displacement assays for herbicide detection by binding 7-carboxymethoxy-4-methylcoumarin to a molecularly imprinted cross-linked polymer of 4-vinylpyridine and ethylene glycol dimethacrylate. The fluoroprobes play important roles in domain-forming polymers, and as an aid in measuring diffusion

[119-121]. When the herbicide went into the polymer and the imprinted regions, the coumarin probe was replaced and lead to the decrease of fluorescence of the imprinted polymer. The sensitivity of the system was determined to be approximately 100 nM [120,122].

Similarly, coumarin 343 was coupled to poly(organosiloxane) microgels (radius~10 nm), the particles can be used as tracers in diffusion studies using fluorescence correlation spectroscopy [121]. Schmidt et al. attached the coumarin to the core of the particles in order to prevent them from interfering with the diffusion behavior of the particles under investigation.

Thermo-responsive nanogels based on photo-controllable crosslinking reactions of coumarin have successfully been proposed and demonstrated by Zhao et al.[123,124] They synthesized diblock copolymers comprised of poly (ethylene oxide) and poly [2-(2-methoxyethoxy) ethyl methacrylateco-4-methyl-[7-(methacryloyl) oxyethyloxy] coumarin] (PEO-b-P (MEOMA-co-CMA)). In their studies, introducing stimuli of temperature and light can change the size of nano aggregates and networks. These smart nanogels can be obtained by photo-crosslinking of the micellar aggregates at temperatures below the LCST of the P (MEOMA-co-CMA) block through dimerization of coumarin side groups at a wavelength higher than 310 nm. Under $\lambda<260$ nm, the reverse photocleavage of the network was observed, consequently resulted in a

decrease of the crosslinking density which followed a swelling of the nanogel.

Novel polyurethane was synthesized by Zhang et al.[64] The polyurethane was consisted of isophorone diisocyanate, polyethylene glycol and photo-reversible moiety 5, 7-bis (2-hydroxyethoxy)-4-methylcoumarin. By taking advantage of reversible photodimerization and photocleavage habit of coumarin, the polyurethane can be repeatedly crosslinked and de-crosslinked under successive UV irradiations at 350 and 254 nm. Therefore the polyurethane exhibited self-healing properties and can be ideal for making UV stimulated self-healing products.

In recent years, most reported coumarin-containing polymers focused on supramolecular science. Although many supramolecular architectures have been synthesized [125-129], the self-healing of macroscopic materials [130-132] through molecular recognition is one of the biggest challenges [133-135]. By introducing as a pendent group or terminal group to the polymer chain could provide a means for structural changes and achieve self-healing process triggered by a stimulus.

In this context, biomimetic self-healing might be available based on the photo-responsive behavior in nature. However, so far, most previous work only focuses into this aspect on the reaction mechanism, and there are only a few studies have applied into photo-controlled drug release with solvent [65,66] and photo-alignment of

liquid crystalline polymers [67,68]. Currently, work on the biological application of coumarin and coumarin derivatives in self-healing macro hydrogels has been rarely reported based on feature of reversible photo-crosslinking.

2.2.3 Gel Forming Materials

A variety of synthetic and naturally derived materials may be used to form hydrogels for tissue engineering scaffolds. However, because their chemistry and properties are controllable and reproducible, synthetic hydrogels are widely used in tissue engineering [12]. For instance, synthetic hydrogels can be specified by tuning the molecular weights, changing the block structures, degradable linkages, or crosslinking modes, which decide the crosslinking density, and consequently, dictate material mechanical and degradation properties [136].

2.2.3.1 Polyethylene Glycol (PEG)

Poly (ethylene glycol) (PEG) is appealing for human medicine, has been approved by FDA for several medical applications. It is one of the most commonly applied synthetic hydrogel polymers for tissue engineering. PEG is a hydrophilic polymer that can be crosslinked by modifying each end of the polymer with either acrylates or methacrylates [137-139]. Hydrogels are then formed when the modified PEG is mixed with the appropriate crosslinkers [138,140].

Research show that if PEG was labeled with a near-infrared fluorophore, it can be used in preclinical work as a vascular agent, lymphatic agent, and general tumor-imaging agent which can be used to exploit the enhanced permeability and retention effect (EPR) of tumors [141].

PEG is also used in the repair of motor neurons damaged in crush or laceration incidents *in vivo* and *in vitro*. if coupled with melatonin, 75% of damaged sciatic nerves were rendered viable [142].

2.2.3.2 Thermo-sensitive Hydrogels

Thermo sensitive polymers exhibit lower critical solution temperature (LCST) behavior. The transition of sensitive soluble polymers from a homogeneous to a heterogeneous state is called the cloud point or phase transition temperature (Tc)[38]. This behavior is derived from changes in the balance of interactions of hydrophilic and hydrophobic groups in the polymer chains at the LCST [143-146]. These properties of the thermo sensitive polymers result in interesting properties of their polymer gels, i.e., significant and sharp changes in swellability upon raising the temperature above the LCST.

Among the thermo responsive polymers, poly (N-isopropylacrylamide) (NIPAM) and its copolymers have been investigated extensively theoretically and experimentally [143-157]. Much of the published work has concentrated on PNIPAM-based hydrogels

as they have potential applications in a broad range of areas, such as drug delivery systems, separation systems and controlled flocculation for enhanced oil recovery [144,158,159]. These applications were also found to be especially attractive with dispersions of thermo sensitive hydrogels.

Poly (N, N-diethylacrylamide (PDEAAM) is also another materials used widely because of its lower critical solution temperature (LCST) in the range of 25-32°C, close to the body temperature. Copolymers of PDEAAM can be made with other monomers, e.g. butylmethacrylate (BMA), to adjust the LCST.

Some types of block copolymers made of poly (ethylene oxide) (PEO) and poly (propylene oxide) (PPO) also have an inverse thermo sensitive property. Due to their LCST around the body temperature, they have been widely used in the development of controlled drug delivery systems based on the sol-gel phase conversion at the body temperature.

The feature of PNIPAM that makes it an attractive polymer support for synthesis and catalysis chemistry is its inverse temperature-dependent solubility. This property is often discussed in terms of the temperature at which the polymer phase separates from a solution the LCST [160]. In water, PNIPAM has an LCST of 31 °C. This behavior results from the unfavorable entropy changes associated with polymer dissolution and

is affected by the presence of a comonomer. The LCST of PNIPAM derivatives allows PNIPAM derivatives to be separated and recovered from solutions of other polymers, substrates, or reagents by heating. Subsequent centrifugation and trituration allows recovery of the PNIPAM-bound species [161].

2.2.3.3 Polyacrylamide (PAM)

Polyacrylamide (PAM) is a polymer formed from acrylamide units. It is available as either a simple linear or cross-linked chain structure, typically using N, N'-methylenebisacrylamide. Polyacrylamide has highly water content and low toxicity. It forms a soft gel when hydrated, applications of PAM such as polyacrylamide gel electrophoresis and soft contact lenses have been frequently studied [162]. Another development is the thickener and suspending agent in the linear chain form. Moreover, it has been used as subdermal filler for aesthetic facial surgery [163].

2.2.4 Preparation of Hydrogels

The physical properties of the materials are critical for the successful applications of the scaffold. Natural materials for hydrogels are usually linear polysaccharide polymers, and don't have sufficient mechanical and swelling properties for most applications. Chemical or physical methods are therefore used to improve their mechanical properties.

For example, scaffolds can be created and their mechanical properties enhanced by introducing various chemical crosslinkers (i.e. glutaraldehyde, formaldehyde, carbodiimide) [164,165], by crosslinking with physical treatments (i.e. UV irradiation, freeze-drying, heating) [164,166], and by blending it with other polymers (i.e. HA, PLA, poly(glycolic acid) (PGA), poly(lactic-coglycolic acid) (PLGA), chitosan, PEO) [164,165,167-169].

Poly (N-isopropylacrylamide) is readily prepared by radical polymerization [76]. High molecular weight copolymers can be prepared by using mixtures of N-isopropylacrylamide and other acrylamide derivatives or acrylic acid derivatives. Both PNIPAM homopolymers and copolymers have been studied previously. PNIPAM and PNIPAM derivatives have received particular attention as materials for use in drug delivery and as coatings due to their thermally sensitive solubility or swellability in water [76,89,160,161].

Hydrogels with dimensions in the range of submicrons (namely microgels of nanogels) could be conventionally prepared by free-radical polymerization in dilute solutions or by emulsion polymerizations[104]. Microgels were first synthesized by Staudinger and Husemann[170] in 1935. Pelton and his coworkers [171-176] have systematically prepared and described PNIPAM latex in water since the 1980s. The colloidal microgel

systems were conventionally prepared using NIPAM, with potassium persulfate as the initiator, sodium dodecyl sulfate (SDS) as the surfactant and methylene bisacrylamide as the cross-linker. The authors reported that under these conditions the microgels could only be formed above a critical temperature, i.e., 55°C. Uzum OB et al. [175] prepared Acrylamide/mesaconic acid (AAm/MA) hydrogels by free radical solution polymerization. The aqueous solution contained acrylamide (AA) with mesaconic acid (MA) as comonomer and two multifunctional crosslinkers, e.g. ethylene glycol dimethacrylate (EGDMA) and 1, 4-butanediol dimethacrylate (BDMA).

Using similar procedures, Murray et al. [177] and Snowden et al. [178] have tailored various colloidal microgels from NIPAM, NIPAM with acrylic acid (AAc) and other thermo sensitive polymers. Duracher and et al. [179] prepared PNIPAM lattices via precipitation polymerization. Jones and Lyon [180] recently developed multiresponsive core-shell multiresonsive microgels were synthesized via precipitation polymerization and then used as nuclei for shell formation.

In addition to the polymerization/crosslinking of monomers, crosslinking of polymer chains with metal ions, freeze-thawing, and irradiation techniques are also utilized to obtain 3D polymer networks[181,182]. Water-in-oil (w/o) microemulsions have been widely used to synthesize particles of controlled size and shape, and provide a simple tool to fabricate hydrogel micro/nanoparticles[183,184]. In this kind of preparation, a

biocompatible surfactant for the formulation of w/o microemulsion for the hydrogel micro/nano-particle syntheses is a very promising prospect. One such surfactant is L-α-phosphatidylcholine or lecithin. Lecithin has a zwitterionic head group and belongs to an essential class of biomolecules known as phosphoglycerides or phospholipids. Thus it is widely used as a biocompatible emulsifier in food processing, medicine, and cosmetics[185].

C.Duan Vo et al.[38] report a new route to prepare thermo sensitive colloidal nanogels based on photopolymers of PNIPAM. The photo-cross-linkable polymers described have gained considerable technological interest as the polymers exhibit many interesting properties [186-190]. They also developed hydrogel films based photo-cross-linkable polymers of NIPAM and dimethyl maleinimido acrylamide (DMIAAm) for microsystem applications [191-194].

2.2.5 Potential Application of Thermo-sensitive Hydrogels

Thermo sensitive hydrogels have enormous applications. They can be used in site-specific drug controlled delivery, biosensors, tissue engineering, enzyme immobilization, flow control, fabric surface modification etc.

2.2.5.1 PNIPAM Hydrogels for Drug Delivery

As for drug carrier, PNIPAM hydrogels own many advantages. The advantages, such as

hydrophilicity, flexibility, high water absorptivity, and good biocompatibility, are characteristic of hydrogels, while the advantages such as long life span in circulation and the possibility of being actively or passively targeted to the desired biophase, e.g. tumor sites, originate from their size which falls in the colloidal range [195].

Li et al.[196] produced a biochemically and stimulus responsive triblock copolymer. a micellar, dithiol cross-linked NIPAM gel was formed at 37°C. When the gel was treated by glutathione, it will be degraded via cleavage of a central disulfide bond. Therefore, such system provides the possibility of carrier/release from a loaded gel by glutathione-stimulated degradation.

M. Das et al. synthesized a pH responsive PNIPAM microgel to delivery anti-cancer drugs to cancer cells [197]. The microgel size was controlled to be small (~150 nm), which maximizes extravasation into tumors. Receptorspecific ligand (transferrin) was conjugated onto the microgel surface for targeting the diseased cells. Drugs were loaded by physical means (via electrostatic interaction), instead of covalent attachment, which may potentially alter the drug's effectiveness. A release mechanism, which is triggered by biological stimuli, i.e., pH change from 7.4 in the extracellular matrix to 4.5 in lysosome, was selected. An *in vitro* study reveals that the biofunctionalized, pH-responsive microgels can selectively carry the chemotherapeutic agent into tumor cells and cause significant cytotoxicity.

2.2.5.2 PNIPAM Hydrogels for Biosensing

Wu et al.[198] designed a composite PNIPAM microgel which is both pH and H_2O_2 responsive. The gel used in their study is a copolymer microgel of poly (N-isopropylacrylamide-acrylic acid-acrylamide) [P (NIPAM-AAc-AAm)]. Calcon dye was applied as an optical identification code and H_2O_2 sensitive component.

Because H_2O_2 can break the azo bond in the Calcon dye, the PL intensity of the composite microgel decreases with time in the presence of H_2O_2. As result, this novel composite microgel can be developed as an optical pH and H_2O_2 sensor.

2.2.5.3 PNIPAM Hydrogels in Tissue Engineering

Kim et al.[199] have created an injectable hydrogel of PNIPAM-co-AAc to mimic the ECM. These hydrogels are prepared by cross-linking an MMP-13/collagenase-3-degradable peptide sequence and NIPAM in the presence of Arg-Gly-Asp-modified poly (AAc). The proteolytic degradation and cell adhesion properties of this hydrogel were studied using rat calvarial osteoblasts. Collagenase was found to degrade the hydrogel, with the rate dependent on the concentration of collagenase in relation to the poly (AAc) chain. Migration of osteoblasts is observed in hydrogels both with and without the Arg-Gly-Asp peptide. However, greater migration is seen in those hydrogels that contain Arg-Gly-Asp. There is also an increase in cell

migration in MMP-degradable hydrogels compared with nondegradable gels, indicating the advantage of bioresponsive hydrogels.

Chen et al. [200] have grafted a PNIPAM hydrogel onto nonwoven fabrics by photo-induced graft polymerization and studied the fabrics' temperature-responsive characteristics. In their work, a temperature-sensitive PNIPAM hydrogel was grafted onto a plasma activated polyethylene terephthalate (PET) film and a polypropylene (PP) nonwoven fabric surface. The results showed that the additives of APS, TEMED, and MBA were beneficial in promoting the grafting yield. These grafted hydrogels exhibited a LCST of about 32 °C, indicating that the temperature-sensitive behavior of the bulk PNIPAM hydrogel was maintained.

The practical applications of hydrogels require significant improvements in the hydrogel properties. Clinical applications of thermo sensitive hydrogels based on NIPAM and its derivatives also have limitations. The monomers and crosslinkers used in the synthesis of the hydrogels are not known to be biocompatible, some of they may be toxic. In addition, the polymers of NIPAM and its derivatives are not biodegradable. The observation that acrylamide-based polymers activate platelets upon contact with blood, together with the unclear metabolism of PNIPAM, requires extensive toxicity studies before clinical applications can emerge [78]. For successful applications, further development of new polymers and crosslinkers with more biocompatibility and

better biodegradability would be essential.

Chapter 3. Hydrogels Based on Cell-compatible Crosslinkers

3.1 Materials and Methods

3.1.1 Materials

2-Bromo-2-methylpropionyl bromide, methylacryloyl chloride, 7-Hydroxy-4-methylcoumarin, 2-bromoethanol, methyl methacrylate, triethylamine, potassium carbonate, ethanol, ether, anhydrous sodium sulfate, dichloromethane, sodium chloride, DMSO, acrylamide, poly (ethylene glycol) diacrylate (PEGDA, Mw=700), N-Isopropyl acrylamide (NIPAM), N,N'-Methylene bis(acrylamide) (MBA), agmatine sulfate salt (AS), 1-(2-Aminoethyl)-piperozine(AEPZ), N,N,N',N'-Tetramethylethanediamine (TEMED), ammonium persulfate (APS), and lithium hydroxide (LiOH) were all purchased from Sigma-Aldrich without further purification. PBS 1X powder, Hoechst 33342, BODIPY®FL phallacidin, To-Pro-3 iodide and Live-Cell staining kit were all purchased from Invitrogen. The 3-(4, 5-dimethyl thiazolyl-2)-2, 5-diphenyltetrazolium bromide (MTT) cell viability assay kits were from Biotium Inc. (Hayward, CA). O.C.T. compounds were purchased from V.W.R. The RT-PCR kit was purchased from Thermo Scientific.

3.1.2 Synthesis of Linear PAA Crosslinker

The agmatine containing poly (amidoamine) (PAA) crosslinker was synthesized via Michael-addition polymerization as shown in Figure 1:

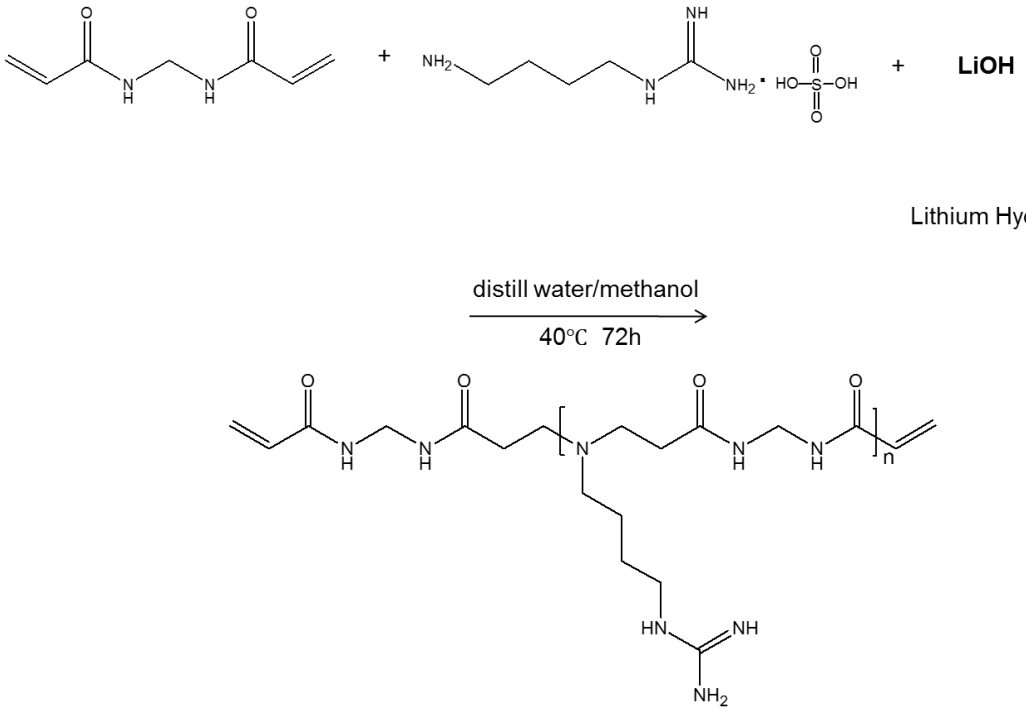

Figure 1.Schematic illustration of the preparation of linear PAA crosslinker.

MBA (185mg, 1.2 mmol) and AS (228 mg, 1.0 mmol) were dissolved in water/methanol (v/v =5/1, total in 5ml) while stirring. When the solution was clear, $LiOH \cdot H_2O$ (42 mg, 1.0 mmol) was added to the solution. The mixture was then gently stirred and allowed to react at 40 ˚C in the dark for 72h. After reaction, the solvent was evaporated using a rotary- evaporator. The product was finally recovered by lyophylization and stored in-20 ˚C refrigerator for future use.

3.1.3 Characterization of Linear PAA Crosslinker

3.1.3.1 Fourier Transforms Infrared Spectroscopy (FTIR)

FTIR spectra were recorded with a Thermo Scientific IR100 FT-IR Spectrometer. Both G1 and G2 hydrogels were freeze-dried in order to remove the residual chemicals. Then dried hydrogels were ground to powder, mixed with KBr, and compressed into pellets. As shown in Figure 2, the sharp peaks appeared around 1666.49cm^{-1} was attributed to the C=O stretching frequency from MBA. While peaks located at 1539.84cm^{-1} was attributed to the NH_2 group from agmatine, the results show successful conjugation of linear PAA crosslinker.

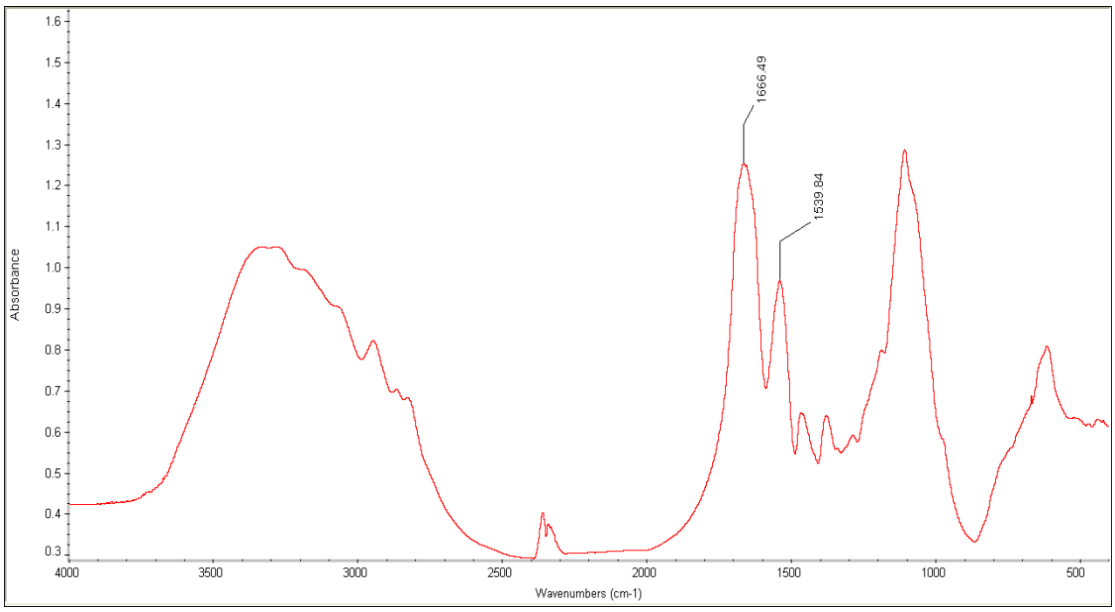

Figure 2.FTIR spectra of linear crosslinker.

3.1.3.2 1H NMR

In order to characterize the PAA crosslinker, 1H NMR spectra was recorded on an Advance 300 MHz spectrometer. 8 mg of PAA crosslinker powders were dissolved in 800µl of D_2O. Chemical shifts (δ) were reported in parts per million (ppm). The molecular weight of PAA crosslinker was calculated from the 1H NMR spectrum (Figure 3). 1H NMR (ppm): δ, 1.40–1.60 (–$CH_2(CH_2)_2CH_2$–), 2.40–2.50 (–CH_2(C=O)NH–), 2.50–2.60 (–CH_2–N$(CH_2)_2$–), 2.80–2.90 (–CH_2–N$(CH_2)_2$–, 3.20–3.30 (–CH_2–NH(C=NH)NH_2), 3.40–3.60 (–(C=O)NH–CH_2–), 4.40-4.60(-NH(CH_2)NH-), 5.60–6.40 (CH_2=CH–(C=O)–).

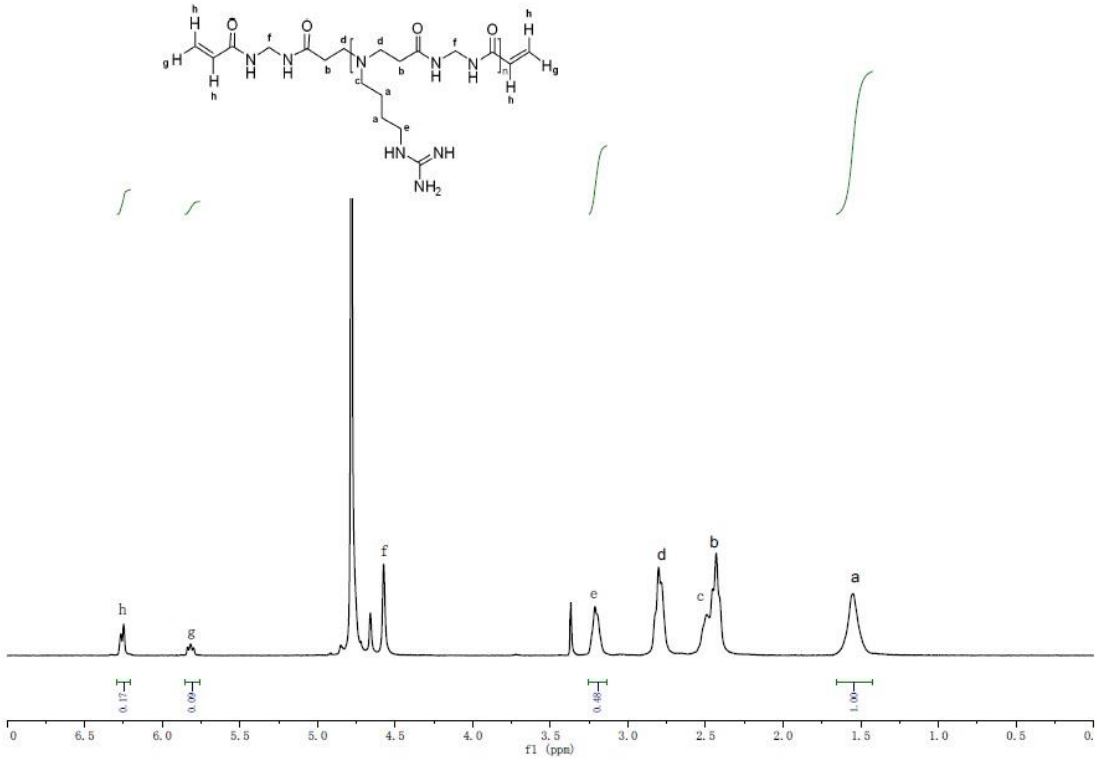

Figure 3.1H NMR spectrum of the PAA crosslinker.

3.1.4 Fabrication of Hydrogels with Linear PAA Crosslinker

3.1.4.1 Fabrication of Hydrogels with Tunable Stiffness

Pure PEG hydrogels and PEG containing PAA hydrogels were prepared at three different concentration 60mg/ml, 120mg/ml and 240mg/ml aim to obtain different stiffness. Gels were fabricated in distill water by initiator APS (5.7mg/ml) and catalyst TEMED (2.9mg/ml) at room temperature for a couple of minutes. Hydrogel labeled G1 are pure PEG hydrogel which is set as control group, G2 are experimental groups with different PAA crosslinker mass ratios. In order to obtain different swelling behavior,

biodegradation and cell adhesive property, they were designed at three different ratios, PEG: PAA=100:5,100:20 and 100:50, labeled as G2-1, G2-2 and G2-3 respectively.

3.1.4.2 Fabrication Thermo-sensitive Hydrogel

NIPAM containing PAA hydrogels were prepared at the concentration 60mg/ml with the ratio NIPAM: PAA=100:20. Gels were fabricated in distill water by initiator APS (5.7mg/ml) and catalyst TEMED (2.9mg/ml) at room temperature for a couple of minutes.

3.1.5 Mechanical Properties of Hydrogels

The stiffness and young's modulus of hydrogels were tested by INSTRON® materials testing machine. The hydrogels were formed in 24-well plate, in order to get a uniform shape with 15mm in diameter and 6mm in height. The test speed was set at 0.2 mm per minute. All measurements were carried out at constant temperature and humidity room. The stiffness curve and young's modulus values were recorded by the INSTRON® software. The sample size of each group is 3 (n=3).

3.1.6 Swelling Behavior Test

Hydrogels were prepared in a specific size in 24-well plate as described before. Then weighed and immersed in vials which containing PBS buffer (pH=7.4) at room temperature. At designed time intervals, the hydrogels were taken out from solution,

and weighed after wiping off any visible surface moisture. The percentage amount of buffer absorbed can be calculated using the following formula:[201]

$$\text{Water (\%)} = (W_t - W_0)/W_0 * 100 \quad (1)$$

Where W_t is the weight of hydrogels at weighing time and W_0 is the weight of the initial weight hydrogel. In order to reduce errors, all swelling ratio results should be obtained from triplicate samples.

3.1.7 Morphology of Hydrogel

Cryosection was used to investigate the morphology of hydrogel. The original gel and healed gel were transferred to 80 ˚C overnight, and then gels were embedded in a half-filled cryomold by an O.C.T. compound. The cryomold was under 20 ˚C until O.C.T. compounds became translucent; finally, the frozen block was removed from the cryomold and mounted on the cryostat to collect the slides. Slides were stained by FITC, fluorescent images were recorded.

Hydrogels for AFM were prepared between two glass cover slips (25 mm × 25 mm) by adding 250 ul of gel precursor solution. After gelation under 60 ˚C for 20 minutes, the cover slips were removed and then the gel was thoroughly washed with sterilized PBS solution to remove chemical residuals.

3.1.8 *In vitro* Degradation Analysis

Since the PEG hydrogels have the similar structure of protein, proteinase K was applied in this enzymatic degradation experiment. Again hydrogels were prepared in a specific size in 24-well plate as described before. Before test, the hydrogels were put into PBS solution for 24h in order to get the hydrogel full swelling. Then move to the enzyme buffer solution. The mixture was then incubated at 37 ˚C with constant shaking [202]. At each time interval, the hydrogels will be taken out from the buffer. Any visible surface moisture should be wiped off before weighing. Afterward, the hydrogel will be returned to the vial. Two different concentrations of Proteinase K (0.05mg/ml and 0.2mg/ml) were designed to get different degradation results. The percentage of weight remaining can be calculated using the following formula:[203]

$$\text{Wet weight remaining (\%)} = W_t/W_0 * 100 \quad (2)$$

Where W_t is the weight of hydrogels at weighing time and W_0 is the initial weight of the hydrogel at maximum mass in water. In order to reduce errors, all swelling ratio results were obtained from triplicate samples.

3.1.9 Cell Culture and Growth on Hydrogel

3.1.9.1 BMSCs Culture

The hydrogels precursor for cell culture were prepared first and mixed evenly. Then drop 100μl precursor onto glass cover slips (diameter: 10mm). After gelation under 37

˚C, the glass cover slips were put into PBS solution for 2h, in order to remove chemical residuals. Then the glass cover slips were taken out and irradiated under UV light in a bio-safety hood for 30 minutes. Finally, the gels coated glass cover slip will be place in cell culture dishes (35 mm x 10 mm). Mouse bone marrow stromal cell lines (BMSCs from ATCC, USA) were cultured with Dulbecco's Modified Eagle's Medium (DMEM, GIBCO) supplemented with 10% fetal bovine serum (FBS, GIBCO), 1.0 x 10^5 U l -1 penicillin (Sigma) and 100 mg l -1 streptomycin (Sigma) at 37 ˚C in 5% CO_2.

3.1.9.2 ASCs Culture

Mouse inguinal fat pad adipose tissue samples were acquired from 6-week-old green fluorescent protein (GFP)-expressing mice, which were provided by the Model Animal Research Center of Nanjing University (Nanjing, China). Then they were cut into pieces and digested with 0.075% type I collagenase (Sigma–Aldrich, St. Louis, MO) under gentle agitation for 45 min at 37˚C. Mature adipocytes and indigested connective tissue were separated from pellets by centrifugation (800 g for 10 min) and then discarded. The pellets were suspended in phosphate-buffered saline (PBS) and filtered through a 200 μm mesh followed by centrifugation (800 g for 10 min) to spin down stromal-vascular fraction cell pellets. The retrieved cell fraction was cultured overnight at 37˚C with 5% CO_2 in a control medium (Dulbecco's modified Eagle media, 10% fetal bovine serum, 100 units/mL penicillin, 100 mg/mL streptomycin). The resulting cell population was cultured for 3 to 5 days until confluent. ASCs were cultured and

expanded in the control medium. Cells from P3 to P5 were used in the following experiments.

3.1.10 MTT Assay

The gelation was first conducted in 96 well culture plates for 5 min at 37 ºC. Then BMSCs were seeded onto the hydrogels. The culture medium was changed every 2 days. For this assay, 100 μL of the provided MTT reagent (tetrazolium salt solution) was added directly to the wells and placed in an incubator at 37 ˚C for 4 h. The purple formazan produced by active mitochondria was solubilized by constructing homogenization in 1 200μl of the DMSO. The absorbance of these solutions was read at 570 nm (n=3) by Molecular Devices Spectra [204].

Live/dead staining was carried out to evaluate the cytotoxicity of hydrogels, according to a protocol from Invitrogen Inc., Canada. BMSC cultures were performed using hydrogels and stained at 24h, 3 days and 7 days. Images were taken by confocal laser scanning microscopy (CLSM) (Olympus FV1000, Japan).

3.1.11 CCK-8 Assay

A volume of 10 μl of hydrogel solutions were added into 96-well culture plates. Then the plates were put into an incubator at 37 ˚C to form the solid hydrogel. ASCs were suspended at a density of 5×10^4 cells/ml, and 100 μl of this cell suspension was added

into each well (a total of 0.5× 10^4 cells/well) containing the hydrogel and into other blank wells without hydrogel. After incubated for 24, 48 and 72 h, cell viability was assessed using CCK-8 (Boster, Wuhan, China) according to the manufacturer's instructions, based on measuring NADH production, resulting from dehydrogenase activity in viable cells. Briefly, each well was incubated with 10 µL of CCK-8 solution at 37 ˚C for 1 h. Thereafter, the optical density (OD) for each well was measured at 450 nm using a micro plate reader (Bio-Rad Model 680, USA). Each experiment was repeated three times and the mean values were considered. The cell survival rate was calculated according to the following equation: cell survival rate = (OD experiment – OD blank)/ (OD control - OD blank) × 100 %.

To assess cellular viability further, 50 µl hydrogel solutions were added into a 24-well plate, and allowed to hydrogel at 37 ˚C. ASCs were then suspended at a density of 5 × 10^4 cells/ml and 650 µl of this solution were added per well (a total of 3.3 × 10^4 cells/well). The hydrogel-ASCs constructs were then stained using a Live/Dead Viability/ Cytotoxicity Kit (Invitrogen, UK) at the end of 3 days of culture, and observed under a fluorescence inverted microscope.

3.1.12 Cell Morphology Investigation

The morphologies of BMSC were also investigated using CLSM, according to the protocol which we used in our former experiments [100], the hydrogel-laden cells

should be fixed with 4% paraformaldehyde solution at room temperature for 20 min. After washing with PBS, samples will be permeabilized using 0.5% Triton X-100 in PBS solution at room temperature for 5 min. Then they will be blocked in 1% bovine serum albumin PBS solution at room temperature for 10 min. The samples will be incubated in BODIPY®FL phallacidin solution for 20 minutes at room temperature and stained with TO-PRO3 for 15min before CLSM investigation.

3.1.13 Observation by scanning electron microscopy (SEM)

The hydrogel was conducted in 6-well culture plates at 37°C to form the solid hydrogel. ASCs were seeded onto the hydrogel and incubated for 24 h. Morphology was examined using scanning electron microscopy (SEM, HITACHI S-3000N) with an accelerating voltage of 20 kV. The samples were quickly frozen in liquid nitrogen and then freeze-dried for 3 days. The freeze-dried samples were vacuum-coated with a gold layer prior to Scanning Electron Microscopy (SEM) examination.

ETHICS APPROVAL

The following part (In vivo Biological Experiments of Hydrogels) of the experiment is done by the department of plastic surgery, Southern Medical University, Guangzhou, P.R. China. This study was approved by the Animal Care and Ethics Committee of Southern Medical University, Guangzhou, P.R. China.

3.1.14*In vivo* Biological Experiments of Hydrogels

3.1.14.1 Depressed Scars Model

Adult Sprague-Dawley rats weighing 350 to 400 g were used under an approved animal protocol in Southern Medical University. Twenty-four hours prior to surgery, the dorsal skin was depilated with a hair remover. On the day of the surgery, animals were anesthetized with 60 mg/kg Nembutal (Sigma-Aldrich, CHN). Four round templates with the diameter of 1cm were marked on the dorsal skin. For a depressed defect model, subcutaneous fat layer and panniculus carnosus muscle tissue were both excised. Following that the defect between skin and muscle layer was sewed throughout a silicone tube (Fig.24). To determine whether the model construct is successful, we select multiple time points to test. After 8 weeks when the scars in defect sites had formed (Fig.24), four fillers 1) the hydrogel-ASCs mixture, 2) the hydrogel only, 3) HA, 4) PBS were injected to the four depressed defect sites randomly. At week 2, 4 and month 6, rats were euthanized and the depressed scars including the underlying part muscle were harvested, then were fixed in 10% neutral-buffered formalin solution for 48 hours and then stored in 70% alcohol at 4 ˚C for further H&E staining.

3.1.14.2 Gross Analysis

After pitted skin scars were harvested at different time points, each sample was photographed immediately by a digital camera (Canon 550D, Tokyo, Japan).

3.1.14.3 Histological Analysis

The samples were fixed in formalin and embedded in paraffin for routine histological processing. A 3 µm section obtained from each paraffin block was stained using routine H&E protocol, and digital images of each H&E stained section were taken and analyzed using Adobe Photoshop CS Software (Adobe Systems Incorporated, San Jose, CA).

3.1.14.4 Immunohistochemical Study of s100 protein

Samples were fixed with 4% paraformaldehyde in PBS, permeabilized with 0.2% Triton X-100 for 15 minutes and blocked for 30 minutes at 21°C. Samples were incubated with S-100 primary antibody (1:3000, Abcam, Cambridge, UK) for 15 hours at 4°C and followed by anti-mouse-HRP secondary antibody (Dako, Shanghai, CHN).

3.1.14.5 Immunofluorescence for GFP

Samples were paraformaldehyde fixed, permeabilized with 0.5% triton and blocked with 2% antibody dilution buffer for 2 hours. Cells were incubated with the anti-GFP primary antibody (1:1000, Abcam, Cambridge, UK) for 1 hour at 25°C. A Goat anti-chicken IgY-488 (1:100, Thermo Fisher Scientific Inc., USA) was used as the secondary antibody. Nuclei were counterstained with 4′, 6′-diamidino-2-phenylindole dihydrochloride (DAPI).

3.1.15 Statistical Analysis

All experiments were repeated three or more times with triplicate samples. Significant differences between two groups were evaluated using a one way analysis of variance (ANOVA) with a 95% confidence interval. When $P < 0.05$, differences was considered to be statistically significant.

3.2 Results and Discussion

3.2.1 Synthesis and Characterization of PAA Crosslinker

It has been reported that guanidine group from agmatine can promote proliferation of various cell types[99,205]. Poly (amidoamine) (PAA) crosslinker was synthesized via Michael-addition polymerization by copoolymering agmatine with MBA. (Figure 1). Cell attachment is obviously improved through adding agmatine which contains a guanidine group. The guanidine group from agmatine combined with the carbonyl group from MBA can provide functions as peptide ligands [206] which is important to enhance the cell adhesion. Both MBA and agmatine are biodegradable and nontoxic to human body. The chemical structure of PAA crosslinker was confirmed by 1H NMR spectra (Figure 2). The integral of peaks between 5.6 and 6.4 ppm represents the residual vinyl groups at the end of polymer chains [207]. According to the integral curve, molecular weight of the PAA crosslinker was calculated to be about 905.

3.2.2 Fabrication and Characterization of Tunable Stiffness Hydrogels

Different mass ratios of PEG and PAA were fabricated via radical polymerization due to the vinyl groups from the PAA crosslinker. Gel formation was show in Figure 4.

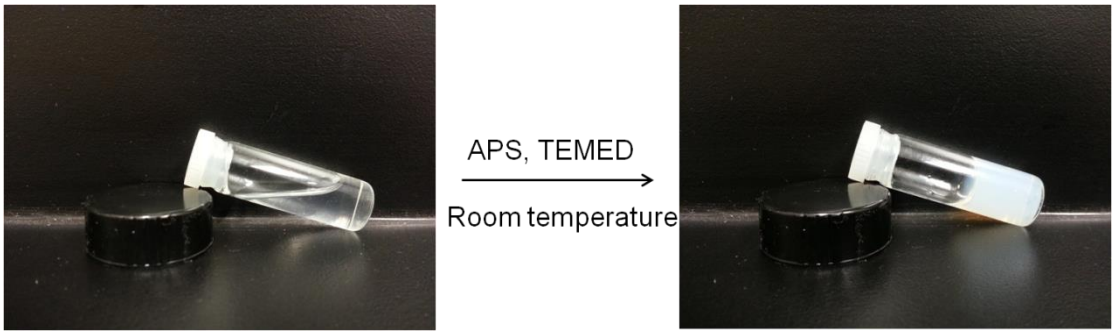

Figure 4. Tunable stiffness PEG hydrogel formation.

The FTIR spectra (Figure 5) conducted the comparison between pure PEG hydrogels and PAA crosslinked PEG hydrogels. As shown in Figure 5, the sharp peaks appeared in both spectra around 1733.8cm^{-1} was attributed to the C=O stretching frequency from ester groups. While new peaks located between 1500cm^{-1} and 1700cm^{-1}(i.e. 1666.3cm^{-1}) in Figure 5 (a) were attributed to the C=O from Amide group and C=N from imines group in the PAA crosslinker. The results show successful conjugation of PAA into PEG hydrogel.

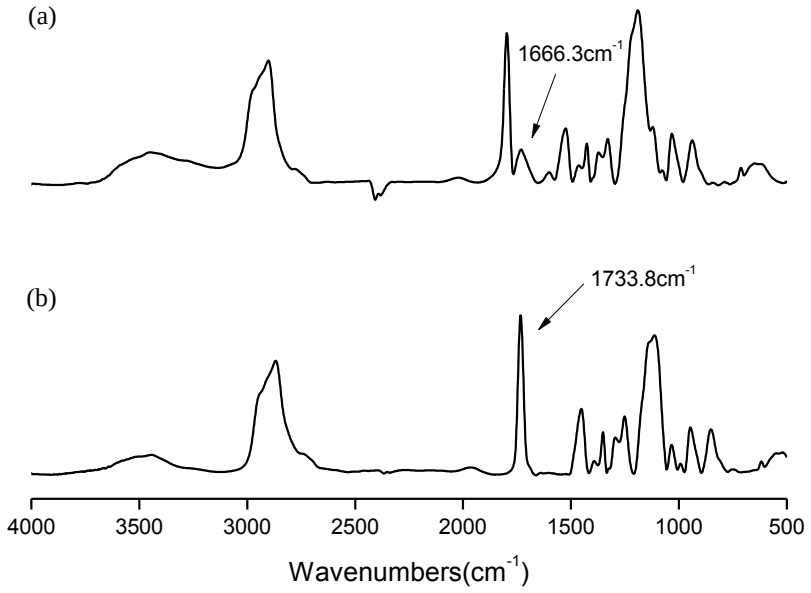

Figure 5. FTIR spectra of (a) hydrogel containing PAA crosslinker (G2) and (b) pure PEG hydrogel (G1).

3.2.3 Mechanical Profiles of Hydrogels

Many scaffolds for tissue engineering initially fill a space otherwise occupied by natural tissue, and then provide a framework by which that tissue may be regenerated. In this capacity, the physical properties of the material are inherent to the success of the scaffold [11]. In addition to genetic and molecular mediators, other physical properties of the artificial ECM may also give effects on cell proliferation [208]. Mechanical properties can affect cellular locomotion, morphology, adhesion, and cytoskeletal protein expression [209].

Adding PAA crosslinker is not only to bind functional groups to hydrogel, but also to tune the stiffness of hydrogels. In our study, pure PEG hydrogel were control group. Experimental groups were PEG hydrogel with PAA crosslinker. In order to get a desired stiffness, these two groups were designed at three different concentrations; they are 60mg/ml, 120mg/ml and 240mg/ml, respectively. The stiffness was evaluated by an INSTRON® materials testing machine. Load-extension curves (Figure 6) were recorded and Young's modulus (Figure 7) was calculated showing different stiffness. Hydrogel's stiffness and crosslinking density were affected by the concentration of hydrogel[210]. As shown in Figure 6, hydrogel fabricated at different concentrations changes the extension properties significantly. When the weight fraction of hydrogel increased, obvious increases appeared in Young's modulus as shown in Figure 7. For the pure PEG hydrogel, Young's modulus was as high as 110 kPa at the concentration of 240mg/ml. When adding PAA into the gel (PEG: PAA=100:5), Young's modulus changed gradually as the precusor's concentration increased. The results showed that at the low concentration, which is 60mg/ml for both pure PEG hydrogel and PEG containing PAA hydrogel, their stiffness were around 20 kPa. Young's modulus at this value was very close to nature ECM property, and promising to provide an ideal stiffness for cell growth and differentiation. However, if the concentration of hydrogel was increased, the gel's stiffness increased remarkably. This is due to the crosslinking density increased. Base on aforementioned results, in the later experiment we chose 60mg/ml as the basic concentration, through adjusting the mass ratio of PAA

crosslinker to obtain different adhesive properties.

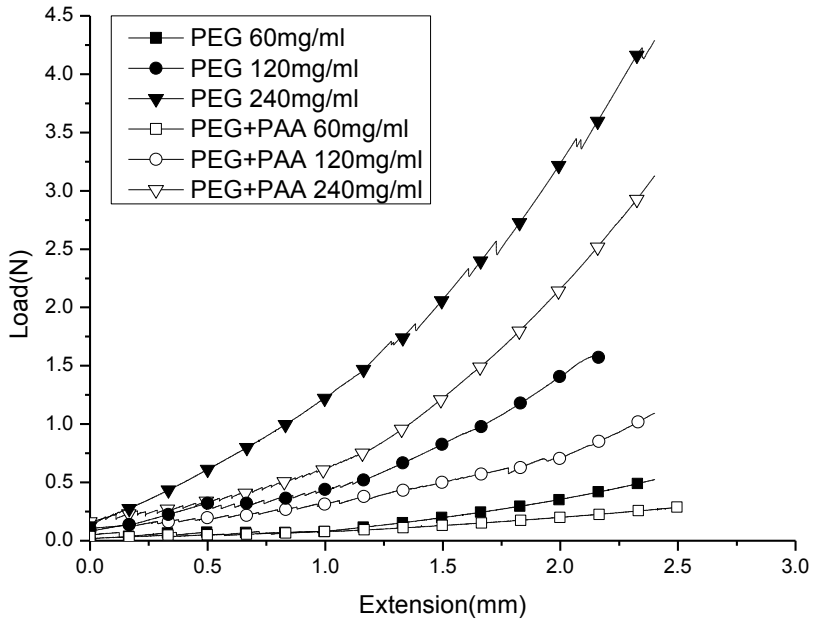

Figure 6. Typical load-extension curves of hydrogels at different concentrations.

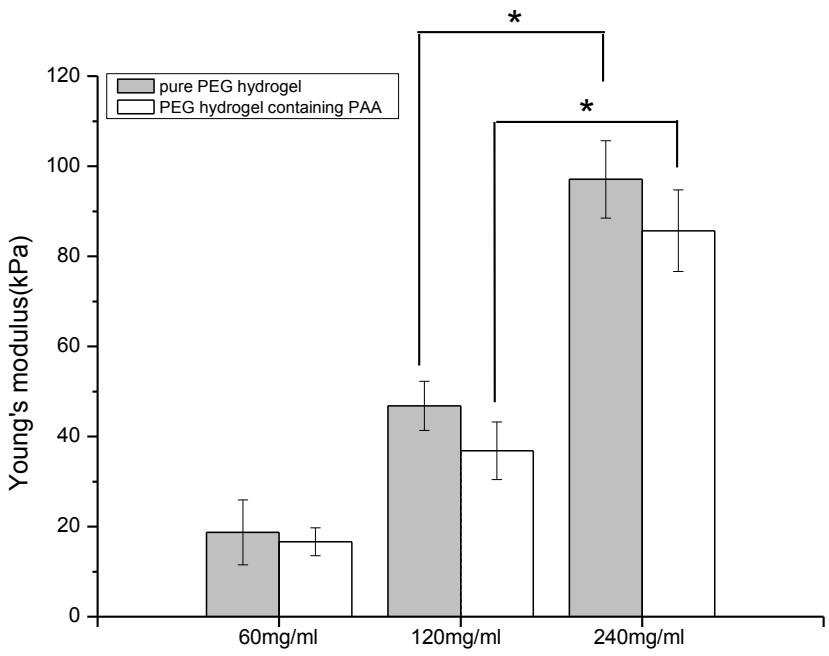

(b)

Figure 7. Young's modulus of hydrogels at different concentrations. (n=3).

3.2.4 Swelling Behavior Results

Because of the high water content and low interfacial tension to surrounding biological environment, hydrogels are usually considered to be biocompatible which are similar to the highly macromolecular based materials in the body [211]. It is very important to take the gel's properties into consideration when it is applied into ECM replacement in tissue engineering [11]. Except the mechanical property, swelling property is also important to evaluate the scaffold's biocompatibility. Samples were molded as previously described and a 72h study was performed to determine percent

swelling of the hydrogels using eqn (1). The results are shown in Figure 8. The swelling ratio of both G1 and G2 hydrogels increased gradually as time grows. Adding crosslinker into hydrogels decreased the swelling ratio slightly as the crosslinking density changes. When the concentration of PAA crosslinker increased, the swelling ratio decreased slightly. This is because as the crosslinking density of hydrogel increased, the aperture size of the polymer network is minimized, thus hydrogels with a lower crosslinking density has a better capacity of water absorbance than hydrogels with higher crosslinking density [99,211].

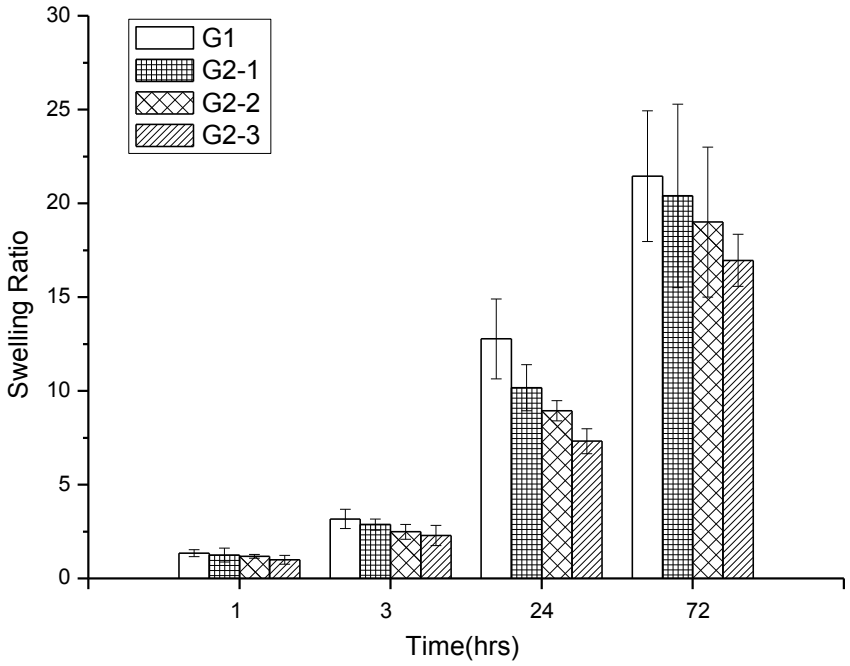

Figure 8. Swelling ratio of hydrogels at different PAA concentrations. (G1 was control group only contains PEG, G2-1, G2-2, G2-3 were experimental groups with PEG: PAA=100:5,100:20,100:50 respectively.) (n=3).

3.2.5 Analysis of Vitro Enzymatic Degradation

PAAs are, normally, biodegradable, with a degradation rate depending on their specific structure [212] and, what is most relevant for biomedical applications, most of them are almost nontoxic, despite their polycationic nature. agmatine used in this study is to provide a functional group which is part of the sequence in proteins [213]. Therefore, in this study, proteinase K was used to analysis the biodegradable property of the hydrogels. Two kinds of concentrations were chose to perform the degradation tests.

0.05mg/ml and 0.2mg/ml proteinase K solution in PBS (pH=7.4) were prepared. The tests were carried out in a 37°C water bath with constant shaking. All these conditions were designed to mimic the physiological environment in human body. The amount of PAA in G2 hydrogels is controlled by varying the mass ratios to PEG. Two ratios were used in the experiment, one is PEG: PAA=100:5, another is PEG: PAA=100:50. The degradation profiles of hydrogels are illustrated in Figure 9 by plotting the remaining wet weight (%) vs. time. Hydrogels with low concentration of PAA showed no significant weight change both in 0.05mg/ml and 0.2mg/ml solution. However, when PAA occupied 33.3% of the whole mass, the gels displayed an obvious weight loss after incubating in proteinase K solution for 10 days. Only 60% of the weight remained after the degradation by 0.2mg/ml Proteinase K, and 30% weight lost in a 0.05mg/ml Proteinase K solution over a period of 10 days.

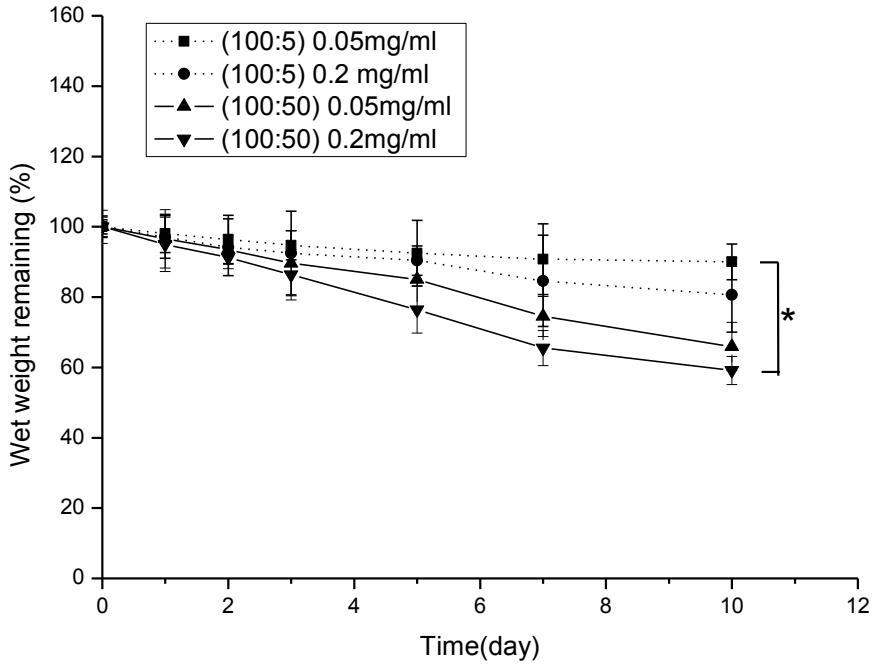

Figure 9. *In vitro* enzymatic degradation profiles of hydrogels with different enzyme concentrations (0.05mg/ml and 0.2mg/ml) and different PAA monomer mass ratios (PEG: PAA = 100: 5 and 100: 50).

3.2.6 Cell Viability

Mouse bone marrow stromal cell lines (BMSCs) were seeded on to the hydrogels. MTT assay was used to evaluate the cell viability for 24h and 7 days. Viability of cells seeded on tissue culture plates (TCPS) was normalized to 100%. In order to eliminate errors come from the gel themselves, hydrogels without cells were also conducted. As shown in Figure 10 and Figure 11, hydrogels with PAA crosslinker had higher cell viability than pure PEG hydrogels after 24h and 7 days' culture. Because the guanidine group

from agmatine combined with the amido group from MBA significantly promotes cell attachment. After one week's culture, cell viability in the hydrogels containing PAA was much higher than cells seeded on pure PEG hydrogels. Hydrogels containing PAA had almost the same cell viability as cell growth on TCPS (Figure 11).

Live/Dead staining was further used to evaluate cell viability (Figure 12-17). BMSCs were seeded on the pure PEG hydrogels (G1) and PEG hydrogels with PAA crosslinker (G2) to evaluate the cell proliferation and compared the cell attachment. After 24h's culture, most cells attached to the gels. Almost 100% of BMSCs on the hydrogel G2 were alive. After 3 days' culture, some dead cells were found but most of them were alive. The number of BMSCs increased significantly in the hydrogel G2, they began to connect with each other. However, cells did not grow well on the hydrogel G1. After one week's culture, this phenomenon is more obvious. Cells grew on the hydrogel G2 started to form a tissue, a spreading out morphology was observed. But for hydrogels G1, cells began to withered and no more cells grew due to the poor adhesion of pure PEG hydrogel. The results suggested that adding PAA crosslinker can improve the cell attachment for the hydrogels.

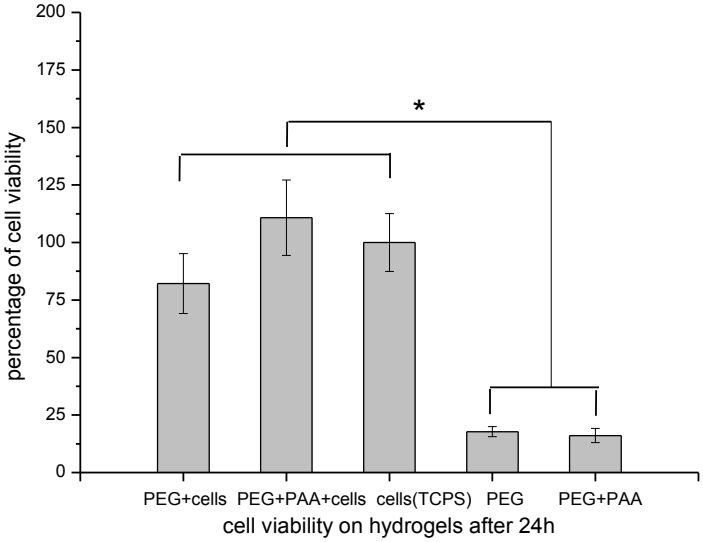

Figure 10. Cell viability on hydrogels after 24h culture based on MTT assay (absorbance is normalized to 1 for the TCPS control sample; PEG and PEG+PAA are hydrogels but without cells for MTT assay); (n=3).

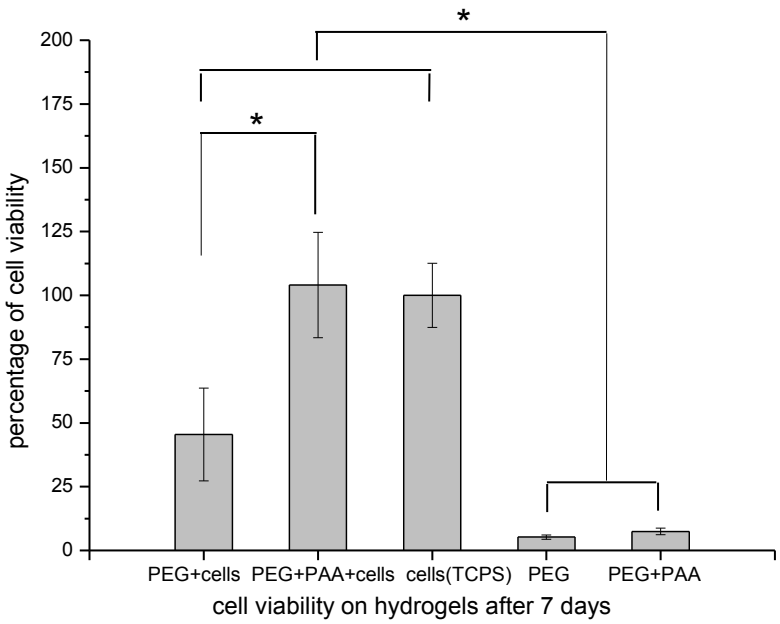

(b)

Figure 11. Cell viability on hydrogels after 7 days culture based on MTT assay (absorbance is normalized to 1 for the TCPS control sample; PEG and PEG+PAA are hydrogels but without cells for MTT assay); (n=3).

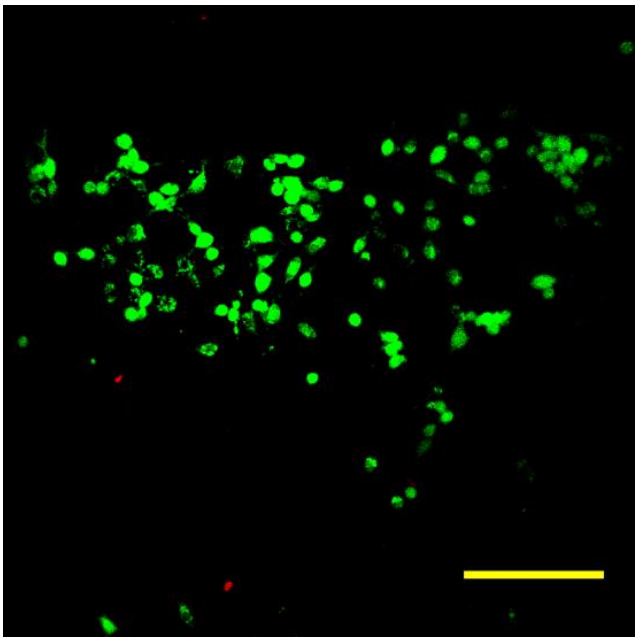

Figure 12. Live/Dead assay of BMSCs cultured on pure PEG hydrogels (G1) after 24 hours, green for live cells and red for dead cells (all scale bars are 200 μm).

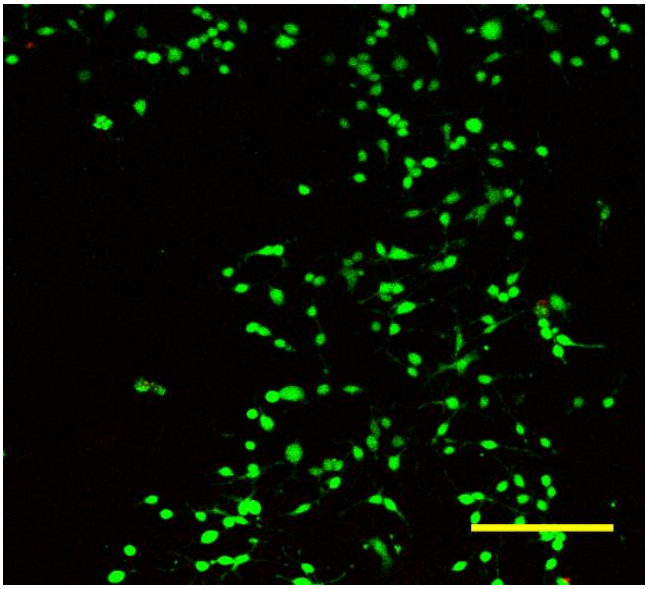

Figure 13. Live/Dead assay of BMSCs cultured on pure PEG hydrogels (G1) after 3 days, green for live cells and red for dead cells (all scale bars are 200 μm).

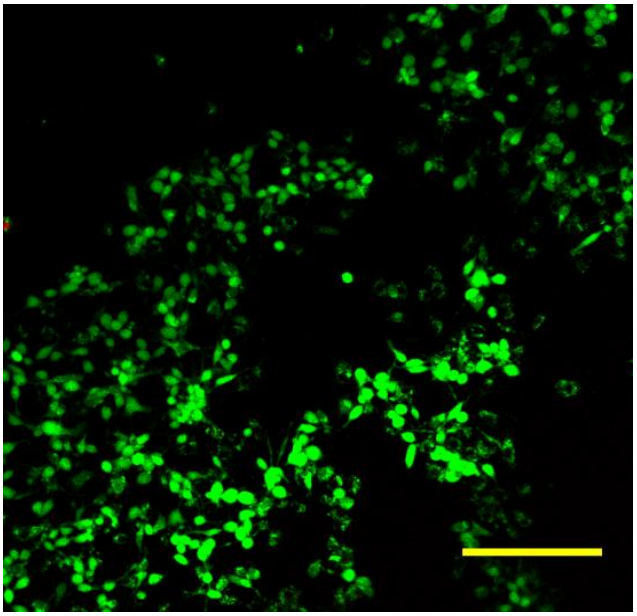

Figure 14. Live/Dead assay of BMSCs cultured on pure PEG hydrogels (G1) after 7 days, green for live cells and red for dead cells (all scale bars are 200 μm).

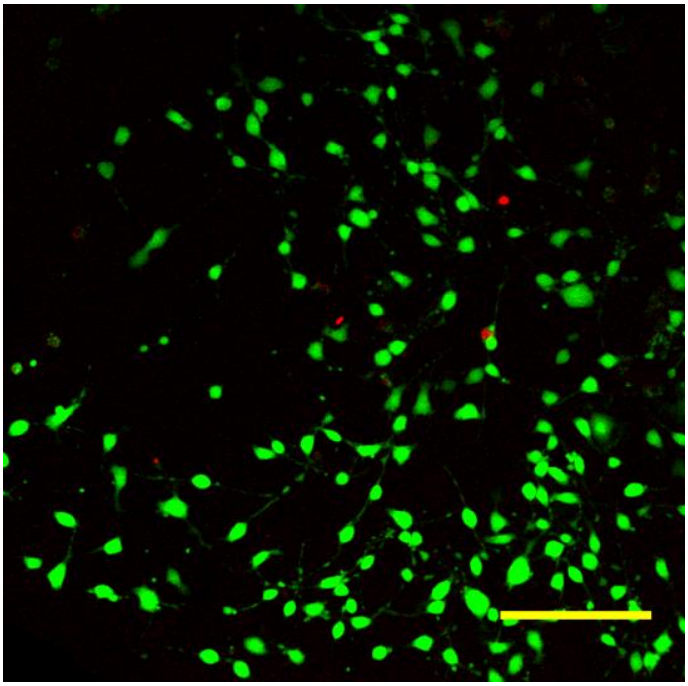

Figure 15. Live/Dead assay of BMSCs cultured on PEG hydrogels containing PAA (G2); green for live cells and red for dead cells (all scale bars are 200 μm).

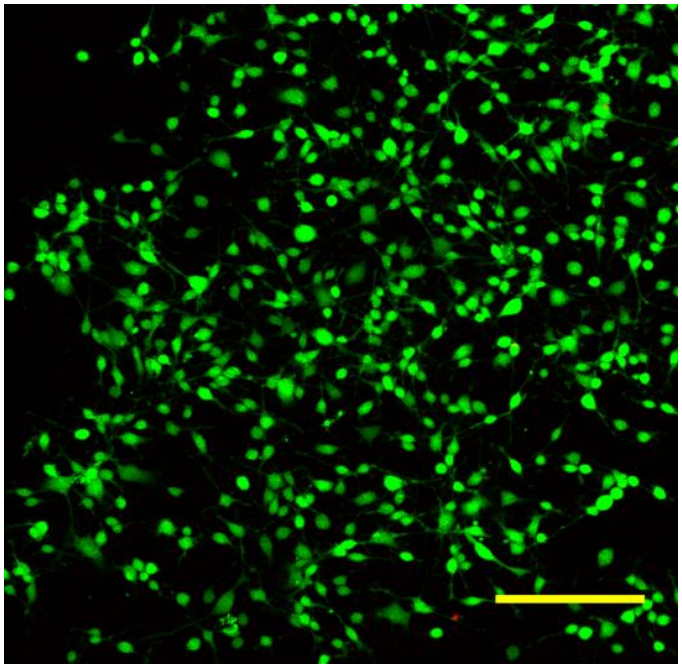

Figure 16. Live/Dead assay of BMSCs cultured on PEG hydrogels containing PAA (G2); green for live cells and red for dead cells (all scale bars are 200 μm).

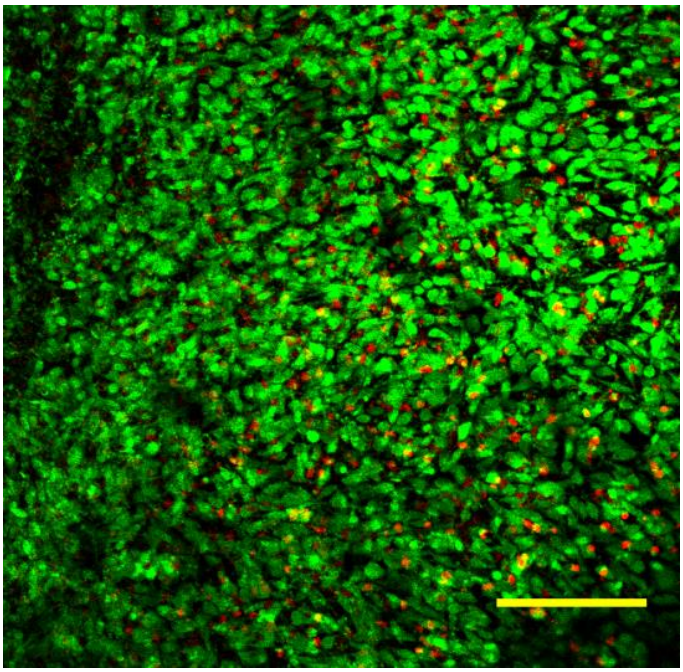

Figure 17. Live/Dead assay of BMSCs cultured on PEG hydrogels containing PAA (G2); green for live cells and red for dead cells (all scale bars are 200 μm).

3.2.7 Cell Morphology on Hydrogels

Morphology of BMSCs seeded on the hydrogels was also investigated by confocal laser scanning microscope. BMSCs were seeded on hydrogels with different mass ratios of PAA crosslinkers. We hope to see different stiffness's effects on the cell attachment. As shown in Figure 18-21, all the cells on the hydrogels were observed to be spreading and migration extensively. However, the distribution of cytoskeleton BMSCs on G2-2 seemed to have a better spread out morphology than that on G2-2 which is harder than G2-1. After one week's observation, the results indicated that cells can adhere to the hydrogels favourably. In this study, the PAA crosslinker incorporated

PEG hydrogel improve the cell attachment significantly. The effects of hydrogel stiffness on cell state likely have important implications for development, differentiation, disease, and regeneration, but still need further investigation [214].

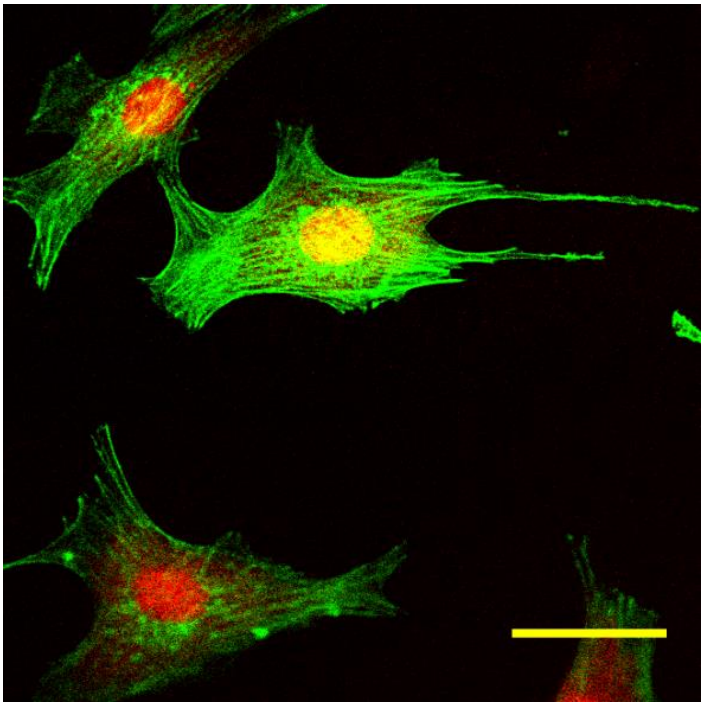

Figure 18. Morphology of BMSCs on hydrogels G2-1 for 24h.(G2-1 is PEG:PAA=100:5, scale bar is 50μm).

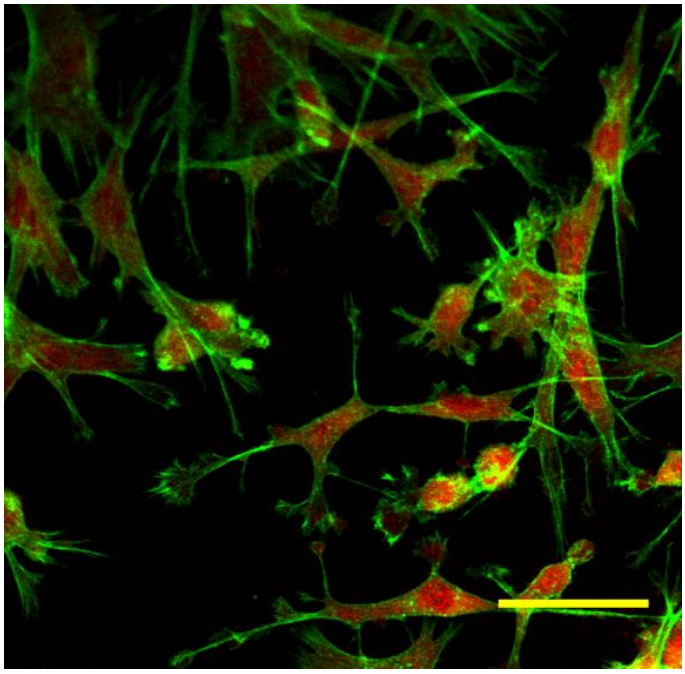

Figure 19. Morphology of BMSCs on hydrogels G2-1 for 7days.(G2-1 is PEG:PAA=100:5, scale bar is 50μm).

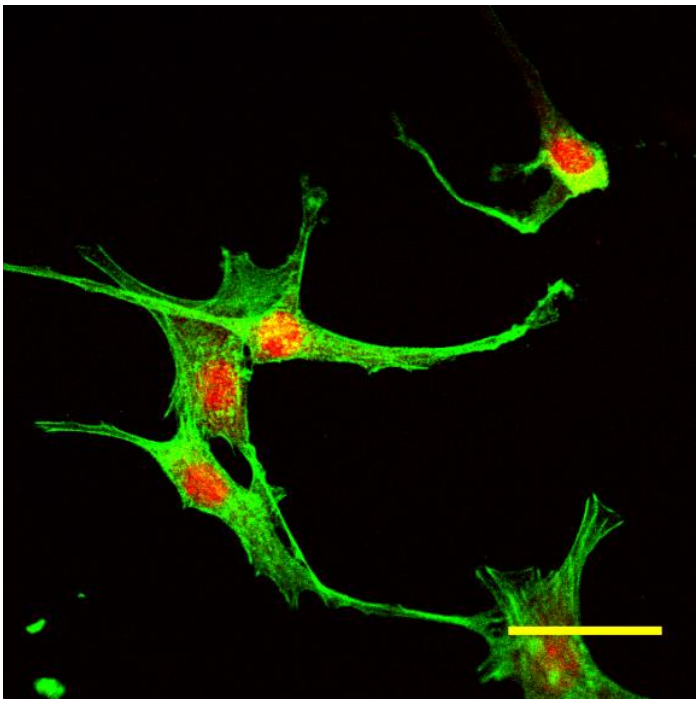

Figure 20. Morphology of BMSCs on hydrogels G2-2 for 24 hours.(G2-2 is PEG:PAA=100:20, scale bar is 50μm).

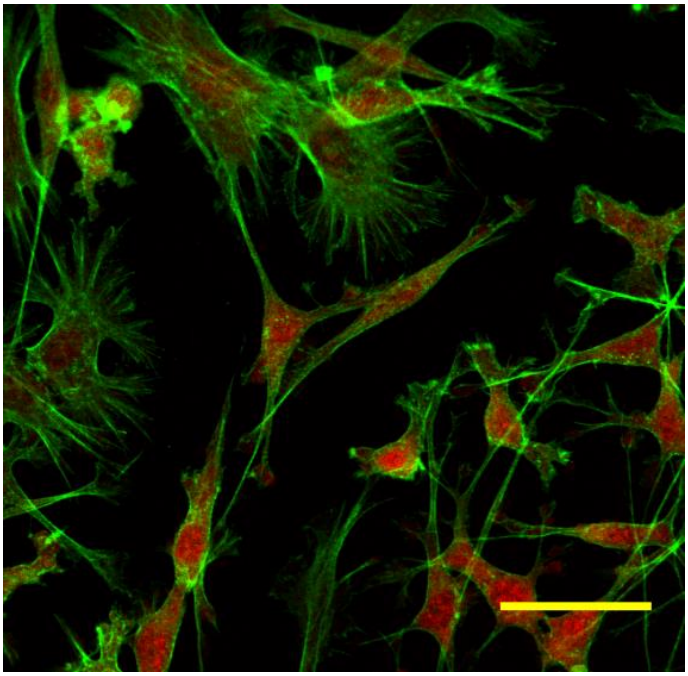

Figure 21. Morphology of BMSCs on hydrogels G2-1 for 7days.(G2-2 is PEG:PAA=100:20, scale bar is 50μm).

3.2.8 Fabrication and Characterization of Thermo-sensitive Hydrogels

Copolymerization of NIPAM with different types of monomers results in hydrogels with more versatile properties, such as faster rates of shrinking when heated through the LCST[88], and sensitivity to additional stimuli. In our experiment, NIPAM and PAA were fabricated via radical polymerization due to the vinyl groups from the PAA crosslinker. As shown in Figure 22, gel was transparent and soft, more like liquid in room temperature. When it was heated to 37°C, gel became white and solid, thus can

perform as a filling material for depressed defects.

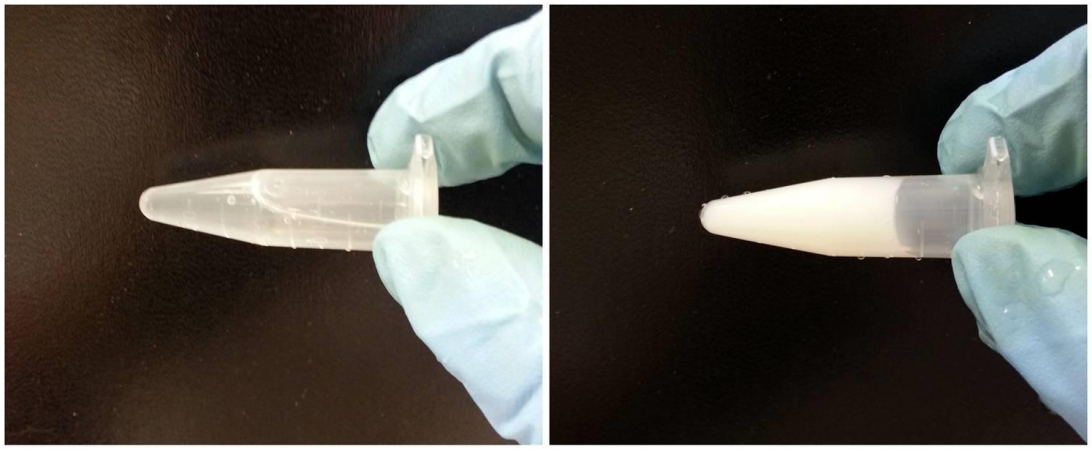

Figure 22. Thermo-sensitive behavior of NIPAM hydrogel.

3.2.9 ASCs Culture and Viability Tests

ASCs were cultured and expanded in the control medium. Cells from P3 were investigated using light microscopy in fluorescent. ASCs were observed to display a relatively homogenous population that exhibited a spindle-shaped phenotype (Fig.23A). For further biomedical applications, it is important to ensure the biocompatibility and the cytocompatibility of the hydrogel materials. The cellular viability of the cultured ADSCs under different conditions was assessed through a Live/Dead Viability/Cytotoxicity kit and is shown in Fig. 23B. The green spindle-shaped cells are live cells, whilst the red and round cells are dead. Only a minority of the cells apoptotic indicates low cytotoxicity of hydrogel. Cell viability was also assessed using CCK-8 assay after 24, 48, 72 hours cultivation. Cell viability value of the control (ASCs only)

was set as 100 percent. The viability of ASCs seeded on the hydrogel was found to beyond 90% (Fig.23 C, $P>0.05$). SEM Images directly showed that ASCs could attach to the hydrogel contained PAA crosslinker and cells can stretch out on it (Fig.23 D). It showed excellent biocompatibility and cytocompatibility of the hydrogel, which is necessary for filler.

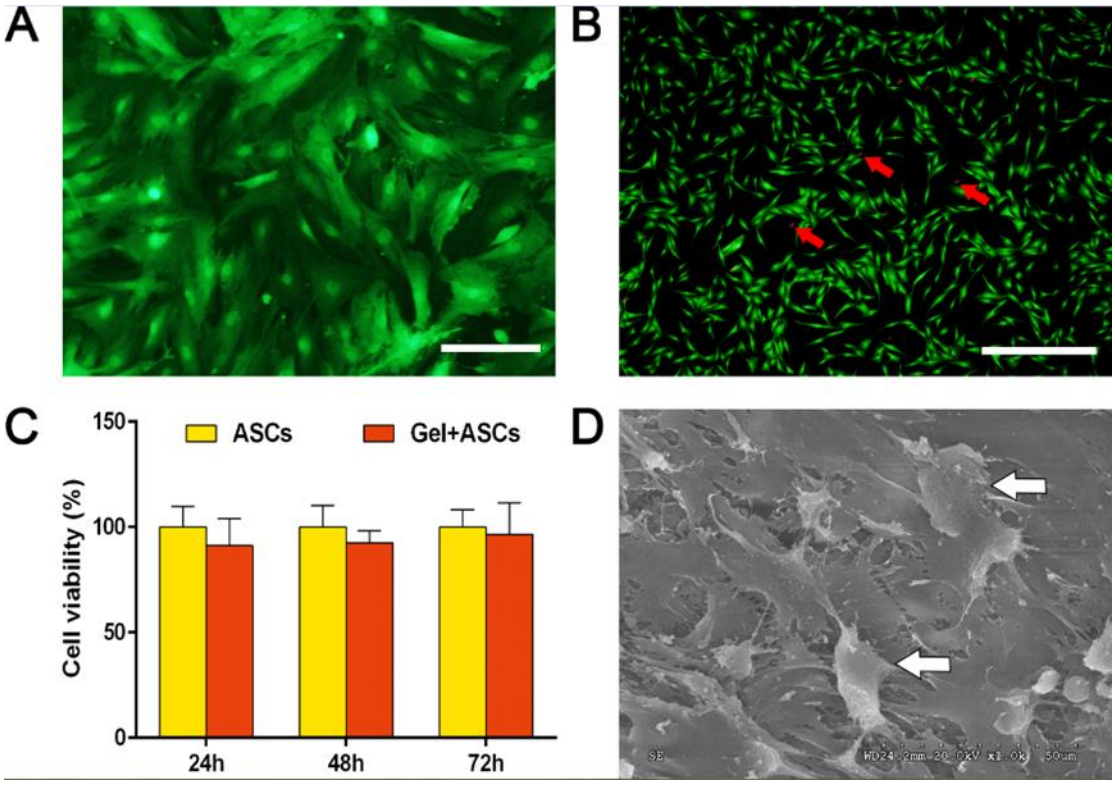

Figure 23. ASCs and hydrogel Cytotoxicity tests. ASCs imaged with Light Microscopy in fluorescent (A, Scale bars = 100 μm). Photographs of ASCs cultured on hydrogel after live/dead staining. Live cells fluoresce green, whereas dead cells with compromised membranes fluoresce red (red arrows) (B, Scale bars = 1 mm).The viability test of ASCs seeded on the hydrogel using CCK-8 (C, P>0.05). SEM images show that ASCs attach to the hydrogel (D, white arrows point ASCs).

3.2.10 Rat model

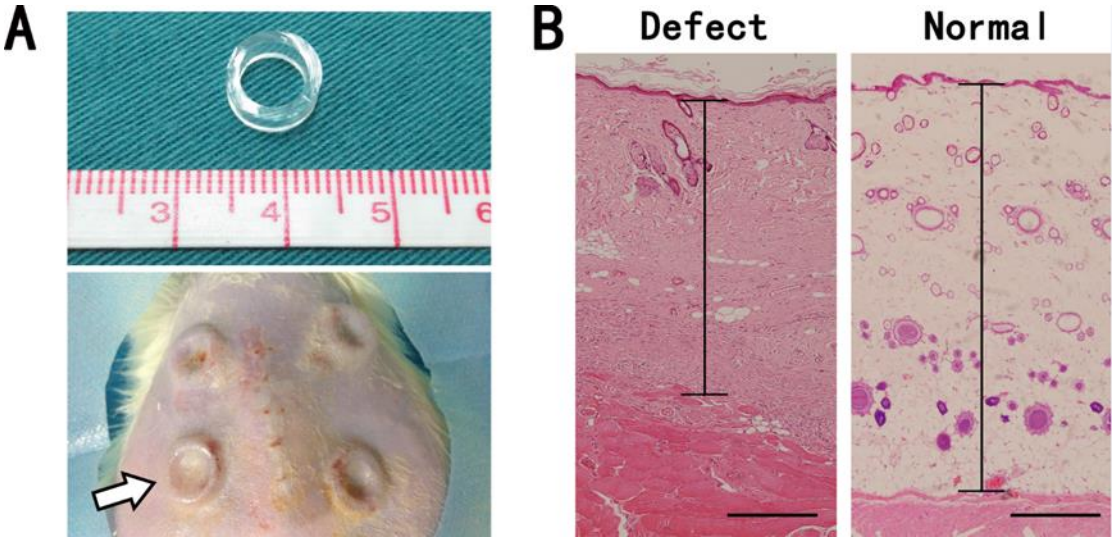

Figure 24. Rat depressed defect model. The silicone tubes used in operation and constructed depressed defect model (A, white arrow). Defect site was replaced by fibrous connective tissue. Thickness from skin to muscle layer was thinner than the normal group (B, Scale bars = 1 mm).

The silicone tubes were used in operation as seen in Fig.24A. The internal diameter of the tube is 0.65 cm and height is 0.3cm. Four depressed defect models showed on each rat dorsal skin after 8 weeks (Fig.24A below). For test the scars in defect sites had formed, we tried to pull the skin and subcutaneous muscle defect separately, it failed. Furthermore, H&E staining showed normal structure of the skin was damaged and replaced by fibrous connective tissue. Thickness from skin to muscle layer in depressed defect group was thinner than the normal group (Fig.24B). Four different fillers 1) the hydrogel-ASCs mixture, 2) the hydrogel only, 3) HA, 4) PBS were injected to the four

depressed defect sites randomly. The doses were all 0.1 ml. ASCs density was 5×10^4 cells/ml.

3.2.11 Gross and Histological Analysis

After 4 weeks，the depressed defect samples were harvested. Defects in hydrogel, hydrogel-ASCs, and HA groups recovered significantly and there were no significant differences among them. However, PBS group still remained depressed (Fig. 25A). Just like the results of the macroscopic, defect sites were filled with materials themselves in the front three groups, whereas PBS had already been absorbed at earlier stage. HA and hydrogel both had good filling effects (Fig. 25B). After 6 months，defects in hydrogel group and hydrogel-ASCs group remained recovery significantly and there were no significant differences between them. However HA group became depressed again, like PBS group. Histologically, HA was degraded mostly during 6 months in vivo, but the hydrogels had more retention (Fig. 25B). This indicated they were biodegradable. More surprisingly, with the hydrogel degraded gradually, at the same time tissue regeneration in depressed defect area was seen. Regenerated tissues consisted of multilocular immature adipocytes (Fig. 25B). No similar phenomenon occurred in the HA group. We speculate that the hydrogel played a scaffold role that recruit mesenchymal cells to repair defects by adipose regeneration.

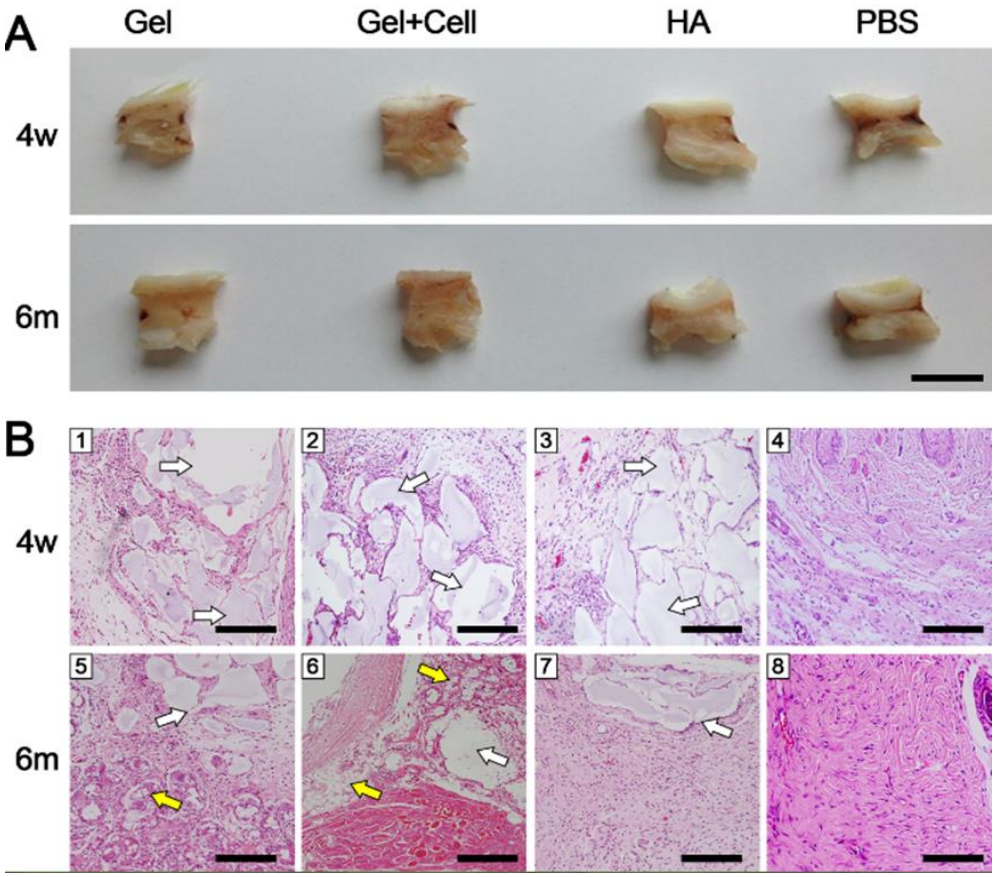

Figure 25. Gross and HE staining Analysis. 4 weeks after injection, Hydrogel, Hydrogel + cell, and HA group recovered significantly. PBS group remained depressed. After 6 months，Hydrogel and Hydrogel + cell group still recovered significantly, but HA group became depressed again, like PBS group (A, Scale bars = 1 cm). HE staining Analysis showed defect sites were filled with material itself In Hydrogel , Hydrogel + cell and HA groups (white arrow) at 4week. At 6 months，in Hydrogel and Hydrogel + cell group tissue regeneration in depressed defect area was seen. HA was a little remaining, fibrous connective tissue presented in depressed defect site again, like PBS group (B, Scale bar=300 μm)

3.2.12 ASCs Mixed with Hydrogel Differentiated into Immature Adipocytes

In the injection site, some regenerated small cells like immature adipocytes were found in Hydrogel-ASCs group (Fig. 26). Immunohistochemical staining for S100 was tested. The result showed s100 positive cells could be seen in the regenerated tissues (Fig. 26). They may be immature adipocytes. Previous studies also reported host mesenchymal cells differentiated into adipocytes via attaching to some biological materials [12,13].

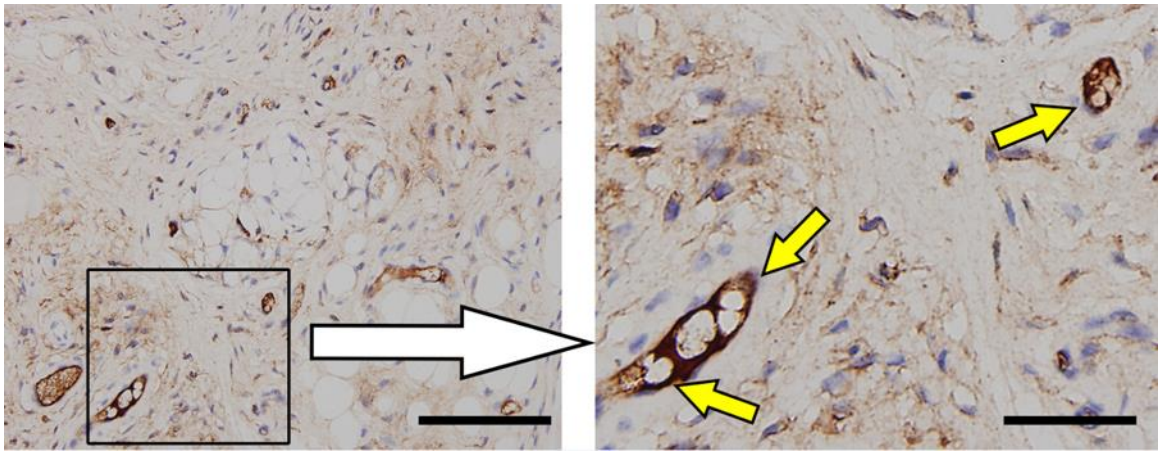

Figure 26. S100-positive cells (yellow arrows) were seen in the regenerated tissues (Scale bar=100 μm).

3.2.13 Localization of GFP-ASCs in Regenerated Tissue

To examined whether the regenerated immature adipocytes were differentiated partly from the injected ASCs of GFP expressing mice, the sample from hydrogel group and

hydrogel-ASCs group were both tested in Immunofluorescence for GFP. We found the regenerated adipose tissue were some GFP positive as shown in Fig. 27. Therefore, we can speculate that the hydrogel played scaffold for host mesenchymal stromal cells which differentiated into adipocytes. And for our study, host mesenchymal stromal cells were mainly from adipose-derived stromal cells. In the future, this hydrogel are promising in tissue engineering for repairing various other damaged tissues. Of course, it needs more experimental evidences.

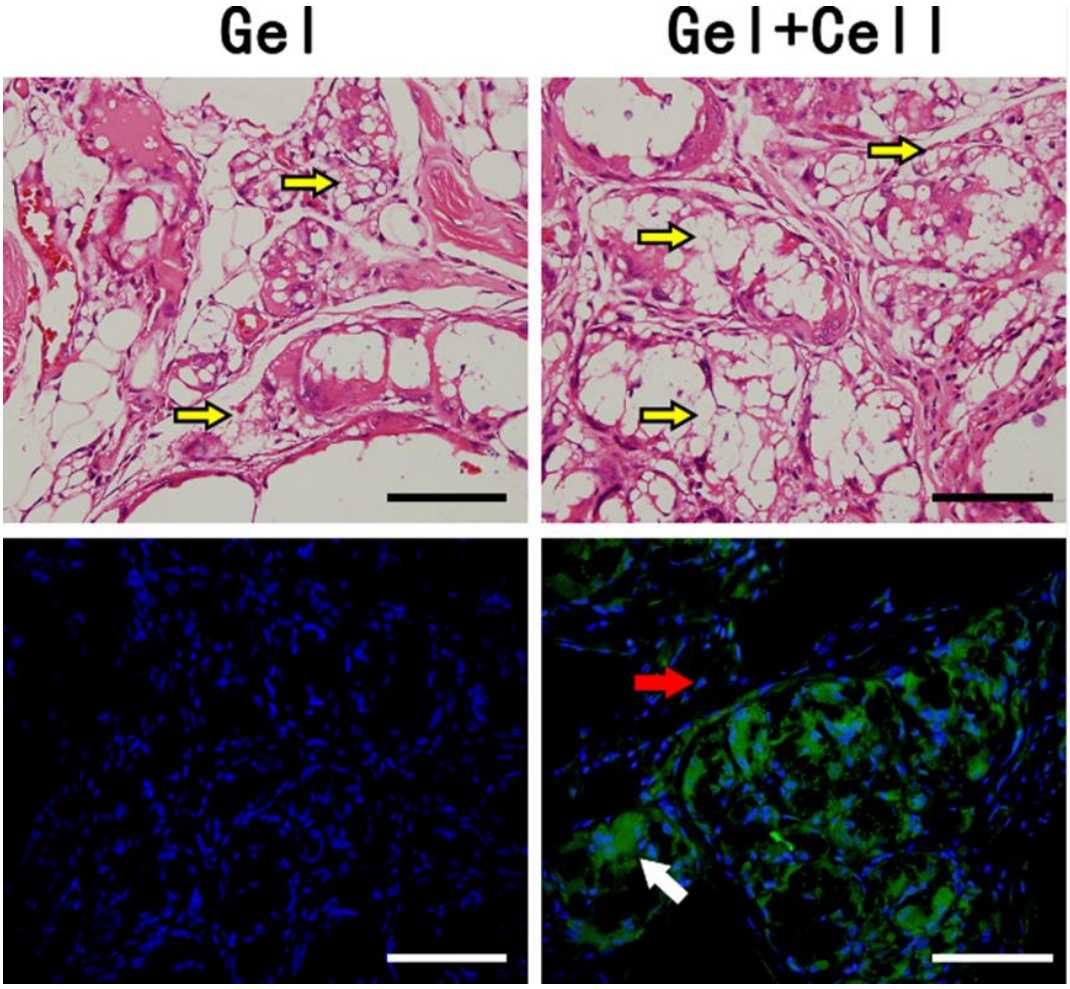

Figure 27. HE staining and Immunofluorescence for GFP in hydrogel and hydrogel-ASCs group. Adipose regeneration can be seen both in hydrogel and hydrogel-ASCs group from HE staining (yellow arrow show the regenerated adipocytes, Scale bar=100 μm). In the hydrogel group, regenerated tissues were negative in Immunofluorescence for GFP. In hydrogel-ASCs group, some GFP positive cells (green) in Immunofluorescence for GFP (Scale bar=100 μm).

3.3 Summary

Here we report the preliminary evaluation of novel biodegradable and biocompatible

agmatine-containing PAA crosslinker. Hydrogels fabricated by this crosslinker can obtain controllable stiffness and excellence cell adhesion. Results shows changing the mass ratio of crosslinker can achieve the ideal stiffness which is most close to nature ECM to support cells' growth. In vitro tests also demonstrate that PAA crosslinked hydrogels can successfully provide a 3D structure to let the cells adhere and grow. Hereby PAA containing hydrogels might be promising for implantable scaffolds for tissue regeneration.

A novel multifunctional poly (amidoamine) was synthesized as a crosslinker and applied to NIPAM to form an injectable and biocompatible hydrogel. The PAA contained hydrogel reported here is an innovative newcomer as implantable material, first employed as filler for pitting defects in rats. The data reported in this article are preliminary but clearly support that such hydrogel is promising in many important respects, such as biodegradability, biocompatibility which were confirmed by In vitro and in vivo tests. In conclusion, such cell attachable thermo sensitive hydrogel definitely warrant potential as a filling material for small pitting defects and ultimately might become a new material in plastic surgery in the clinic. Hydrogels prepared from this novel multifunctional crosslinker are promising in tissue engineering applications.

Chapter 4. Cell-compatible Photo-reversible Self-healing Hydrogel

4.1 Materials and Methods

4.1.1 Synthesis of CMA Crosslinker

4.1.1.1 Synthesis of 7-(2-Hydroxyethoxy)-4-methylcoumarin

The synthesis of coumarin methacrylate crosslinker (CMA) was conducted by a two-step reaction. As showed in Figure 28. First, a mixture of 5.0 g of 7-hydroxy-4-methylcoumarin, 5.0 g of 2-bromoethanol and 3.0 g of potassium carbonate in 50 mL of ethanol was heated under reflux for 20 h and treated with ether and water after cooling. The organic layer was washed with ether thoroughly and dried over magnesium sulfate, followed by the removal of the solvent. The residual solid was pure enough to use in the next step without further purification.

4.1.1.2 Synthesis of 7-(2-Methacryloyloxyethoxy)-4-methylcoumarin

5.0 g of methacryloyl chloride was added dropwise to a mixture of 5.0 g of triethylamine and 5.0 g of 7-(2-hydroxyethoxy)-4-methylcoumarin in 80 mL of chloroform. After being stirred for 12 h at room temperature, the reaction mixture was treated with dichloromethane and the organic layer was washed with an aqueous solution of NaCl, followed by drying over anhydrous sodium sulfate and the removal of

the solvent to give a solid. The crude product was recrystallized from ethanol to afford colorless powdery crystals.

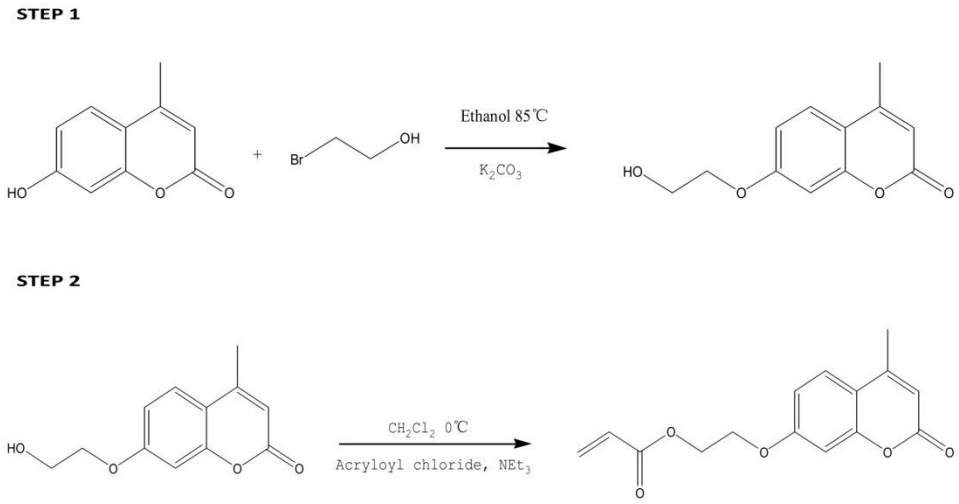

Figure 28. Schematic illustration of two-step synthesis of the CMA crosslinker

4.1.2 Synthesis of Hyper branched PAA Crosslinker

The agmatine and AEPZ contained hyper branched poly (amidoamine) (PAA) crosslinker was synthesized via Michael-addition polymerization as shown in Figure 29:

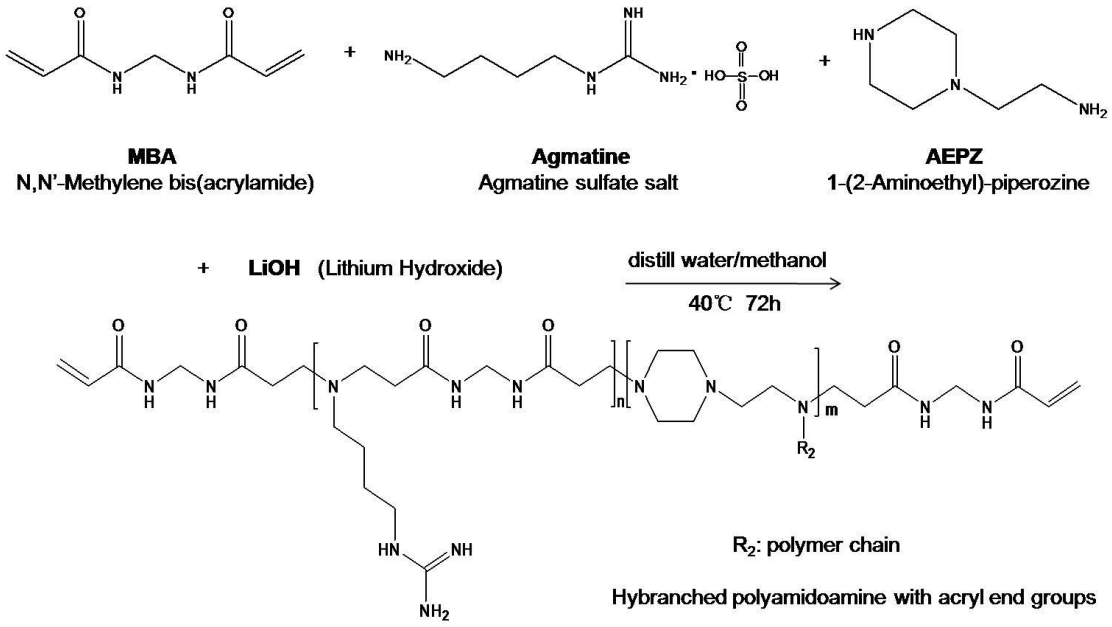

Figure 29. Schematic illustration of the preparation of hyperbrached PAA crosslinker

MBA (234mg, 1.52 mmol), Agmatine (138 mg, 0.6 mmol) and AEPZ (52mg, 0.4mmol) were dissolved in water/methanol (v/v =5/1, total in 5ml) while stirring. When the solution was clear, $LiOH \cdot H_2O$ (25.2 mg, 0.6 mmol) was added to the solution. The mixture was then gently stirred and allowed to react at 40 ˚C in the dark for 72h. After reaction, the solvent was evaporated using a rotary- evaporator. The product was finally recovered by lyophylization and stored in-20 ˚C refrigerator for future use.

4.1.3 Characterization of CMA Crosslinker and Hyper Branched PAA Crosslinker

4.1.3.1 Fourier Transforms Infrared Spectroscopy (FTIR)

FTIR spectra were recorded with a Thermo Scientific IR100 FT-IR Spectrometer. Hydrogels were freeze-dried in order to remove the residual chemicals. Then dried hydrogels were ground to powder, mixed with KBr, and compressed into pellets.

4.1.3.2 1H NMR

In order to characterize the CMA crosslinker and hyper branched PAA crosslinker, 1H NMR spectra (Figure 30 and Figure 31) was recorded on an Advance 300 MHz spectrometer. 8 mg of PAA crosslinker and CMA crosslinker powders were dissolved in 800µl of DMSO and D_2O respectively. Chemical shifts (δ) were reported in parts per million (ppm). 1H NMR (ppm): δ, 1.7 (H_2O), 2.44 (–CH_3,s, 3H), 4.28(-CH_2-C***H₂***-O-Ph,t, 2H), 4.55(-C***H₂***-CH_2-O-O-Ph,t, 2H), 6.10(C***H₂***=CH-COO-,d, H), 6.28(-C(CH_3)=CH-CO-,s, H), 6.38(CH_2=C***H***-COO-,q, H), 6.68(C***H₂***=CH-COO-,d, H), 7.14(O-C_6H_3-,d, H), 7.17(O-C_6H_3-,s, H), 7.64(O-C_6H_3-,d, H)

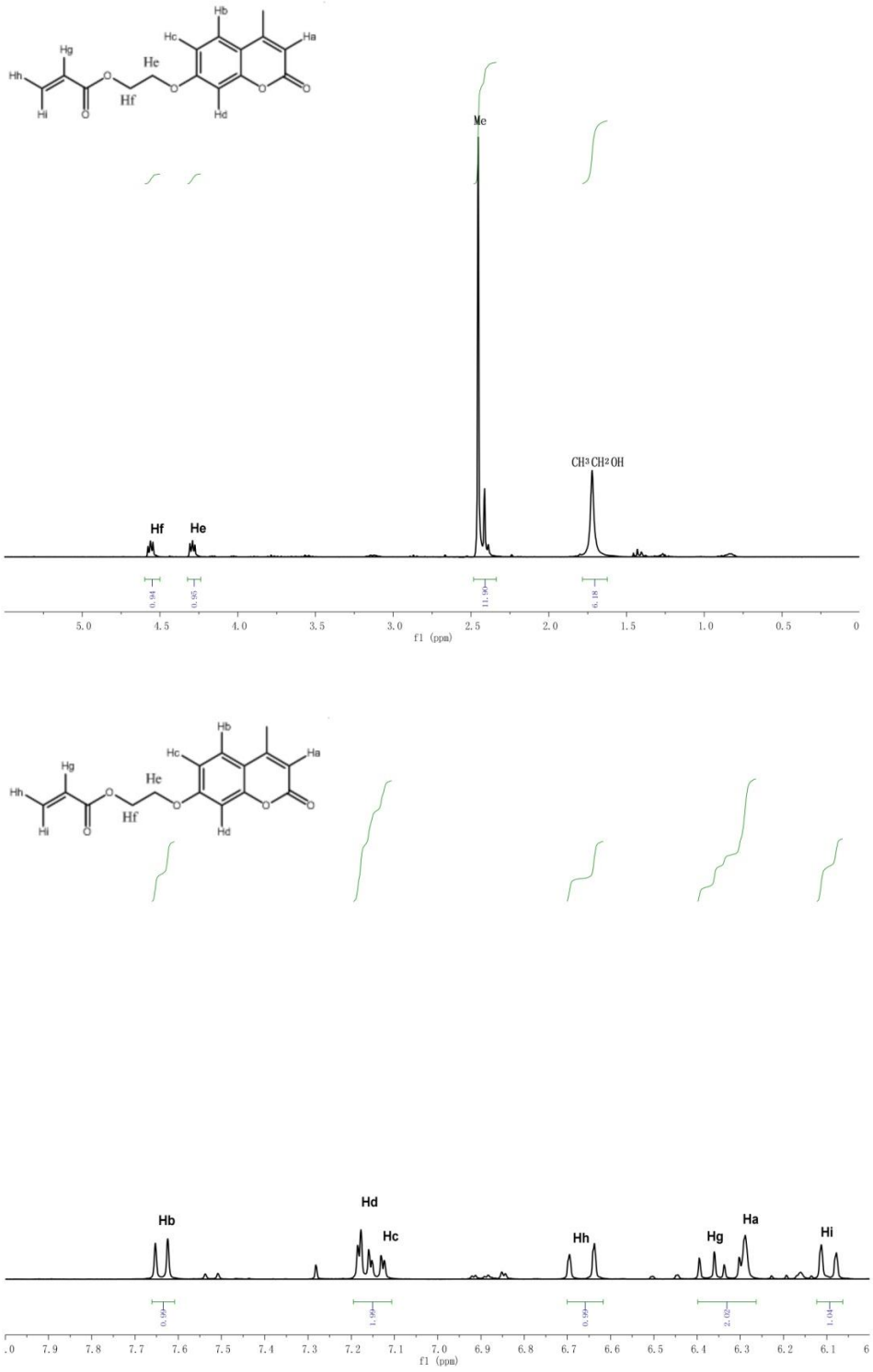

Figure 30. 1H NMR spectrum of the CMA crosslinker

1H NMR (ppm): δ, 1.5 (-N-CH_2-C***H*****$_2$**-C***H*****$_2$**-CH_2-NH-,s, 4mH),

2.0-3.0(CO-C***H*****2**-C***H*****2**-N,m, 8(m+2)H, -N_2C_4***H*****8**-C***H*****2**-C***H*****2**-N-,m, 8nH), 3.17(-N-C***H*****2**-CH_2-,s, 2mH), 4.53 and 4.62(-NH-C***H*****2**-CH-,s, 2m+2H), 5.77 (C***H*****2**=CH-,t, 2H), 6.21(CH_2=C***H***-,s, 2H), 6.225 (-C***H*****2**=CH,s, 2H).

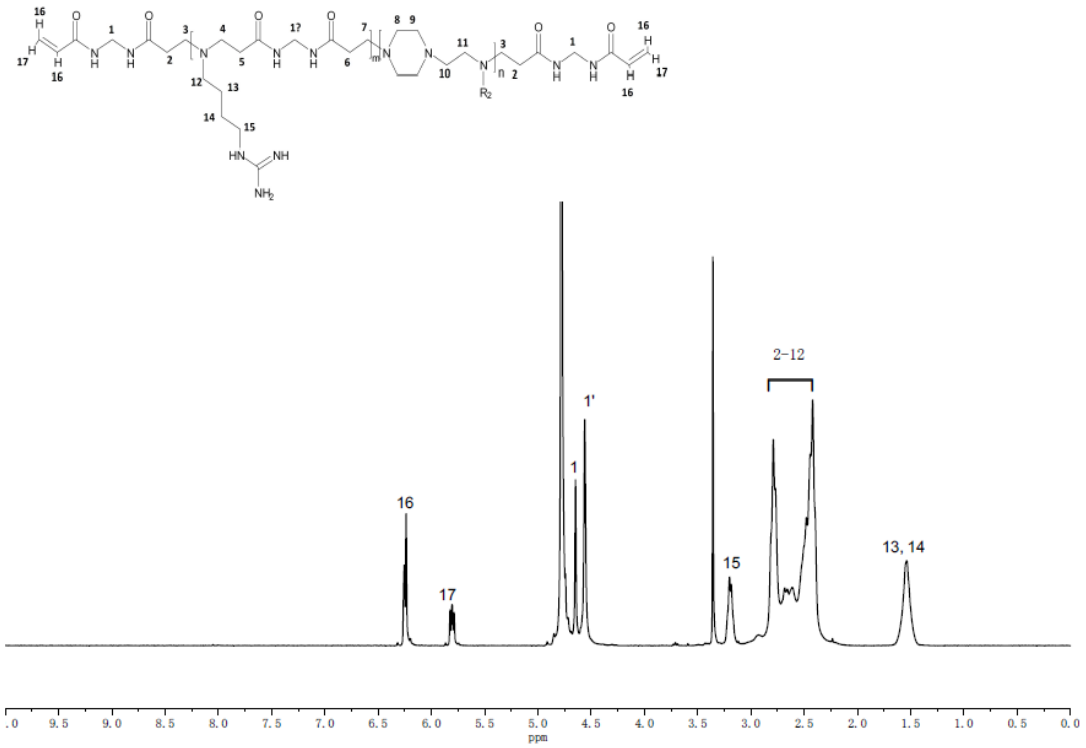

Figure 31. 1H NMR spectrum of the PAA crosslinker

4.1.4 Fabrication of Self-healing Hydrogel with CMA Crosslinker and Hyper branched PAA Crosslinker

Coumarin-containing hydrogel was prepared by copolymerization of acrylamide (6.2 mmol), 7-(2-Methacryloyloxyethoxy)-4-methylcoumarin (0.31 mmol), PAA crosslinker (0.97 mmol) using APS (0.20 mmol) and TEMED in 1.0 ml of DMSO at

65°C. The gel was purified by washing with large amounts of DMSO, followed by exposure to water over several hours, then repeated washing with water. To form the gel with conductive property, the gel precursor was added with carbon nanotubes（CNTs) at concentration of 10mg/ml, and then ultrasonic for 1h to get a homogeneous solution.

4.1.5 Evaluation of Self-healing Property of Hydrogel

4.1.5.1 Elongation Test

To evaluate the intrinsic healing behavior of hydrogels, Hydrogels contain CMA crosslinker were synthesized. Specimen of 20 mm in length, 4mm in width and 2mm in thickness was firstly cut by a razor. Samples were kept in alignment and intimate contact without pressure. After irradiation, the healed gel bars were fixed on the tensile test machine stress-strain curves were recorded as showed in Figure 32.

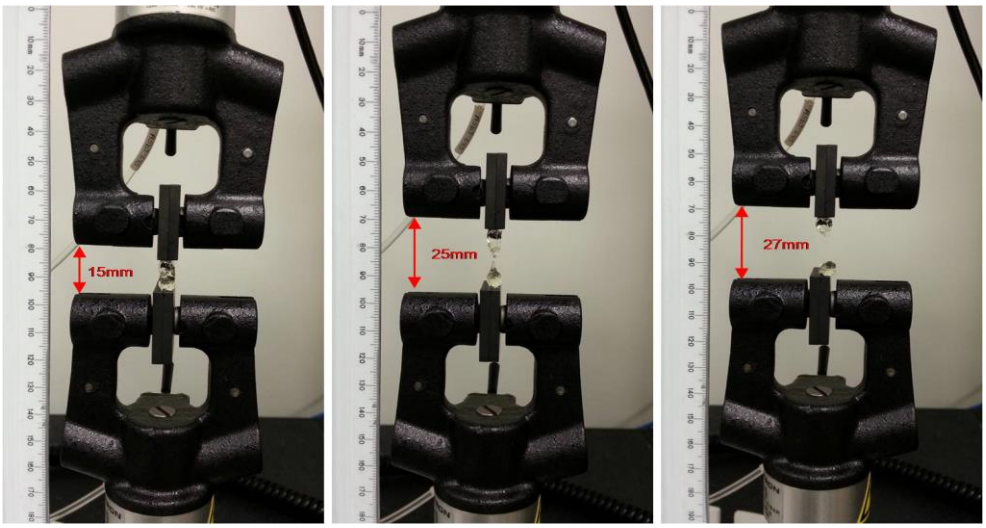

Figure 32. Images of sample test setting.

Samples were then irradiated under UV light at the wavelength of 365nm for 10min, 20min, 30min and 60min respectively. After the self-healing process, the connected bars were fixed onto the INSTRON® materials testing machine. The test speed was set at 0.1 mm per minute. The tensile stress and elongation were recorded by the INSTRON® software. All measurements were carried out at Constant temperature and humidity room. The sample size of each group is 3 (n=3).

4.1.5.2 Self-Healing Behavior Test

The hydrogels precursor were prepared first and mixed evenly. Then drop 200μl precursor onto square glass cover slips (length: 20mm). After gelation at 65°C, the slips with hydrogels on the surface were stained by FITC fluorescence dye. Then a crack was made by a blade. Fluorescence pictures before and after UV healing process (λ=365nm) were recorded by confocal laser scanning microscopy (CLSM) (Olympus FV1000,

Japan).

4.1.5.3 Photo Reversible Test

In order to verify the photo reversible property of hydrogels, UV light (λ<280nm) at another wavelength was applied to the mechanically bisected samples. Two halves which had been healed for 30min were exposed to the UV light at the wavelength of 260nm for 10min and 20min. then the tensile stress and elongation were again recorded by INSTRON®. All the parameters and methods were set the same as the former test.

4.1.6 Swelling Behavior Test

Hydrogels were prepared in a specific size in 24-well plate as described before. Then weighed and immersed in vials which containing PBS buffer (pH=7.4) at room temperature. At designed time intervals, the hydrogels were taken out from solution, and weighed after wiping off any visible surface moisture. The percentage amount of buffer absorbed can be calculated using the following formula:[201]

$$\text{Water (\%)} = (W_t - W_0)/W_0 * 100 \quad (1)$$

Where W_t is the weight of hydrogels at weighing time and W_0 is the weight of the initial weight hydrogel. In order to reduce errors, all swelling ratio results should be obtained from triplicate samples.

4.1.7 Cell Culture and Growth on Hydrogel

4.1.7.1 BMSCs Culture

The hydrogels precursor for cell culture were prepared first and mixed evenly. Then drop 100μl precursor onto glass cover slips (diameter: 10mm). After gelation under 37 ˚C, the glass cover slips were put into PBS solution for 2h, in order to remove chemical residuals. Then the glass cover slips were taken out and irradiated under UV light in a bio-safety hood for 30 minutes. Finally, the gels coated glass cover slip will be place in cell culture dishes (35 mm × 10 mm). Mouse bone marrow stromal cell lines (BMSCs from ATCC, USA) were cultured with Dulbecco's Modified Eagle's Medium (DMEM, GIBCO) supplemented with 10% fetal bovine serum (FBS, GIBCO), 1.0 x 10^5 Ul^{-1} penicillin (Sigma) and 100 mg l^{-1} streptomycin (Sigma) at 37 ˚C in 5% CO_2.

4.1.7.2 MTT Assay

The gelation was first conducted in 96 well culture plates for 5 min at 37 ˚C. Then BMSCs were seeded onto the hydrogels. The culture medium was changed every 2 days. For this assay, 100 μL of the provided MTT reagent (tetrazolium salt solution) was added directly to the wells and placed in an incubator at 37 ˚C for 4 h. The purple formazan produced by active mitochondria was solubilized by construct homogenization in 200μl of the DMSO. The absorbance of these solutions was read at 570 nm (n=3) by Molecular Devices Spectra [204].

Live/dead staining was carried out to evaluate the Cytotoxicity of hydrogels, according to a protocol from Invitrogen Inc., Canada. BMSC cultures were performed using hydrogels and stained at 24h, 3 days and 7 days. Images were taken by confocal laser scanning microscopy (CLSM) (Olympus FV1000, Japan).

4.1.8 Quantitative Real-time PCR Analysis

100 ml of mouse bone marrow stromal cells (BMSCs) in medium at a density of $2x10^6$ cells per ml was seeded onto the hydrogels for 30 minutes. Then, 2 ml medium were added to the disk. After 2 days, cell-encapsulating hydrogels were transferred to FBS-supplemented DMEM containing a combination of osteogenic chemical supplements: 50 mg/ml L-ascorbic acid 1-phosphate (Sigma), 10 mM b-glycerophosphate (Sigma) and 100 nM dexamethasone (Sigma). Gels with cells were incubated for various time points. The osteogenic medium was changed for every 2 days. At predetermined time intervals, the media were aspirated with the unattached cells and the wells were washed with DPBS. Then, cells on hydrogels were treated with liquid nitrogen and smashed. In order to validate the gene expression of osteogenic differentiation in all samples, total RNA isolation and cDNA synthesis were conducted using TRIzol and Oligo dT (Thermo Scientific, USA), according to the standard procedures. Then quantitative real-time PCR (qPCR) was performed by SYBER Green assays (Applied Biosystems, USA). Amplification conditions were as follows: hold at

95 ˚C for 10 minutes, followed by 40 cycles at 15 seconds at 95 ˚C and 1 minute in 60 ˚C. Thermal cycling and fluorescence detection were done using the StepOnePlus™ real-time PCR System (Applied Biosystems, USA). The mRNA expression levels were determined relative to the GAPDH by the ΔCt method.

4.2 Results and Discussion

4.2.1 Synthesis and Characterization of Hyperbranched PAA Crosslinker and CMA Crosslinker

As shown in Figure 33, the sharp peaks appeared around 1736.15cm^{-1} was attributed to the ester group and the small peak around 1508.18cm^{-1} indicated the double bond at the end of molecule. Peaks located at 1163.06cm^{-1} was attributed to the C-O-C group, the results show successful conjugation of CMA crosslinker.

Figure 34 showed the spectra of hyper branched crosslinker, the sharp peaks appeared around 1650.66cm^{-1} was attributed to the C=O stretching frequency from MBA. While peaks located at 1533.51cm^{-1} was attributed to the NH_2 group from agmatine and AEPZ, the results show successful conjugation of hyper branched PAA crosslinker.

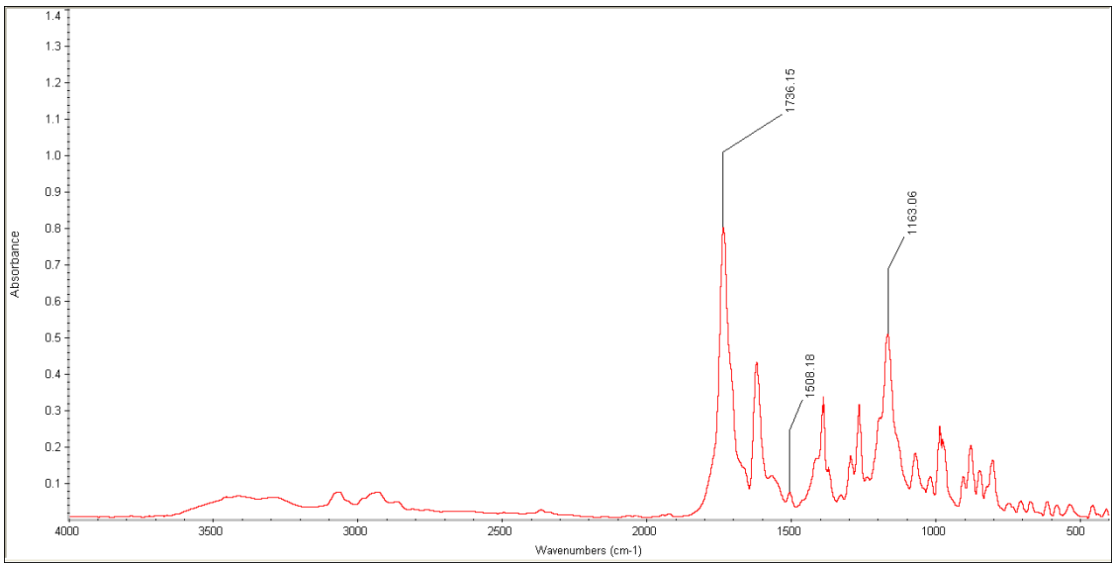

Figure 33. FTIR spectra of CMA crosslinker.

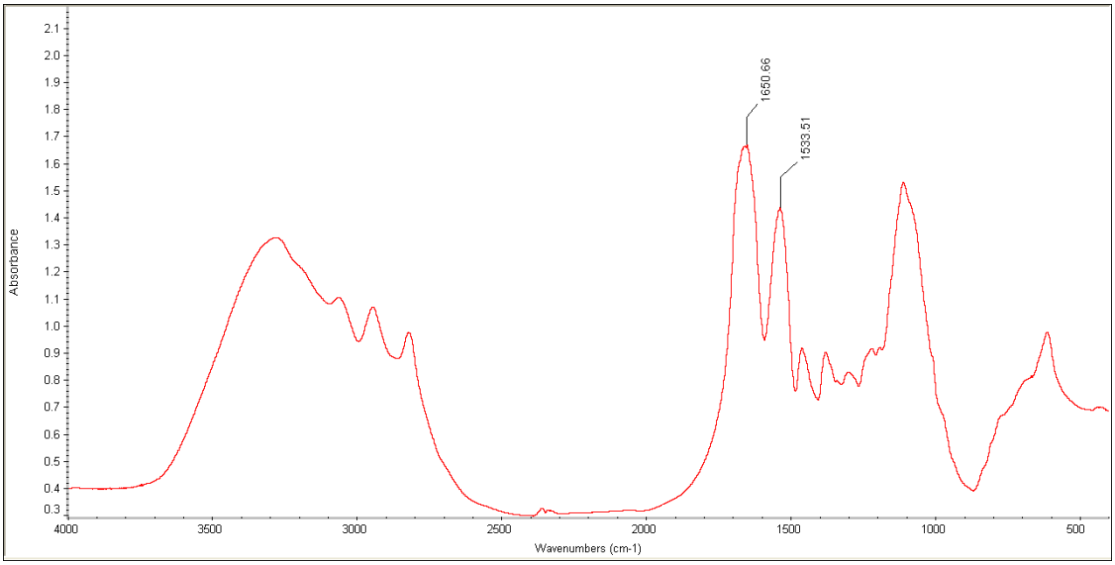

Figure 34. FTIR spectra of hyper branched crosslinker.

4.2.2 Synthesis of Self-healing Hydrogel

The synthesis of coumarin methacrylate crosslinker (CMA) was conducted by a two-step reaction.[64,215] (>20% yield over two steps; for details see the Supporting Information). In order to introduce an agmatine group into the N, N'-Methylene bis

(acrylamide), the poly (amidoamine) (PAA) crosslinker was synthesized via Michael-addition. FTIR and NMR were conducted to verify the successful synthesis of both crosslinkers. Chemical structure of gels and mechanism of self-healing process were showed in Figure 36 and Figure 37. According to the structural requirements for imparting photochemical reactivity to polyacrylamide, coumarin methacrylate should play dual-role as side groups and crosslinkers. It means that double bond groups have to be present on the main chains of the polymer, connect with PAA crosslinker and acrylamide. As a result, desired multi-functional homopolymer of polyacrylamide that contains coumarin groups and agmatine groups were synthesized. Figure 35 shows the gel formation.

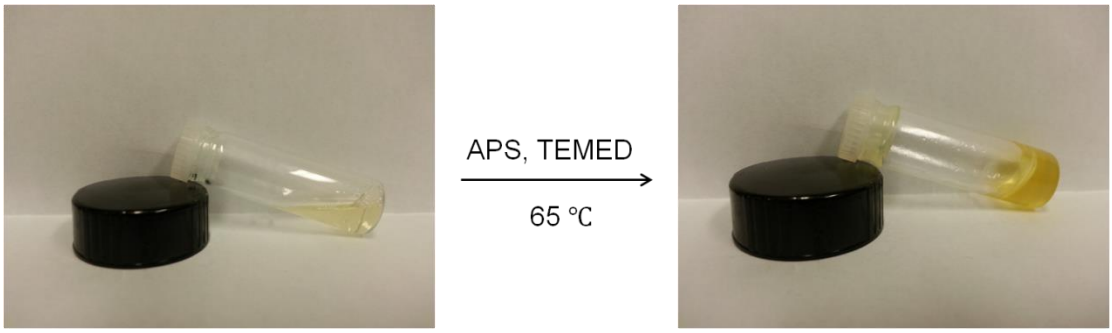

Figure 35. Self-healing hydrogel formation.

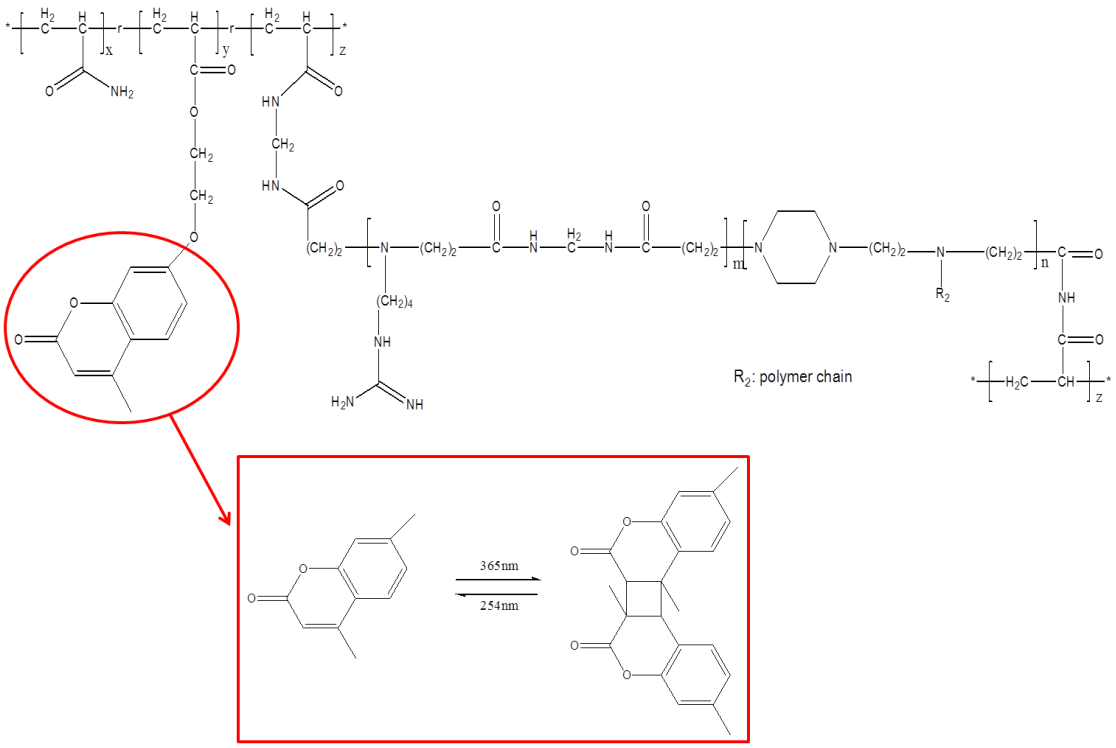

Figure 36. Chemical structure of the polyacrylamide gels and the photodimerization and photocleavage of coumarin side groups.

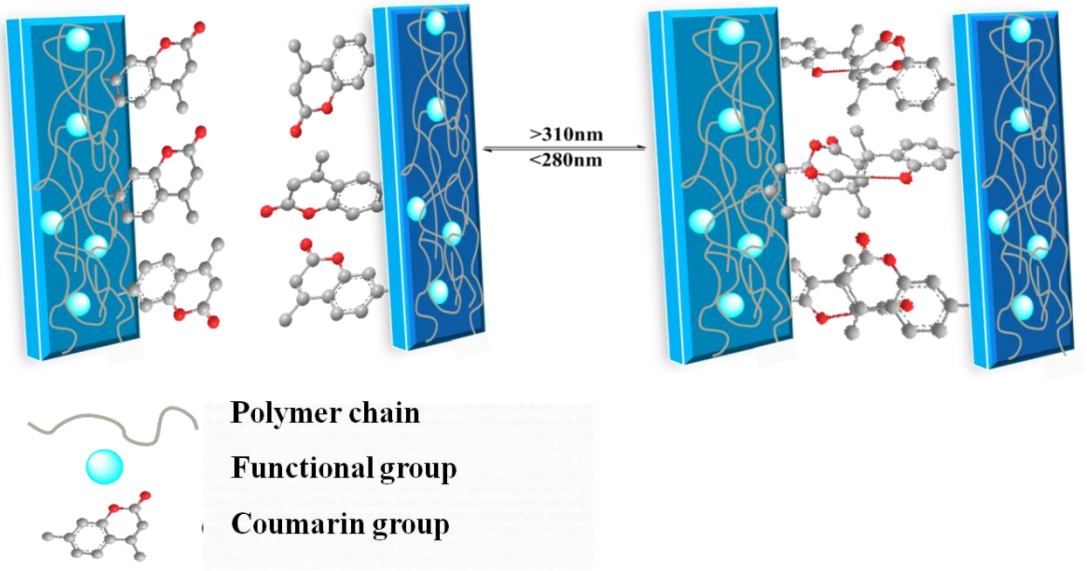

Figure 37. Schematic illustration of the self-healing process.

4.2.3 Self-healing Property in Terms of Tension Test

Movies were recorded to test self-healing properties of CMA contained gels. Generally, for damaged gels contained coumarin groups shows significant self-healing feature upon the irradiation of 365nm UV light (see movie 1).

Movie 1. Video for hydrogel with coumarin groups

However for control group, gels without coumarin groups, the two halves cannot bind each other as supposed (see movie 2).

Movie 2. Video for hydrogel without coumarin group

With the treatment of UV light (365nm), the results reflect contribution of π-π* transitions of the conjugated benzene nucleus and pyrone nucleus in 4-methylcoumarin chromophores [216]. Because the double bonds of 4-methylcoumarin gradually dimerize to form cyclobutane rings under 365 nm UV illumination, the conjugation between double bonds and phenyl groups has to be destructed (Figure 36). As a result, the two halves can connect together.

Stress−strain tests were conducted to investigate the mechanical properties of CMA contained gels. Samples were first cut into half, and then were mechanically bisected and then the two halves were brought into contact (Figure 38). Samples under irradiated

with 365 nm UV light for 10 min, 20min, 30min and 60min respectively.

Tensile tests were conducted to quantify the ability of the damaged gels to restore strength. For instance, the tensile stress of gel which was irradiated for 60 minutes (200.26kPa) is nearly five times that of the one which was only irradiated for 10 minutes (44.93kPa). Moreover, increasing the irradiation time gives rise to a remarkable improvement in the stress intensity as well as in the elongation to break.

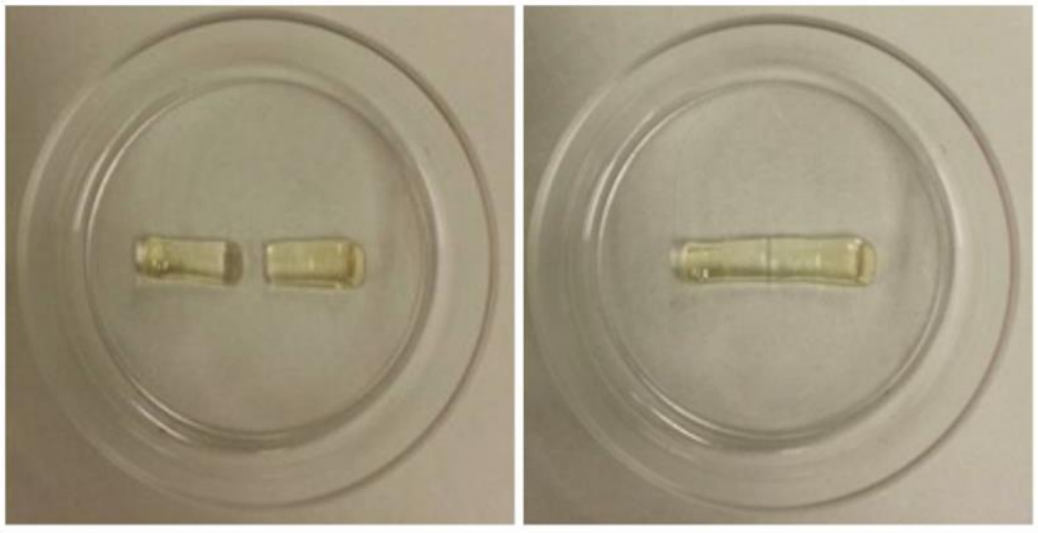

Figure 38. Images of sample preparation.

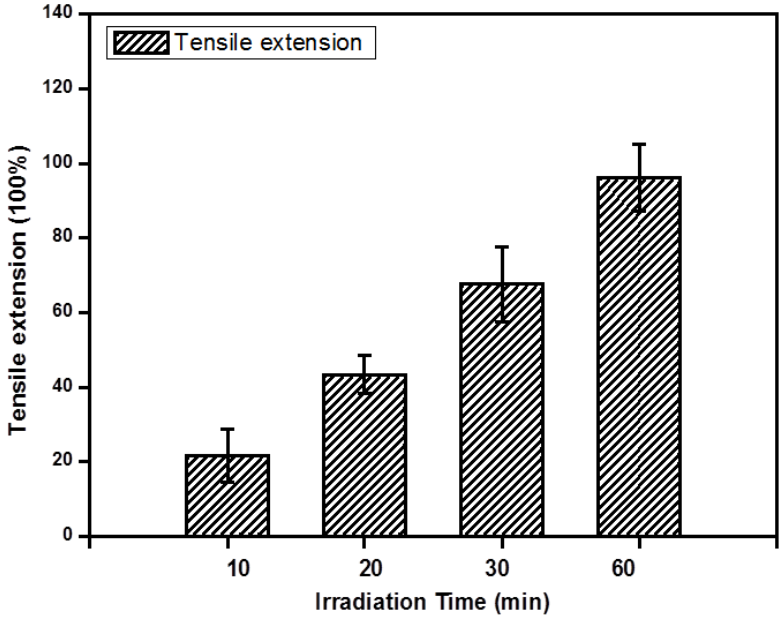

Figure 39. Tensile elongations after different healing time.

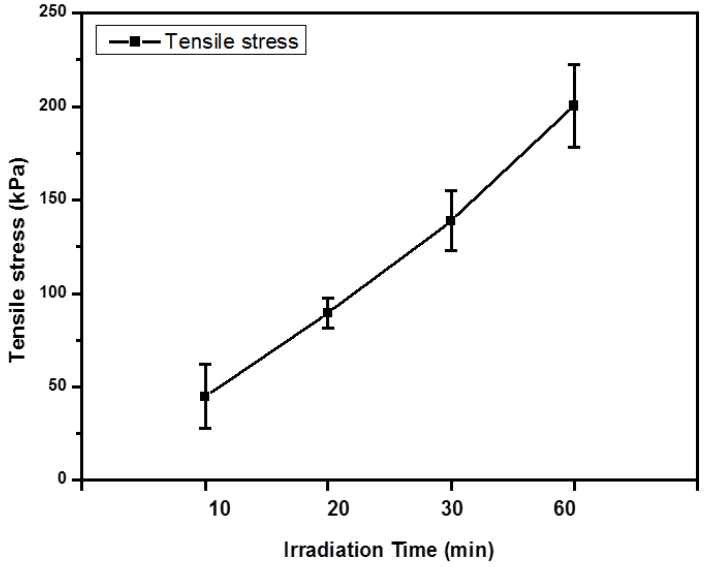

Figure 40. Tensile stresses after different healing time.

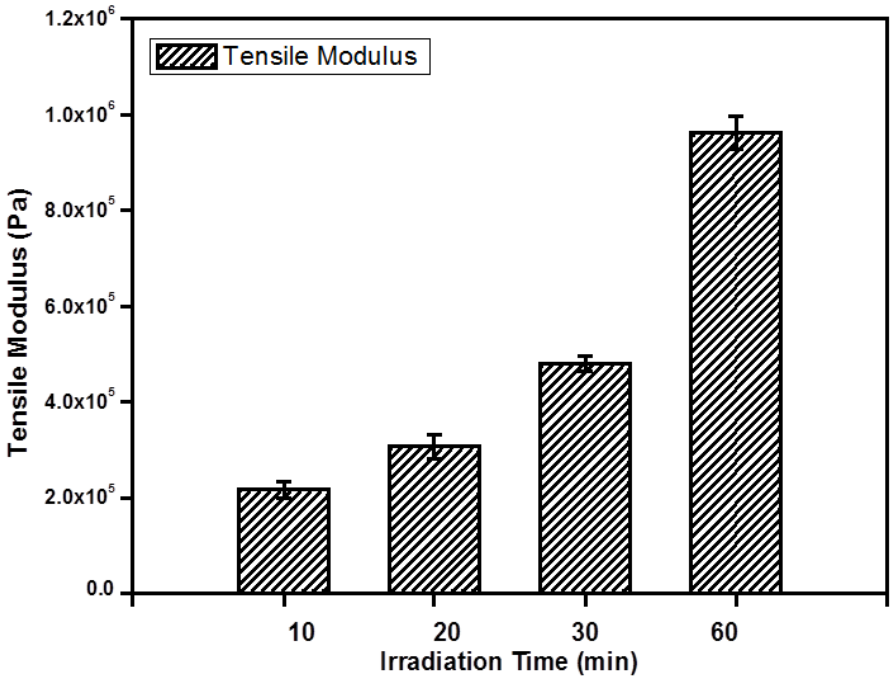

Figure 41. Tensile modulus values versus different UV healing time (365nm) for gels. (n=3)

When irradiation time for cut samples increases from 10min to 60min, stress intensity increases from 44.94kPa to 200.26kPa(Figure 40), indicating that the introduction of coumarin groups improve the self-healing performance of gels. Gels which were irradiated for 10min, 20min, 30min, 60min, show the elongation at break over 21.6%, 43.4%, 67.7% and 96.2% respectively (Figure 39). The results reveal that the CMA contained gels have good self-healing property.

In addition, the tensile modulus of gels was also investigated. Figure 41 shows the

tensile modulus as a function of healing time for healed samples of gels. It is obvious that the restorability relies greatly on the irradiation time, and gel which was irradiated for 1h showed high healing efficiency to give tensile modulus of 2.08×10^5 Pa.

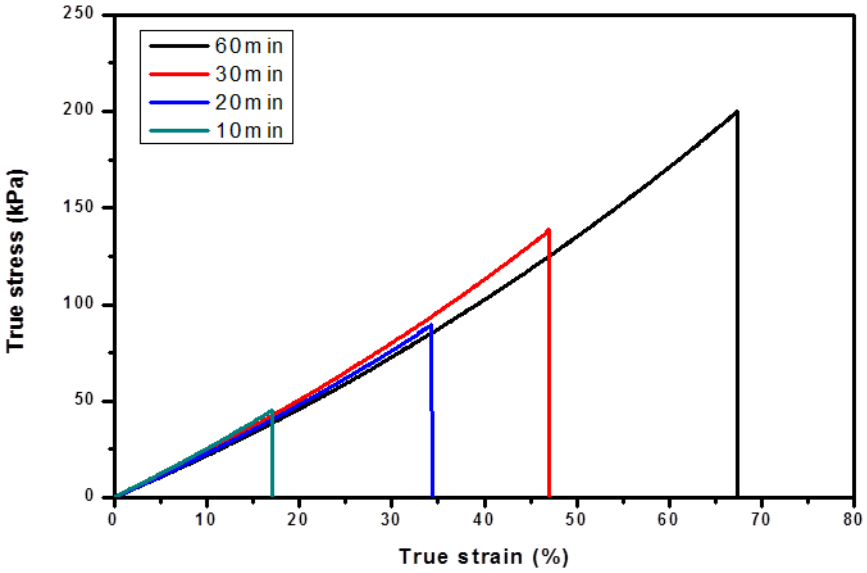

Figure 42. Representative stress-strain curves at different healing time. Healing conditions: 365nm.

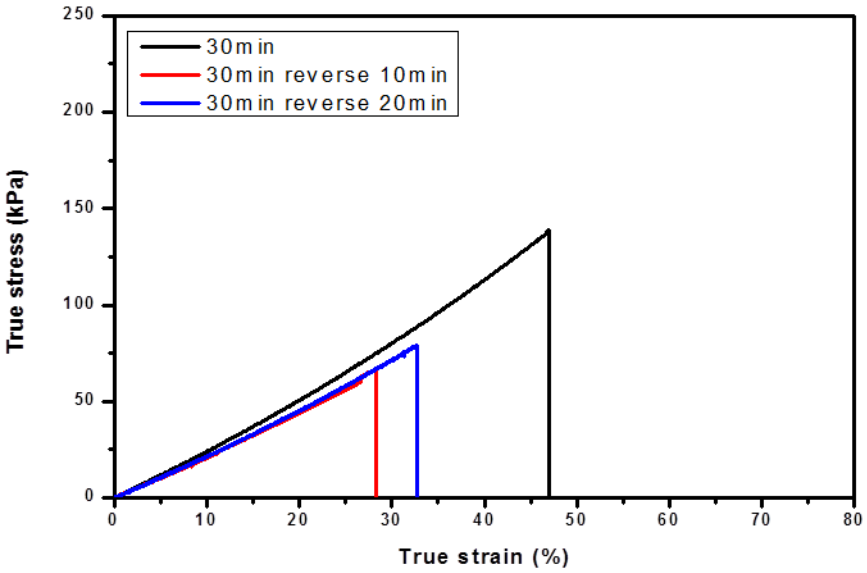

Figure 43. Representative stress-strain curves at different reverse time. Reverse conditions: 254 nm.

To further confirm the photo reversible property of gels. UV light (λ<280nm) at another wavelength was applied to the mechanically bisected samples. Two halves which had been healed for 30min at 365 nm (Figure 42) were then exposed to 254nm (Figure 43) UV for 10min and 20min. then the train-stress curves were again recorded. Figure 43 showed that the UVC light can photo cleave the formed cyclobutane rings at 254 nm UV.

4.2.4 Morphology of Hydrogel

To evaluate the intrinsic healing behavior of coumarin contained gels, the effect of coumarin on the healing process was explored. A crack was made on the gel by a razor.

Fluorescence confocal microscopy images (Figure 44) exhibited that the autonomic fusion of cut surface occurred after UV treatment.

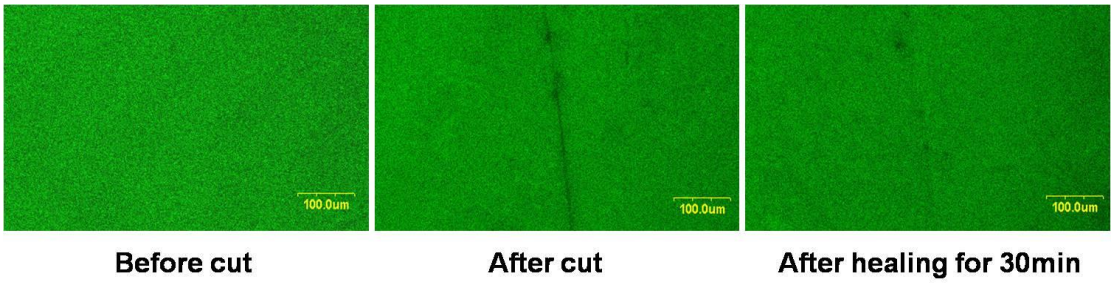

Figure 44. Fluorescence confocal microscopy images of healing process.

Surface changes were also recorded by EVOS® digital microscope. Figure 45(a) demonstrates the topography of the gel before crack creation. The gel were smoother distributed in the gel before UV irradiation, a series images of crack morphology presented the surface after UV treatment as the increase of healing time (Figure 45), which can conclude the proposed protocol results in formation of self-healing process.

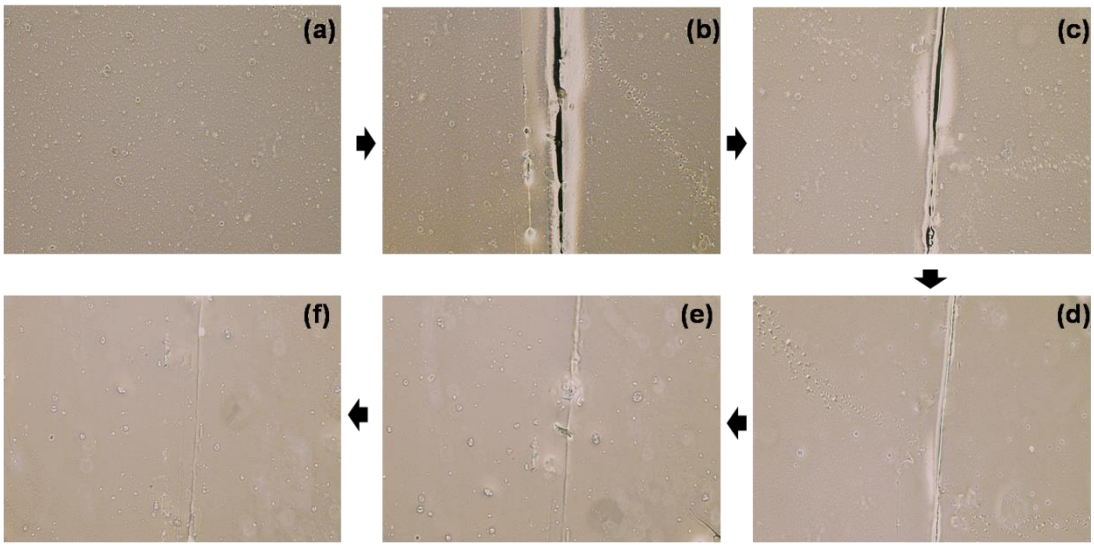

Figure 45. Digital microscopy images of gel surface changes before UV treatment (a) and after treatment for 0 min (b), 15min (c), 30min (d), 45min (e) and 60min (f).

Furthermore, hydrogel was cryosectioned and its inner-morphology was monitored. A micro-scale porous structure was observed, as shown in Figure 46 (a) and (b). The porosity of hydrogel after self-healing process became more compact than gel before treatment. Therefore, healed samples show excellent healing efficiency.

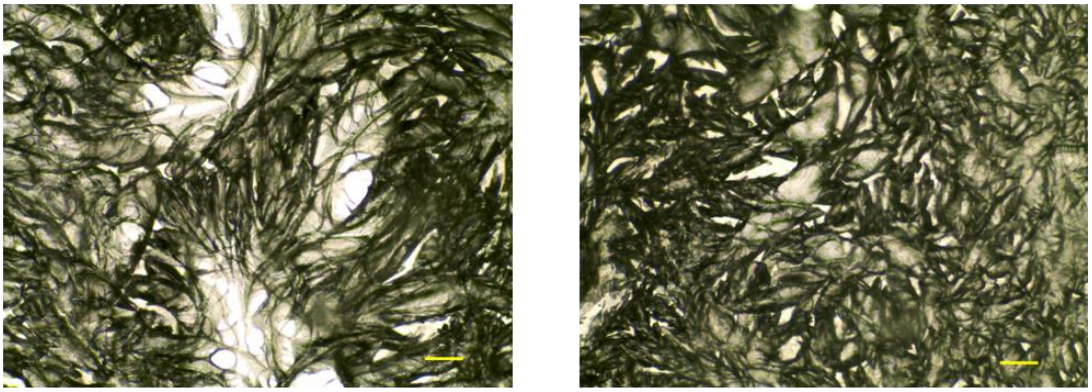

Figure 46. Cryosection images of hydrogels before UV treatment (a) and after treatment (b). (Scale: 100μm)

4.2.5 Swelling Test

Hydrogels are necessary for their high water content and low interfacial tension with the surrounding biological environment [99]. Understanding the role of gel properties on ECM formation is important for numerous biomedical applications [117]. Samples were molded as previously described and a 72h study was performed to determine percent swelling of the hydrogels using eqn (1). Figure 47 shows that the swelling ratio of both gels with and increased gradually as time grows. Hydrogels adding with CMA presented a little lower in swelling ratio compared to no CMA gels, which may be resulted from the changes in the crosslinking density [99,108].

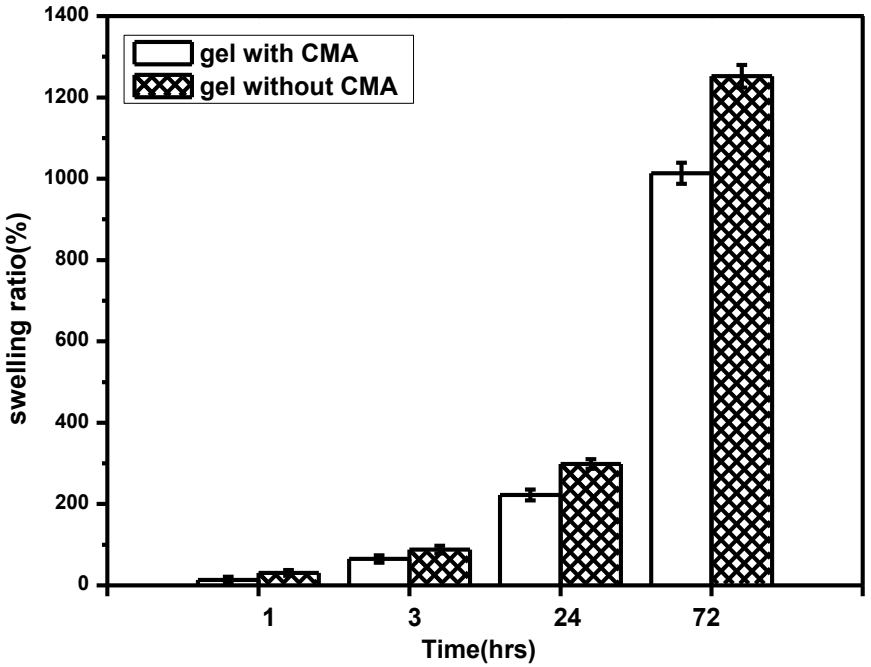

Figure 47. Swelling ratio of hydrogels with and without CMA (n=3).

4.2.6 Cell Viability

Mouse bone marrow stem cells (BMSCs) were seeded onto the hydrogels. MTT assay was used to evaluate the cell viability for 24hrs. Viability of cells seeded on tissue culture plates (TCPS) was normalized to 100%. As the control group, hydrogels without cells were also evaluated. As shown in Fig.48, hydrogels with the PAA crosslinker had high cell viability after 24hrs culture. The guanidine groups from agmatine combined with the amido groups from MBA may have significantly promoted cell attachment [100].

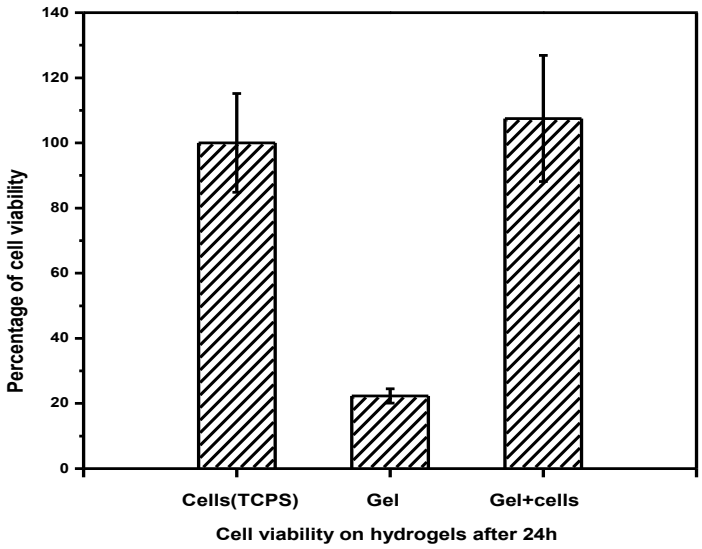

Figure 48. Cell viability on hydrogels after 24h culture based on MTT assay (absorbance is normalized to 1 for the TCPS control sample) (n=3).

Live/dead assay was used to evaluate the cell viability for 72h. Hydrogels with and without the PAA crosslinker were evaluated for the cell proliferation and cell attachment. After 24hs culture, most cells were found to attach to the gels. After 72hs culture, some dead cells were found but most of them were still alive (Fig.49-52). The number of BMSCs increased significantly in the hydrogels that contain the PAA crosslinker. However, in the control group, a significantly lower cell density was observed, which may be due to the poor adhesion to the untreated hydrogel. The results suggest that the PAA cross-linker may improve the cell attachment to the hydrogels, therefore, endowing the self-healing gels wider applications.

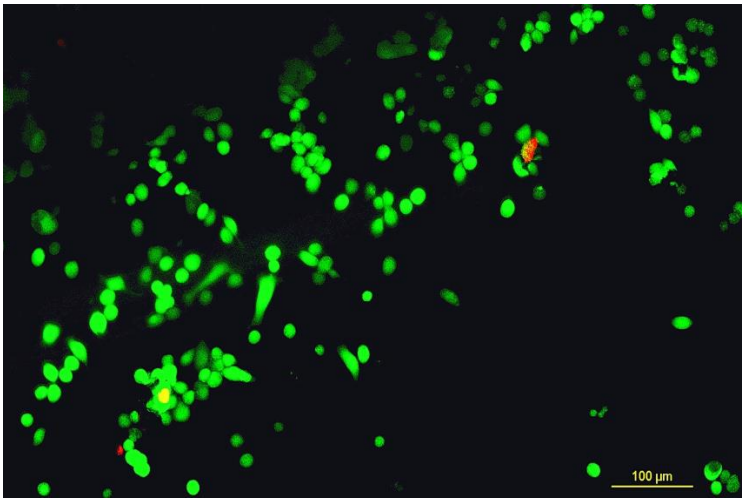

Figure 49. Live/Dead assay of BMSCs cultured on pure hydrogels (without PAA) after 24h. (Green for live cells and red for dead cells, scale: 100µm)

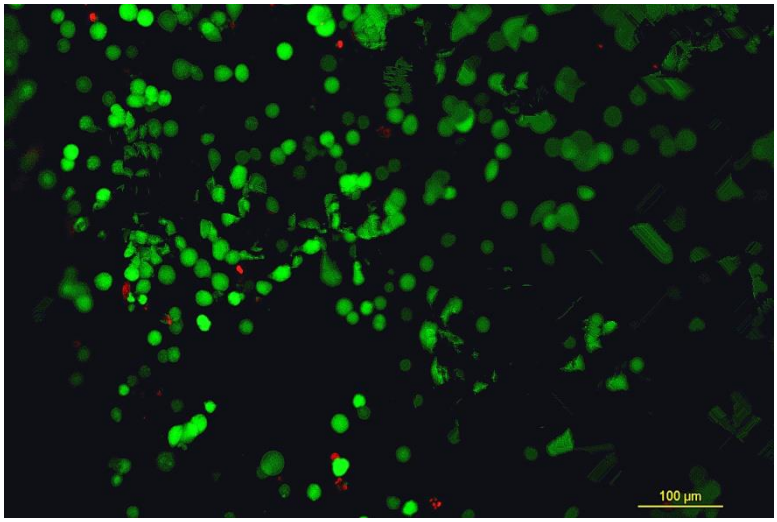

Figure 50. Live/Dead assay of BMSCs cultured on pure hydrogels (without PAA) after 72h. (Green for live cells and red for dead cells, scale: 100µm)

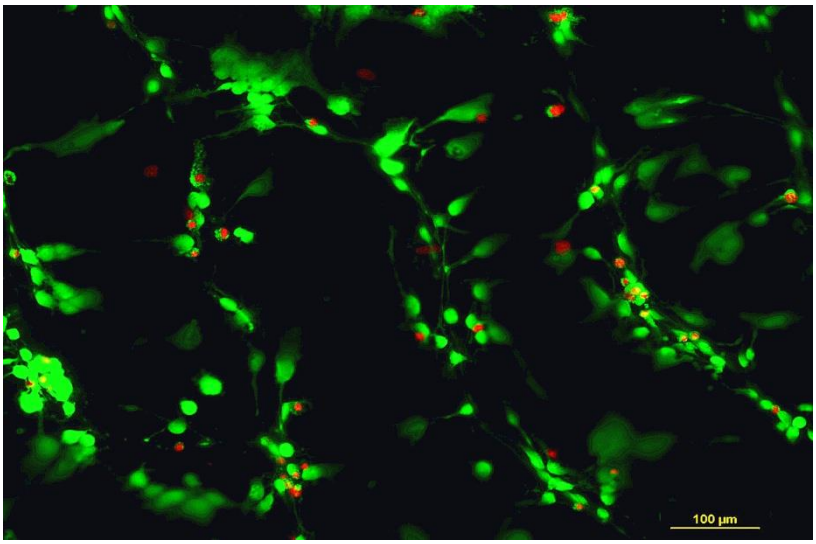

Figure 51. Live/Dead assay of BMSCs cultured on hydrogels containing PAA after 24h. (Green for live cells and red for dead cells, scale: 100µm)

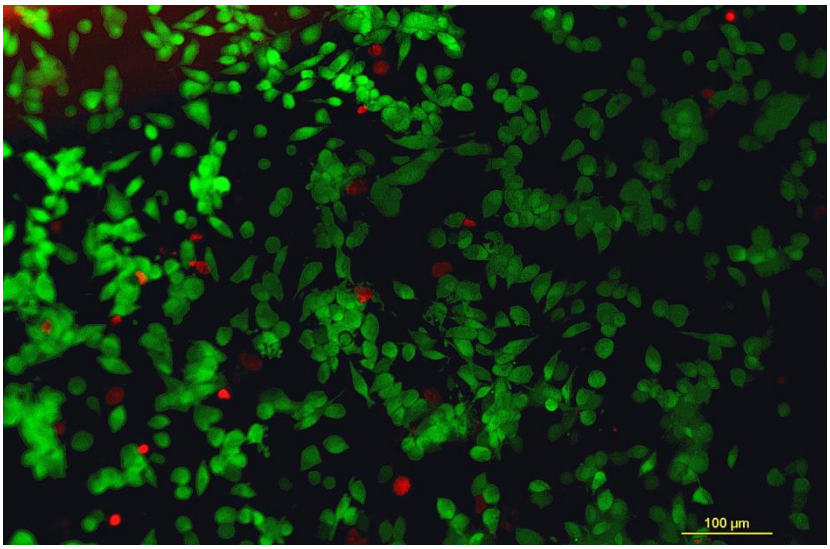

Figure 52. Live/Dead assay of BMSCs cultured on hydrogels containing PAA after 72h. (Green for live cells and red for dead cells, scale: 100µm)

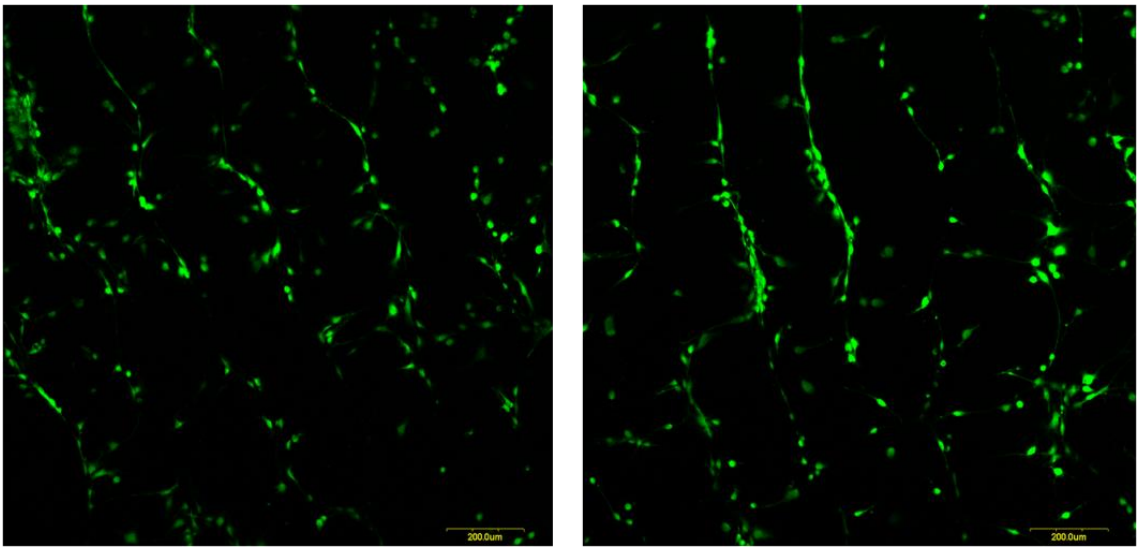

Figure 53. Confocal microscopy images of BMSC cells grown on the gel after 24h. (Scale: 200μm)

More interestingly, a uniform cell pattern was observed after cells grew on the gel for 24h. Confocal laser microscopy images further confirm the pattern (Figure 53), however the mechanism is still under study.

4.2.7 Real Time-qPCR Analysis

To evaluate effects of the hydrogel on the osteogenic differentiation of encapsulated BMSCs, Real time-qPCR was applied to BMSCs seeded hydrogels (Figure 54-57). Changes of response to the hydrogels were recorded using osteogenic marker mRNAs for ALP, BSP, COL and OPN. As shown in Figure 54-57, osteogenic gene expression in BMSCs increased significantly after 7days' culture.

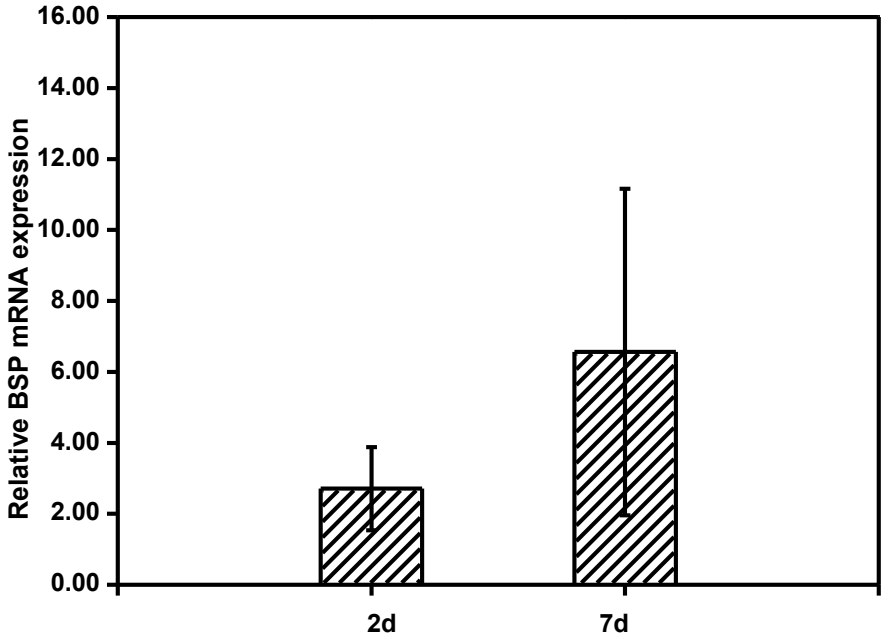

Figure 54. Real time-qPCR of osteogenic gene expression levels of BMSCs cultured *in vitro*. Total RNA was prepared from BMSCs grown on hydrogel for 2 and 7 days. BSP gene expression was quantified using real time-qPCR methods, GAPDH was used as an internal control. Data values are expressed as mean±SE (n=3). "*" means $p < 0.05$ vs. the groups on day 2.

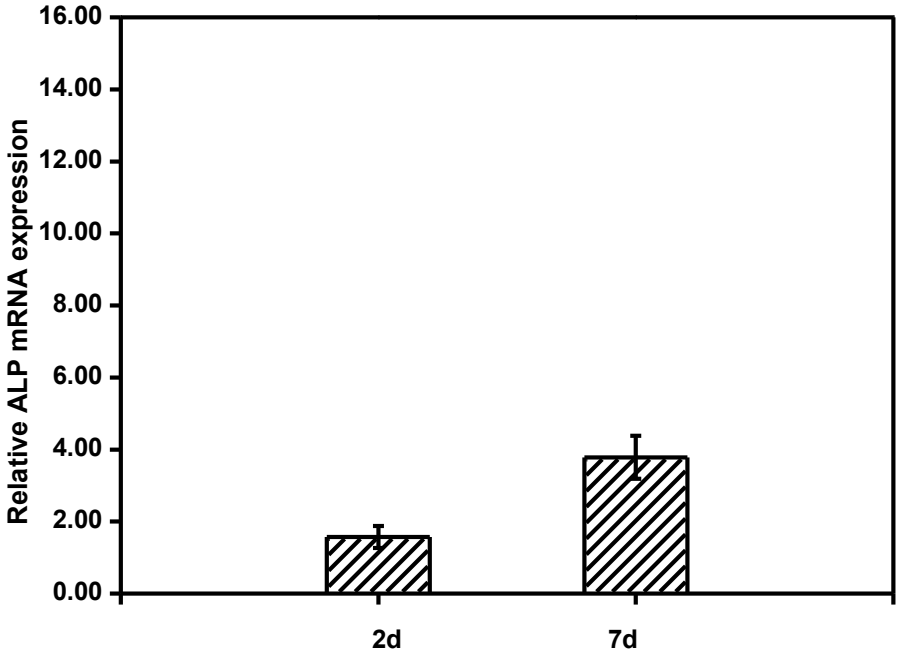

Figure 55. Real time-qPCR of osteogenic gene expression levels of BMSCs cultured *in vitro*. Total RNA was prepared from BMSCs grown on hydrogel for 2 and 7 days. ALP gene expression was quantified using real time-qPCR methods, GAPDH was used as an internal control. Data values are expressed as mean±SE (n=3). "*" means $p < 0.05$ vs. the groups on day 2.

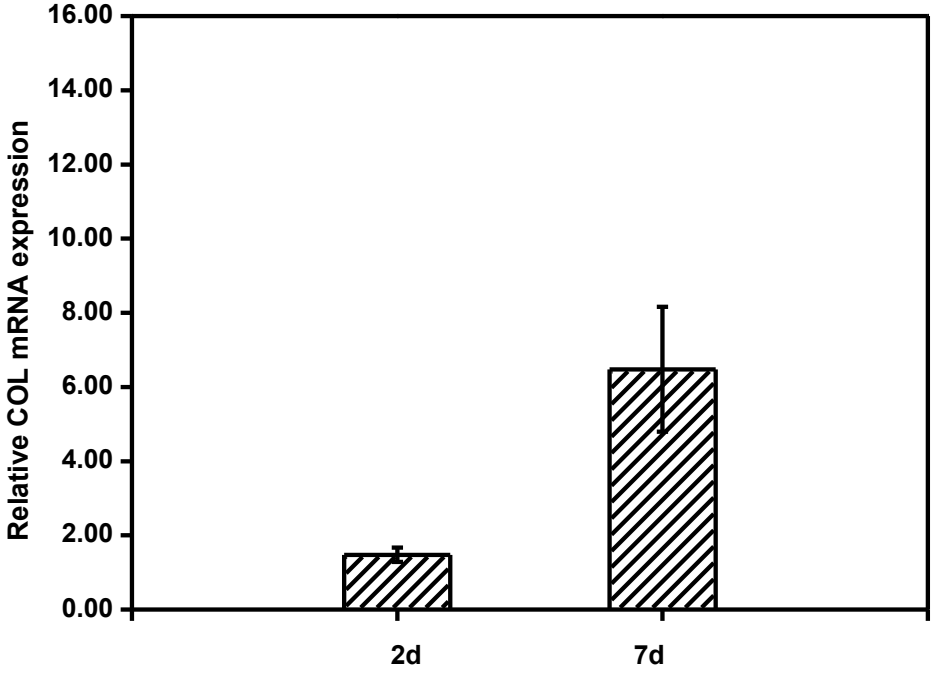

Figure 56. Real time-qPCR of osteogenic gene expression levels of BMSCs cultured *in vitro*. Total RNA was prepared from BMSCs grown on hydrogel for 2 and 7 days. COL (c) gene expression was quantified using real time-qPCR methods, GAPDH was used as an internal control. Data values are expressed as mean±SE (n=3). "*" means $p < 0.05$ vs. the groups on day 2.

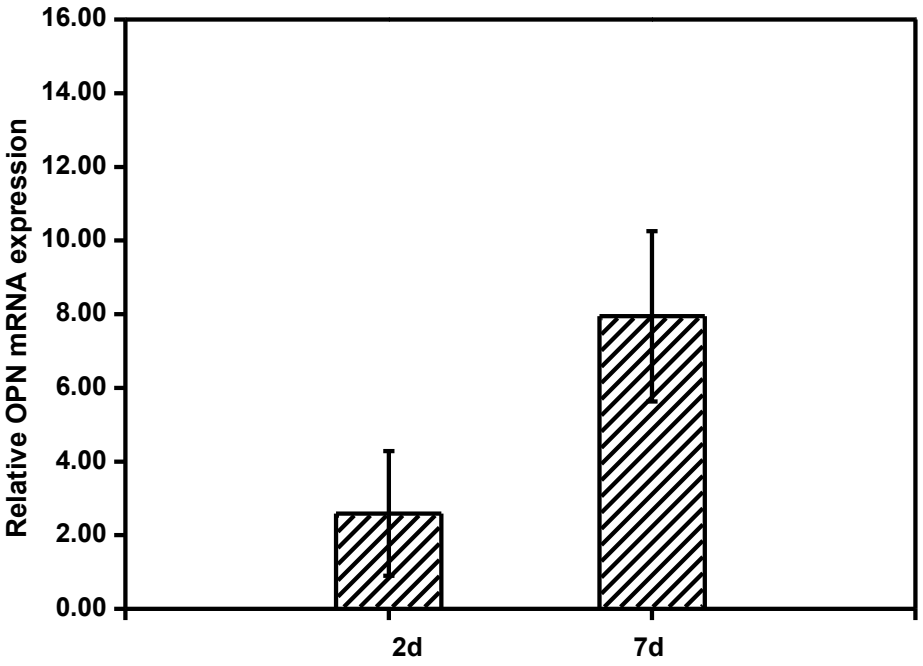

Figure 57. Real time-qPCR of osteogenic gene expression levels of BMSCs cultured *in vitro*. Total RNA was prepared from BMSCs grown on hydrogel for 2 and 7 days. OPN gene expression was quantified using real time-qPCR methods, GAPDH was used as an internal control. Data values are expressed as mean±SE (n=3). "*" means $p < 0.05$ vs. the groups on day 2.

Bone sialoprotein (BSP) is an important protenforosteogenetic differentiation. It can be expressed in osteoblasts or differentiated stem cells [217]. On day 2, the expression of BSP gene is increased and the same trend was observed on day 7 (Figure 54). Collagen (COL) is a critical marker in the late stage of bone differentiation [218]. The expression level of COL (Figure 56) had the similar tendency to that of BSP.

Osteopontin (OPN) is another important human gene product which is related to osteogenesis [218]. It plays a role in organic linking component of bone. As shown in Figure 57, the expression profiling of OPN was relatively lower than that of both BSP and COL. But the expression profiling of OPN still have a positive trend after 7 days during the osteogenetic differentiation. Alkaline phosphatase (ALP) is an enzyme that exists in all tissue in human body, which can remove the phosphate group from nucleotides or proteins etc. ALP may be a marker for bone metabolism if a high level of ALP was observed when active bone was formatted [219]. The ALP expression is evaluated when BMSCs were cultured on hydrogels. The results showed that hydrogel had a high ALP expression level throughout one week (Figure 55).

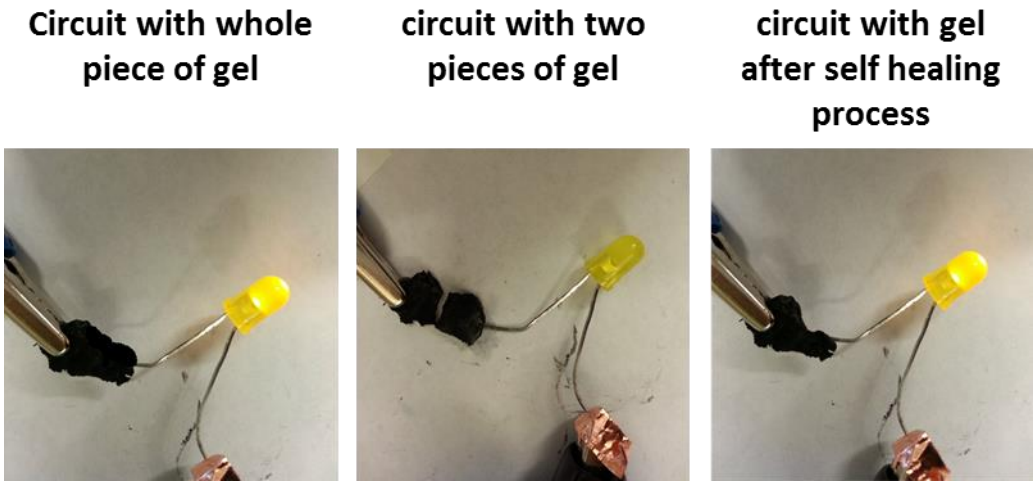

Figure 58. Conductivity test for the gel with MWNTs.

To further test the gel's self-healing property, the gel precursor was added with MWNTs, and then conductive property was tested after self-healing process. As shown in Fig. 58, gel was cut into two pieces, and a simple circuit with a led bulb was constituted. The results showed that gel after UV treatment restored to an integrated

one, acting as a wire in the closed circuit. The electric conductivity of gel was also recorded by a multifunction digital four-probe tester. The resistance of this hydrogel is between 1.16×10^{-3} and 6.55×10^{-4} (Normal) and σ is 1×10^{-3}(Normal).

4.3 Summary

Herein, we demonstrate a novel macro gels with self-healing capability and biocompatibility. Coumarin derivatives are successively introduced to construct into polyacrylamide-based hydrogels. The reversible photodimerization and photocleavage reactivity of coumarin have been imparted to the polymer. The resultant functional gels shows noticeable self-healing property after healing under 365nm UV irradiation ascribed to the intramolecular [2+2] photocycloaddition reactions of coumarins. The self-healing gels also possess high mechanical strength after healing for 60min with stress intensity of 2×10^5 Pa and the elongation at break over 96%. More interestingly, cell attachment property was significantly improved by adding PAA crosslinker. The interesting development of method and materials in this work provides a new insight into the fabrication of novel biocompatible self-healing materials for extensive applications.

Chapter 5. Summary and Conclusion

This thesis reports the preliminary evaluation of novel biodegradable and biocompatible agmatine-containing PAA crosslinker. Hydrogels fabricated by this crosslinker can obtain controllable stiffness and excellent cell adhesion. Results shows changing the mass ratio of crosslinker can achieve the ideal stiffness which is most close to nature ECM to support cells' growth. *In vitro* tests also demonstrate that PAA crosslinked hydrogels can successfully provide a 3D structure to let the cells adhere and grow. Hereby PAA containing hydrogels might be promising for implantable scaffolds for tissue regeneration.

The PAA contained thermo-sensitive hydrogel reported here is an innovative newcomer as implantable material, first employed as filler for depressed defects in rats. The data reported in this article are preliminary but clearly support that such hydrogel is promising in many important respects, such as biodegradability, biocompatibility which were confirmed by *In vitro* and *in vivo* tests. In conclusion, such cell attachable thermo sensitive hydrogel definitely warrant potential as a filling material for small depressed defects and ultimately might become a new material in plastic surgery in the clinic. Hydrogels prepared from this novel multifunctional crosslinker are promising in tissue engineering applications.

The thesis also demonstrated a novel macro gels with self-healing capability and biocompatibility. Coumarin derivatives are successively introduced to construct into polyacrylamide-based hydrogels. The reversible photodimerization and photocleavage reactivity of coumarin has been imparted to the polymer. The resultant functional gels shows noticeable self-healing property after healing under 365nm UV irradiation ascribed to the intramolecular [2+2] photocycloaddition reactions of coumarins. The self-healing gels also possess high mechanical strength after healing for 60min with stress intensity of $2x10^5$ Pa and the elongation at break over 96%. More interestingly, cell attachment property was significantly improved by adding agmatine and AEPZ contained PAA crosslinker. The interesting development of method and materials in this work provides a new insight into the fabrication of novel biocompatible self-healing materials for extensive applications.

In order to further evaluate the biological performance of the proposed hydrogel scaffolds, it is suggested to further study in other kinds of cells except BMSC and also *in vivo* application. For example, carbon nanotubes (CNTs) has been indicated that can Guide the differentiation of neural cells, therefore, adding CNTs into the hydrogels and then study the effects on neural cells can be another direction of further research. Such studies will provide a deeper insight for the scaffold modification and application in tissue engineering.

There is still potential development of the proposed self-healing hydrogels, such as the probability of using far IR for healing treatment replacing UV irradiation. Recent research has showed that a thermal treatment can also induce the photodimerization of coumarin, therefore, using thermal treatment to replace UV treatment would be a promising method.

In vivo application of hydrogels inside living body, or incorporation with growth factor or drugs into hydrogel to give a release system would be another prospect area. Recently, study about reducible and photosensitive polyamidoamine-magnetic iron oxide nanoparticles for doxorubicin delivery has been conducted. The magnetic iron oxide nanoparticles (MNPs) can be the best choice not only for resonance imaging (MRI) contrast agents, but also for carriers for targeted drug delivery. A reducible and photosensitive polyamidoamine polymer was prepared, and this dual functional polymer can not only provide efficient drug loading, but also have reduction-responsive and optical controlled drug release functions. Studies in this area can also become another promising research about targeted drug load and release.

Reference

[1]Sharing, United Network for Organ, Procurement, Organ, & Network, Transplantation. (1996). *1996 annual report, the us scientific registry of transplant recipients and the organ procurement and transplantation network: Transplant data 1988-1995*: United Network for Organ Sharing.

[2]Lanza, Robert, Langer, Robert, & Vacanti, Joseph P. (2011). *Principles of tissue engineering*: Academic press.

[3]Cohen, Smadar, Baño, M Carmen, Cima, Linda G, Allcock, Harry R, Vacanti, Joseph P, Vacanti, Charles A, & Langer, Robert. (1993). Design of synthetic polymeric structures for cell transplantation and tissue engineering. *Clinical materials, 13*(1), 3-10.

[4]Langer, Robert. (1993). I articles. *Science, 260*, 5110.

[5]Cima, LG, Vacanti, JP, Vacanti, C, Ingber, D, Mooney, D, & Langer, R. (1991). Tissue engineering by cell transplantation using degradable polymer substrates. *Journal of biomechanical engineering, 113*(2), 143-151.

[6]Cima, Linda G, Ingber, Donald E, Vacanti, Joseph P, & Langer, Robert. (1991). Hepatocyte culture on biodegradable polymeric substrates. *Biotechnology and bioengineering, 38*(2), 145-158.

[7]Yang, Shoufeng, Leong, Kah-Fai, Du, Zhaohui, & Chua, Chee-Kai. (2001). The design of scaffolds for use in tissue engineering. Part i. Traditional factors. *Tissue engineering, 7*(6), 679-689.

[8]Yang, Shoufeng, Leong, Kah-Fai, Du, Zhaohui, & Chua, Chee-Kai. (2002). The design of scaffolds for use in tissue engineering. Part ii. Rapid prototyping techniques. *Tissue engineering, 8*(1), 1-11.

[9]Thomson, RC, Wake, MC, Yaszemski, MJ, & Mikos, AG. (1995). Biodegradable polymer scaffolds to regenerate organs *Biopolymers ii* (pp. 245-274): Springer.

[10]Wong, Wai Hung, & Mooney, David J. (1997). Synthesis and properties of biodegradable polymers used as synthetic matrices for tissue engineering *Synthetic biodegradable polymer scaffolds* (pp. 51-82): Springer.

[11]Bryant, Stephanie J, & Anseth, Kristi S. (2002). Hydrogel properties influence ecm production by chondrocytes photoencapsulated in poly (ethylene glycol) hydrogels. *Journal of biomedical materials research, 59*(1), 63-72.

[12]Drury, Jeanie L, & Mooney, David J. (2003). Hydrogels for tissue engineering: Scaffold design variables and applications. *Biomaterials, 24*(24), 4337-4351.

[13]Anseth, Kristi S, Bowman, Christopher N, & Brannon-Peppas, Lisa. (1996). Mechanical properties of hydrogels and their experimental determination. *Biomaterials, 17*(17), 1647-1657.

[14]Gunn, Jonathan W, Turner, Suzanne D, & Mann, Brenda K. (2005). Adhesive and mechanical properties of hydrogels influence neurite extension. *Journal of Biomedical*

Materials Research Part A, 72(1), 91-97.
[15]Rehfeldt, Florian, Engler, Adam J, Eckhardt, Adam, Ahmed, Fariyal, & Discher, Dennis E. (2007). Cell responses to the mechanochemical microenvironment—implications for regenerative medicine and drug delivery. *Advanced drug delivery reviews, 59*(13), 1329-1339.
[16]Atala, Anthony, & Mooney, David J. (1997). *Synthetic biodegradable polymer scaffolds*: Springer.
[17]Yu, Woo Jong, Li, Zheng, Zhou, Hailong, Chen, Yu, Wang, Yang, Huang, Yu, & Duan, Xiangfeng. (2013). Vertically stacked multi-heterostructures of layered materials for logic transistors and complementary inverters. *Nature materials, 12*(3), 246-252.
[18]Ceylan, Hakan, Urel, Mustafa, Erkal, Turan S, Tekinay, Ayse B, Dana, Aykutlu, & Guler, Mustafa O. (2013). Mussel inspired dynamic cross-linking of self-healing peptide nanofiber network. *Advanced Functional Materials, 23*(16), 2081-2090.
[19]Barthel, Markus J, Rudolph, Tobias, Teichler, Anke, Paulus, Renzo M, Vitz, Jürgen, Hoeppener, Stephanie, Hager, Martin D, Schacher, Felix H, & Schubert, Ulrich S. (2013). Self-healing materials via reversible crosslinking of poly (ethylene oxide)-block-poly (furfuryl glycidyl ether)(peo-b-pfge) block copolymer films. *Advanced Functional Materials, 23*(39), 4921-4932.
[20]Lipomi, Darren J, Vosgueritchian, Michael, Tee, Benjamin CK, Hellstrom, Sondra L, Lee, Jennifer A, Fox, Courtney H, & Bao, Zhenan. (2011). Skin-like pressure and strain sensors based on transparent elastic films of carbon nanotubes. *Nature nanotechnology, 6*(12), 788-792.
[21]Coope, Tim S, Mayer, Ulrich FJ, Wass, Duncan F, Trask, Richard S, & Bond, Ian P. (2011). Self-healing of an epoxy resin using scandium (iii) triflate as a catalytic curing agent. *Advanced Functional Materials, 21*(24), 4624-4631.
[22]Burnworth, Mark, Tang, Liming, Kumpfer, Justin R, Duncan, Andrew J, Beyer, Frederick L, Fiore, Gina L, Rowan, Stuart J, & Weder, Christoph. (2011). Optically healable supramolecular polymers. *Nature, 472*(7343), 334-337.
[23]Park, Jeong-Ho, & Braun, Paul V. (2010). Coaxial electrospinning of self-healing coatings. *Advanced materials, 22*(4), 496-499.
[24]Ghosh, Biswajit, & Urban, Marek W. (2009). Self-repairing oxetane-substituted chitosan polyurethane networks. *Science, 323*(5920), 1458-1460.
[25]White, Scott R, Sottos, NR, Geubelle, PH, Moore, JS, Kessler, M_R, Sriram, SR, Brown, EN, & Viswanathan, S. (2001). Autonomic healing of polymer composites. *Nature, 409*(6822), 794-797.
[26]Bergman, Sheba D, & Wudl, Fred. (2008). Mendable polymers. *Journal of Materials Chemistry, 18*(1), 41-62.
[27]Yuan, YC, Yin, T, Rong, MZ, & Zhang, MQ. (2008). Self healing in polymers and polymer composites. Concepts, realization and outlook: A review. *Express Polym. Lett, 2*(4), 238-250.

[28]Dazhu, Chen, Pingsheng, He, & Haiyang, Yang. (2004). Self-healing polymeric materials. *Chemistry, 2*, 009.
[29]Ferruti, P. (1996). Ion-chelating polymers (medical applications) (Vol. 5, pp. 3334-3359): CRC Press Inc.: Boca Raton, FL.
[30]Ferruti, Paolo, Marchisio, Maria A, & Duncan, Ruth. (2002). Poly (amido-amine) s: Biomedical applications. *Macromolecular Rapid Communications, 23*(5-6), 332-355.
[31]Fuchs, Julie R, Nasseri, Boris A, & Vacanti, Joseph P. (2001). Tissue engineering: A 21st century solution to surgical reconstruction. *The Annals of thoracic surgery, 72*(2), 577-591.
[32]Niklason, Laura E, & Langer, Robert. (2001). Prospects for organ and tissue replacement. *Jama, 285*(5), 573-576.
[33]Stock, Ulrich A, & Vacanti, Joseph P. (2001). Tissue engineering: Current state and prospects. *Annual review of medicine, 52*(1), 443-451.
[34]Bell, Eugene. (1991). Tissue engineering: A perspective. *Journal of cellular biochemistry, 45*(3), 239-241.
[35]Fenili, Fabio, Manfredi, Amedea, Ranucci, Elisabetta, & Ferruti, Paolo. (2011). Poly (amidoamine) hydrogels as scaffolds for cell culturing and conduits for peripheral nerve regeneration. *International Journal of Polymer Science, 2011*.
[36]Ranucci, Elisabetta, Ferruti, Paolo, Lattanzio, Ettore, Manfredi, Amedea, Rossi, Manuela, Mussini, Patrizia R, Chiellini, Federica, & Bartoli, Cristina. (2009). Acid-base properties of poly (amidoamine) s. *Journal of Polymer Science Part A: Polymer Chemistry, 47*(24), 6977-6991.
[37]Ferruti, Paolo, Bianchi, Sabrina, Ranucci, Elisabetta, Chiellini, Federica, & Caruso, Vincenzina. (2005). Novel poly (amido-amine)-based hydrogels as scaffolds for tissue engineering. *Macromolecular bioscience, 5*(7), 613-622.
[38]Cao, Zheng, Du, Binyang, Chen, Tianyou, Nie, Jingjing, Xu, Junting, & Fan, Zhiqiang. (2008). Preparation and properties of thermo-sensitive organic/inorganic hybrid microgels. *Langmuir, 24*(22), 12771-12778.
[39]Yu, Chao, Wang, Cai-Feng, & Chen, Su. (2013). Robust self-healing host–guest gels from magnetocaloric radical polymerization. *Advanced Functional Materials*.
[40]Tee, Benjamin CK, Wang, Chao, Allen, Ranulfo, & Bao, Zhenan. (2012). An electrically and mechanically self-healing composite with pressure-and flexion-sensitive properties for electronic skin applications. *Nature nanotechnology, 7*(12), 825-832.
[41]Burnworth, M, Tang, LM, Kumpfer, JR, & Duncan, AJ. (2011). Fl 85 beyer, gl fiore, sj rowan and c. Weder. *Nature, 472*, 334-U230.
[42]Fox, Justin, Wie, Jeong J, Greenland, Barnaby W, Burattini, Stefano, Hayes, Wayne, Colquhoun, Howard M, Mackay, Michael E, & Rowan, Stuart J. (2012). High-strength, healable, supramolecular polymer nanocomposites. *Journal of the American Chemical Society, 134*(11), 5362-5368.

[43]Vaiyapuri, Rajendran, Greenland, Barnaby W, Rowan, Stuart J, Colquhoun, Howard M, Elliott, Joanne M, & Hayes, Wayne. (2012). Thermoresponsive supramolecular polymer network comprising pyrene-functionalized gold nanoparticles and a chain-folding polydiimide. *Macromolecules, 45*(13), 5567-5574.
[44]Hoogenboom, Richard. (2012). Hard autonomous self-healing supramolecular materials—a contradiction in terms? *Angewandte Chemie International Edition, 51*(48), 11942-11944.
[45]Chen, Yulin, Kushner, Aaron M, Williams, Gregory A, & Guan, Zhibin. (2012). Multiphase design of autonomic self-healing thermoplastic elastomers. *Nature chemistry, 4*(6), 467-472.
[46]Wang, Xu, Liu, Feng, Zheng, Xiwei, & Sun, Junqi. (2011). Water-enabled self-healing of polyelectrolyte multilayer coatings. *Angewandte Chemie International Edition, 50*(48), 11378-11381.
[47]Wang, Qigang, Mynar, Justin L, Yoshida, Masaru, Lee, Eunji, Lee, Myongsoo, Okuro, Kou, Kinbara, Kazushi, & Aida, Takuzo. (2010). High-water-content mouldable hydrogels by mixing clay and a dendritic molecular binder. *Nature, 463*(7279), 339-343.
[48]Tuncaboylu, Deniz C, Sari, Murat, Oppermann, Wilhelm, & Okay, Oguz. (2011). Tough and self-healing hydrogels formed via hydrophobic interactions. *Macromolecules, 44*(12), 4997-5005.
[49]Jiang, Guoqing, Liu, Chang, Liu, Xiaoli, Chen, Qingrui, Zhang, Guohui, Yang, Meng, & Liu, Fengqi. (2010). Network structure and compositional effects on tensile mechanical properties of hydrophobic association hydrogels with high mechanical strength. *Polymer, 51*(6), 1507-1515.
[50]Cordier, Philippe, Tournilhac, François, Soulié-Ziakovic, Corinne, & Leibler, Ludwik. (2008). Self-healing and thermoreversible rubber from supramolecular assembly. *Nature, 451*(7181), 977-980.
[51]Ciferri, Alberto. (2002). Supramolecular polymerizations. *Macromolecular rapid communications, 23*(9), 511-529.
[52]Schmuck, Carsten, & Wienand, Wolfgang. (2001). Self-complementary quadruple hydrogen-bonding motifs as a functional principle: From dimeric supramolecules to supramolecular polymers. *Angewandte Chemie International Edition, 40*(23), 4363-4369.
[53]Hart, Lewis R, Harries, Josephine L, Greenland, Barnaby W, Colquhoun, Howard M, & Hayes, Wayne. (2013). Healable supramolecular polymers. *Polymer Chemistry, 4*(18), 4860-4870.
[54]Söntjens, Serge HM, Sijbesma, Rint P, van Genderen, Marcel HP, & Meijer, EW. (2001). Selective formation of cyclic dimers in solutions of reversible supramolecular polymers. *Macromolecules, 34*(12), 3815-3818.
[55]ten Cate, A Tessa, Kooijman, Huub, Spek, Anthony L, Sijbesma, Rint P, & Meijer, EW. (2004). Conformational control in the cyclization of hydrogen-bonded

supramolecular polymers. *Journal of the American Chemical Society, 126*(12), 3801-3808.
[56]Burattini, Stefano, Colquhoun, Howard M, Greenland, Barnaby W, & Hayes, Wayne. (2009). A novel self-healing supramolecular polymer system. *Faraday discussions, 143*, 251-264.
[57]Kievit, Forrest M, Stephen, Zachary R, Veiseh, Omid, Arami, Hamed, Wang, Tingzhong, Lai, Vy P, Park, James O, Ellenbogen, Richard G, Disis, Mary L, & Zhang, Miqin. (2012). Targeting of primary breast cancers and metastases in a transgenic mouse model using rationally designed multifunctional spions. *ACS nano, 6*(3), 2591-2601.
[58]Cho, Sung-Youl, Kim, Joong-Gon, Oh, Se-Young, & Chung, Chan-Moon. (2010). Heat-induced crack healing in a perfluorocyclobutane-containing polymer. *Macromolecular Research, 18*(2), 212-214.
[59]Froimowicz, Pablo, Frey, Holger, & Landfester, Katharina. (2011). Towards the generation of self-healing materials by means of a reversible photo-induced approach. *Macromolecular rapid communications, 32*(5), 468-473.
[60]Sottos, Nancy R, & Moore, Jeffrey S. (2011). Materials chemistry: Spot-on healing. *Nature, 472*(7343), 299-300.
[61]Ohkawa, Kousaku, Shoumura, Kenji, Yamada, Masanori, Nishida, Ayako, Shirai, Hirofusa, & Yamamoto, Hiroyuki. (2001). Photoresponsive peptide and polypeptide systems, 14. Biodegradation of photocrosslinkable copolypeptide hydrogels containing l-ornithine and δ-7-coumaryloxyacetyl-l-ornithine residues. *Macromolecular Bioscience, 1*(4), 149-156.
[62]Yamamoto, Hiroyuki, Kitsuki, Tomohiro, Nishida, Ayako, Asada, Kouji, & Ohkawa, Kousaku. (1999). Photoresponsive peptide and polypeptide systems. 13. Photoinduced cross-linked gel and biodegradation properties of copoly (l-lysine) containing ε-7-coumaryloxyacetyl-l-lysine residues. *Macromolecules, 32*(4), 1055-1061.
[63]Brahmbhatt, DI, Singh, Shashibala, & Patel, KC. (1999). Synthesis, characterization and biological activity of some poly (coumarin ethylene) s. *European polymer journal, 35*(2), 317-324.
[64]Ling, Jun, Rong, Min Zhi, & Zhang, Ming Qiu. (2012). Photo-stimulated self-healing polyurethane containing dihydroxyl coumarin derivatives. *Polymer, 53*(13), 2691-2698.
[65]Cheng, Zhiyu, Ren, Biye, Zhao, Dongli, Liu, Xinxing, & Tong, Zhen. (2009). Novel thermotropic liquid crystalline and redox-active complexes of ionically self-assembled poly (ferrocenylsilane) and dendritic amphiphiles. *Macromolecules, 42*(7), 2762-2766.
[66]Zhang, Jingyan, Jiang, Xiaoze, Zhang, Yanfeng, Li, Yuting, & Liu, Shiyong. (2007). Facile fabrication of reversible core cross-linked micelles possessing thermosensitive swellability. *Macromolecules, 40*(25), 9125-9132.

[67]Kishore, Kaushal. (1995). A new class of photo-cross-linkable side chain liquid crystalline polymers containing bis (benzylidene) cyclohexanone units. *Macromolecules, 28*(4), 806-815.
[68]Jackson, Peregrine Orr, O'Neill, Mary, Duffy, Warren Lee, Hindmarsh, Paul, Kelly, Stephen Malcom, & Owen, Gareth James. (2001). An investigation of the role of cross-linking and photodegradation of side-chain coumarin polymers in the photoalignment of liquid crystals. *Chemistry of materials, 13*(2), 694-703.
[69]Kakuta, Takahiro, Takashima, Yoshinori, Nakahata, Masaki, Otsubo, Miyuki, Yamaguchi, Hiroyasu, & Harada, Akira. (2013). Preorganized hydrogel: Self-healing properties of supramolecular hydrogels formed by polymerization of host–guest-monomers that contain cyclodextrins and hydrophobic guest groups. *Advanced Materials, 25*(20), 2849-2853.
[70]Yan, Xuzhou, Xu, Donghua, Chen, Jianzhuang, Zhang, Mingming, Hu, Bingjie, Yu, Yihua, & Huang, Feihe. (2013). A self-healing supramolecular polymer gel with stimuli-responsiveness constructed by crown ether based molecular recognition. *Polymer Chemistry, 4*(11), 3312-3322.
[71]Nakahata, Masaki, Takashima, Yoshinori, Hashidzume, Akihito, & Harada, Akira. (2013). Redox-generated mechanical motion of a supramolecular polymeric actuator based on host–guest interactions. *Angewandte Chemie International Edition, 52*(22), 5731-5735.
[72]Papisov, Mikhail I. (1998). Theoretical considerations of res-avoiding liposomes: Molecular mechanics and chemistry of liposome interactions. *Advanced drug delivery reviews, 32*(1), 119-138.
[73]Qiu, Yong, & Park, Kinam. (2001). Environment-sensitive hydrogels for drug delivery. *Advanced drug delivery reviews, 53*(3), 321-339.
[74]Hoffman, Allan S. (1987). Applications of thermally reversible polymers and hydrogels in therapeutics and diagnostics. *Journal of Controlled Release, 6*(1), 297-305.
[75]Kim, Sung Wan, Bae, You Han, & Okano, Teruo. (1992). Hydrogels: Swelling, drug loading, and release. *Pharmaceutical research, 9*(3), 283-290.
[76]Schild, HG. (1992). Poly (< i> n</i>-isopropylacrylamide): Experiment, theory and application. *Progress in polymer science, 17*(2), 163-249.
[77]Kaneko, Y, Sakai, K, & Okano, T. (1998). Temperature-responsive hydrogels as intelligent materials. *Biorelated Polymers and Gels*, 29-69.
[78]Bromberg, Lev E, & Ron, Eyal S. (1998). Temperature-responsive gels and thermogelling polymer matrices for protein and peptide delivery. *Advanced drug delivery reviews, 31*(3), 197-221.
[79]Ichikawa, Hideki, & Fukumori, Yoshinobu. (2000). A novel positively thermosensitive controlled-release microcapsule with membrane of nano-sized poly (< i> n</i>-isopropylacrylamide) gel dispersed in ethylcellulose matrix. *Journal of Controlled Release, 63*(1), 107-119.

[80]Greene, Larry C, Meyers, Paul A, Springer, Jeff T, & Banks, Philip A. (1992). Biological evaluation of pesticides released from temperature-responsive microcapsules. *Journal of agricultural and food chemistry, 40*(11), 2274-2278.
[81]Wang, Chun, Stewart, Russell J, & KopeČek, JindŘich. (1999). Hybrid hydrogels assembled from synthetic polymers and coiled-coil protein domains. *Nature, 397*(6718), 417-420.
[82]Feil, H, Bae, YH, Feijen, J, & Kim, SW. (1992). Mutual influence of ph and temperature on the swelling of ionizable and thermosensitive hydrogels. *Macromolecules, 25*(20), 5528-5530.
[83]Hirotsu, SHUNSUKE. (1993). Coexistence of phases and the nature of first-order phase transition in poly-n-isopropylacrylamide gels *Responsive gels: Volume transitions ii* (pp. 1-26): Springer.
[84]Irie, Masahiro. (1993). Stimuli-responsive poly (n-isopropylacrylamide). Photo-and chemical-induced phase transitions *Responsive gels: Volume transitions ii* (pp. 49-65): Springer.
[85]Hirotsu, Shunsuke, Hirokawa, Yoshitsugu, & Tanaka, Toyoichi. (1987). Volume-phase transitions of ionized n-isopropylacrylamide gels. *The Journal of chemical physics, 87*(2), 1392-1395.
[86]Yu, Hua, & Grainger, David W. (1993). Thermo-sensitive swelling behavior in crosslinked n-isopropylacrylamide networks: Cationic, anionic, and ampholytic hydrogels. *Journal of applied polymer science, 49*(9), 1553-1563.
[87]Suzuki, Yoshiharu, Tomonaga, Kaoru, Kumazaki, Makoto, & Nishio, Izumi. (1996). Change in phase transition behavior of an nipa gel induced by solvent composition: Hydrophobic effect. *Polymer Gels and Networks, 4*(2), 129-142.
[88]Dong, Liang-Chang, & Hoffman, Allan S. (1990). Synthesis and application of thermally reversible heterogels for drug delivery. *Journal of Controlled Release, 13*(1), 21-31.
[89]Galaev, Igor Yu. (1995). 'Smart'polymers in biotechnology and medicine. *Russian Chemical Reviews, 64*(5), 471.
[90]Taylor, Lloyd D, & Cerankowski, Leon D. (1975). Preparation of films exhibiting a balanced temperature dependence to permeation by aqueous solutions—a study of lower consolute behavior. *Journal of Polymer Science: Polymer Chemistry Edition, 13*(11), 2551-2570.
[91]Pfohl, Oliver, Hino, Toshiaki, & Prausnitz, John M. (1995). Solubilities of styrene-based polymers and copolymers in common solvents. *Polymer, 36*(10), 2065-2073.
[92]Freeman, PI, & Rowlinson, JS. (1960). Lower critical points in polymer solutions. *Polymer, 1*, 20-26.
[93]Magnaghi, Valerio, Conte, Vincenzo, Procacci, Patrizia, Pivato, Giorgio, Cortese, Paolo, Cavalli, Erika, Pajardi, Giorgio, Ranucci, Elisabetta, Fenili, Fabio, & Manfredi, Amedea. (2011). Biological performance of a novel biodegradable polyamidoamine

hydrogel as guide for peripheral nerve regeneration. *Journal of Biomedical Materials Research Part A, 98*(1), 19-30.
[94]Slaughter, Brandon V, Khurshid, Shahana S, Fisher, Omar Z, Khademhosseini, Ali, & Peppas, Nicholas A. (2009). Hydrogels in regenerative medicine. *Advanced Materials, 21*(32-33), 3307-3329.
[95]Salamone, Joseph C. (1998). *Concise polymeric materials encyclopedia* (Vol. 1): CRC press.
[96]Ferruti, Paolo, Manzoni, Sara, Richardson, Simon CW, Duncan, Ruth, Pattrick, Nicola G, Mendichi, Raniero, & Casolaro, Mario. (2000). Amphoteric linear poly (amido-amine) s as endosomolytic polymers: Correlation between physicochemical and biological properties. *Macromolecules, 33*(21), 7793-7800.
[97]Ulijn, Rein V, Bibi, Nurguse, Jayawarna, Vineetha, Thornton, Paul D, Todd, Simon J, Mart, Robert J, Smith, Andrew M, & Gough, Julie E. (2007). Bioresponsive hydrogels. *Materials today, 10*(4), 40-48.
[98]Franchini, Jacopo, Ranucci, Elisabetta, Ferruti, Paolo, Rossi, Manuela, & Cavalli, Roberta. (2006). Synthesis, physicochemical properties, and preliminary biological characterizations of a novel amphoteric agmatine-based poly (amidoamine) with rgd-like repeating units. *Biomacromolecules, 7*(4), 1215-1222.
[99]Jacchetti, Emanuela, Emilitri, Elisa, Rodighiero, Simona, Indrieri, Marco, Gianfelice, Antonella, Lenardi, Cristina, Podestà, Alessandro, Ranucci, Elisabetta, Ferruti, Paolo, & Milani, Paolo. (2008). Biomimetic poly (amidoamine) hydrogels as synthetic materials for cell culture. *Journal of nanobiotechnology, 6*(1), 14.
[100]Shi, Junbin, Ouyang, Jun, Li, Qintao, Wang, Leyu, Wu, Jun, Zhong, Wen, & Xing, Malcolm MQ. (2012). Cell-compatible hydrogels based on a multifunctional crosslinker with tunable stiffness for tissue engineering. *Journal of Materials Chemistry, 22*(45), 23952-23962.
[101]Ekenseair, Adam K, Boere, Kristel WM, Tzouanas, Stephanie N, Vo, Tiffany N, Kasper, F Kurtis, & Mikos, Antonios G. (2012). Synthesis and characterization of thermally and chemically gelling injectable hydrogels for tissue engineering. *Biomacromolecules, 13*(6), 1908-1915.
[102]Urban, Marek W. (2012). Dynamic materials: The chemistry of self-healing. *Nature chemistry, 4*(2), 80-82.
[103]Imato, Keiichi, Nishihara, Masamichi, Kanehara, Takeshi, Amamoto, Yoshifumi, Takahara, Atsushi, & Otsuka, Hideyuki. (2012). Self-healing of chemical gels cross-linked by diarylbibenzofuranone-based trigger-free dynamic covalent bonds at room temperature. *Angewandte Chemie International Edition, 51*(5), 1138-1142.
[104]Bigi, Franca, Chesini, Luca, Maggi, Raimondo, & Sartori, Giovanni. (1999). Montmorillonite ksf as an inorganic, water stable, and reusable catalyst for the knoevenagel synthesis of coumarin-3-carboxylic acids. *The Journal of organic chemistry, 64*(3), 1033-1035.
[105]Maggi, Raimondo, Bigi, Franca, Carloni, Silvia, Mazzacani, Alessandro, &

Sartori, Giovanni. (2001). Uncatalysed reactions in water: Part 2. Part 1: Ref. 1. Preparation of 3-carboxycoumarins. *Green chemistry, 3*(4), 173-174.
[106]Albini, Angelo, & Fagnoni, Maurizio. (2004). Green chemistry and photochemistry were born at the same time. *Green Chemistry, 6*(1), 1-6.
[107]Graf, C, Schärtl, W, & Hugenberg, N. (2000). Photoinduced cluster formation of coumarin-labeled organosilicon micronetworks. *Advanced Materials, 12*(18), 1353-1356.
[108]Mal, Nawal Kishor, Fujiwara, Masahiro, & Tanaka, Yuko. (2003). Photocontrolled reversible release of guest molecules from coumarin-modified mesoporous silica. *Nature, 421*(6921), 350-353.
[109]Hara, Kohjiro, Wang, Zhong-Sheng, Sato, Tadatake, Furube, Akihiro, Katoh, Ryuzi, Sugihara, Hideki, Dan-oh, Yasufumi, Kasada, Chiaki, Shinpo, Akira, & Suga, Sadaharu. (2005). Oligothiophene-containing coumarin dyes for efficient dye-sensitized solar cells. *The Journal of Physical Chemistry B, 109*(32), 15476-15482.
[110]Brun, Marie-Priscille, Bischoff, Laurent, & Garbay, Christiane. (2004). A very short route to enantiomerically pure coumarin-bearing fluorescent amino acids. *Angewandte Chemie International Edition, 43*(26), 3432-3436.
[111]Zhao, Lihua, Vaupel, Matthias, Loy, Douglas A, & Shea, Kenneth J. (2008). Photoresponsive hybrid materials: Synthesis and characterization of coumarin-dimer-bridged polysilsesquioxanes. *Chemistry of Materials, 20*(5), 1870-1876.
[112]Liedtke, Alicia, O'Neill, Mary, Wertmöller, Anke, Kitney, Stuart P, & Kelly, Stephen M. (2008). White-light oleds using liquid crystal polymer networks. *Chemistry of Materials, 20*(11), 3579-3586.
[113]Chen, Ming, Ghiggino, Kenneth P, Launikonis, Anton, Mau, Albert WH, Rizzardo, Ezio, Sasse, Wolfgang HF, Thang, San H, & Wilson, Gerard J. (2003). Raft synthesis of linear and star-shaped light harvesting polymers using di-and hexafunctional ruthenium polypyridine reagents. *Journal of Materials Chemistry, 13*(11), 2696-2700.
[114]Trajkovska, Anita, Kim, Chunki, Marshall, Kenneth L, Mourey, Thomas H, & Chen, Shaw H. (2006). Photoalignment of a nematic liquid crystal fluid and glassy-nematic oligofluorenes on coumarin-containing polymer films. *Macromolecules, 39*(20), 6983-6989.
[115]Karthikeyan, S, & Ramamurthy, V. (2006). Templating photodimerization of coumarins within a water-soluble nano reaction vessel. *The Journal of organic chemistry, 71*(17), 6409-6413.
[116]Russell, Glen A, & Pecoraro, Joseph M. (1979). Electron transfer processes. 20. Conversion to p, p'-dinitrostilbene and other examples of the srn1 substitution reactions of p-nitrobenzyl derivatives. *Journal of the American Chemical Society, 101*(12), 3331-3334.

[117]Trenor, Scott R, Shultz, Allan R, Love, Brian J, & Long, Timothy E. (2004). Coumarins in polymers: From light harvesting to photo-cross-linkable tissue scaffolds. *Chemical reviews, 104*(6), 3059-3078.
[118]Ren, Biye, Zhao, Dongli, Liu, Shanshan, Liu, Xingxing, & Tong, Zhen. (2007). Synthesis and characterization of poly (ferrocenylsilanes) with coumarin side groups and their photochemical reactivity and electrochemical behavior. *Macromolecules, 40*(13), 4501-4508.
[119]Peng, Qian, Soler, Ana Maria, Warloe, Trond, Nesland, Jahn M, & Giercksky, Karl-Erik. (2001). Selective distribution of porphyrins in skin thick basal cell carcinoma after topical application of methyl 5-aminolevulinate. *Journal of Photochemistry and Photobiology B: Biology, 62*(3), 140-145.
[120]Haupt, Karsten, Mayes, Andrew G, & Mosbach, Klaus. (1998). Herbicide assay using an imprinted polymer-based system analogous to competitive fluoroimmunoassays. *Analytical Chemistry, 70*(18), 3936-3939.
[121]Graf, Christina, Schärtl, Wolfgang, Fischer, Karl, Hugenberg, Norbert, & Schmidt, Manfred. (1999). Dye-labeled poly (organosiloxane) microgels with core-shell architecture. *Langmuir, 15*(19), 6170-6180.
[122]Haupt, Karsten, Dzgoev, Anatoli, & Mosbach, Klaus. (1998). Assay system for the herbicide 2, 4-dichlorophenoxyacetic acid using a molecularly imprinted polymer as an artificial recognition element. *Analytical chemistry, 70*(3), 628-631.
[123]He, Jie, Tong, Xia, & Zhao, Yue. (2009). Photoresponsive nanogels based on photocontrollable cross-links. *Macromolecules, 42*(13), 4845-4852.
[124]He, Jie, Yan, Bin, Tremblay, Luc, & Zhao, Yue. (2010). Both core-and shell-cross-linked nanogels: Photoinduced size change, intraparticle lcst, and interparticle ucst thermal behaviors. *Langmuir, 27*(1), 436-444.
[125]Oshovsky, Gennady V, Reinhoudt, David N, & Verboom, Willem. (2007). Supramolecular chemistry in water. *Angewandte Chemie International Edition, 46*(14), 2366-2393.
[126]Ariga, Katsuhiko, Hill, Jonathan P, Lee, Michael V, Vinu, Ajayan, Charvet, Richard, & Acharya, Somobrata. (2008). Challenges and breakthroughs in recent research on self-assembly. *Science and Technology of Advanced Materials, 9*(1), 014109.
[127]Harada, Akira, Hashidzume, Akihito, Yamaguchi, Hiroyasu, & Takashima, Yoshinori. (2009). Polymeric rotaxanes. *Chemical reviews, 109*(11), 5974-6023.
[128]Zayed, Jameel M, Nouvel, Nicolas, Rauwald, Urs, & Scherman, Oren A. (2010). Chemical complexity—supramolecular self-assembly of synthetic and biological building blocks in water. *Chemical Society Reviews, 39*(8), 2806-2816.
[129]Uhlenheuer, Dana A, Petkau, Katja, & Brunsveld, Luc. (2010). Combining supramolecular chemistry with biology. *Chemical Society Reviews, 39*(8), 2817-2826.
[130]Bowden, Ned, Terfort, Andreas, Carbeck, Jeff, & Whitesides, George M. (1997). Self-assembly of mesoscale objects into ordered two-dimensional arrays. *Science,*

276(5310), 233-235.
[131]Tien, Joe, Terfort, Andreas, & Whitesides, George M. (1997). Microfabrication through electrostatic self-assembly. *Langmuir, 13*(20), 5349-5355.
[132]Grzybowski, Bartosz A, Winkleman, Adam, Wiles, Jason A, Brumer, Yisroel, & Whitesides, George M. (2003). Electrostatic self-assembly of macroscopic crystals using contact electrification. *Nature materials, 2*(4), 241-245.
[133]Gartner, Zev J, & Bertozzi, Carolyn R. (2009). Programmed assembly of 3-dimensional microtissues with defined cellular connectivity. *Proceedings of the National Academy of Sciences, 106*(12), 4606-4610.
[134]Harada, Akira, Kobayashi, Ryosuke, Takashima, Yoshinori, Hashidzume, Akihito, & Yamaguchi, Hiroyasu. (2010). Macroscopic self-assembly through molecular recognition. *Nature chemistry, 3*(1), 34-37.
[135]Yamaguchi, Hiroyasu, Kobayashi, Ryosuke, Takashima, Yoshinori, Hashidzume, Akihito, & Harada, Akira. (2011). Self-assembly of gels through molecular recognition of cyclodextrins: Shape selectivity for linear and cyclic guest molecules. *Macromolecules, 44*(8), 2395-2399.
[136]Joralemon, Maisie J, McRae, Samantha, & Emrick, Todd. (2010). Pegylated polymers for medicine: From conjugation to self-assembled systems. *Chemical Communications, 46*(9), 1377-1393.
[137]Cruise, Gregory M, Scharp, David S, & Hubbell, Jeffrey A. (1998). Characterization of permeability and network structure of interfacially photopolymerized poly (ethylene glycol) diacrylate hydrogels. *Biomaterials, 19*(14), 1287-1294.
[138]West, Jennifer L, & Hubbell, Jeffrey A. (1999). Polymeric biomaterials with degradation sites for proteases involved in cell migration. *Macromolecules, 32*(1), 241-244.
[139]Mann, Brenda K, Gobin, Andrea S, Tsai, Annabel T, Schmedlen, Rachael H, & West, Jennifer L. (2001). Smooth muscle cell growth in photopolymerized hydrogels with cell adhesive and proteolytically degradable domains: Synthetic ecm analogs for tissue engineering. *Biomaterials, 22*(22), 3045-3051.
[140]Bryant, Stephanie J, & Anseth, Kristi S. (2001). The effects of scaffold thickness on tissue engineered cartilage in photocrosslinked poly (ethylene oxide) hydrogels. *Biomaterials, 22*(6), 619-626.
[141]Kovar, J, Wang, Ying, Simpson, Melanie A, & Olive, D Michael. (2009). Imaging lymphatics with a variety of near-infrared labeled optical agents. *World Mol Imaging, 56*, 67-68.
[142]Stavisky, Ronda C, Britt, Joshua M, Zuzek, Aleksej, Truong, Elizabeth, & Bittner, George D. (2005). Melatonin enhances the in vitro and in vivo repair of severed rat sciatic axons. *Neuroscience letters, 376*(2), 98-101.
[143]Heskins, Michael, & Guillet, James E. (1968). Solution properties of poly (n-isopropylacrylamide). *Journal of Macromolecular Science—Chemistry, 2*(8),

1441-1455.
[144]Hoffman, Allan S. (1995). *"Intelligent" polymers in medicine and biotechnology.* Paper presented at the Macromolecular symposia.
[145]Winnik, Francoise M. (1990). Fluorescence studies of aqueous solutions of poly (n-isopropylacrylamide) below and above their lcst. *Macromolecules, 23*(1), 233-242.
[146]Vesterinen, Elina, Tenhu, Heikki, & Dobrodumov, Anatoli. (1994). Poly (< i> n</i>-isopropyl acrylamide) derivatives with pendent sulfonic acid groups and nitroxide radicals. *Polymer, 35*(22), 4852-4856.
[147]Schild, Howard G, & Tirrell, David A. (1991). Interaction of poly (n-isopropylacrylamide) with sodium n-alkyl sulfates in aqueous solution. *Langmuir, 7*(4), 665-671.
[148]Meewes, M, Ricka, J, De Silva, M, Nyffenegger, R, & Binkert, Th. (1991). Coil-globule transition of poly (n-isopropylacrylamide): A study of surfactant effects by light scattering. *Macromolecules, 24*(21), 5811-5816.
[149]Han, Chang Kwon, & Bae, You Han. (1998). Inverse thermally-reversible gelation of aqueous< i> n</i>-isopropylacrylamide copolymer solutions. *Polymer, 39*(13), 2809-2814.
[150]Lu, Tao, Vesterinen, Elina, & Tenhu, Heikki. (1998). Dynamic light scattering studies on polyelectrolytic derivatives of poly (< i> n</i>-isopropylacrylamide). *Polymer, 39*(3), 641-650.
[151]Qiu, Xingping, Li, Mei, Kwan, Chi Man Simon, & Wu, Chi. (1998). Light-scattering study of the coil-to-globule transition of linear poly (n-isopropylacrylamide) ionomers in water. *Journal of Polymer Science-B-Polymer Physics Edition, 36*(9), 1501-1506.
[152]Larsson, Anders, Kuckling, Dirk, & Schönhoff, Monika. (2001). 1h nmr of thermoreversible polymers in solution and at interfaces: The influence of charged groups on the phase transition. *Colloids and Surfaces A: Physicochemical and Engineering Aspects, 190*(1), 185-192.
[153]Kuckling, Dirk, Adler, Hans-Jürgen P, Arndt, Karl-Friedrich, Ling, Long, & Habicher, Wolf D. (2000). Temperature and ph dependent solubility of novel poly (n-isopropylacrylamide)-copolymers. *Macromolecular Chemistry and Physics, 201*(2), 273-280.
[154]Jean, B, Lee, L-T, & Cabane, B. (2000). Interactions of sodium dodecyl sulfate with acrylamide–n-isopropylacrylamide) statistical copolymer. *Colloid and Polymer Science, 278*(8), 764-770.
[155]Lee, Lay-Theng, & Cabane, Bernard. (1997). Effects of surfactants on thermally collapsed poly (n-isopropylacrylamide) macromolecules. *Macromolecules, 30*(21), 6559-6566.
[156]Tiktopulo, EI, Bychkova, VE, Ricka, J, & Ptitsyn, OB. (1994). Cooperativity of the coil-globule transition in a homopolymer: Microcalorimetric study of poly (n-isopropylacrylamide). *Macromolecules, 27*(10), 2879-2882.

[157]Shibayama, Mitsuhiro, & Tanaka, Toyoichi. (1993). Volume phase transition and related phenomena of polymer gels *Responsive gels: Volume transitions i* (pp. 1-62): Springer.
[158]Murray, MJ, & Snowden, MJ. (1995). The preparation, characterisation and applications of colloidal microgels. *Advances in colloid and interface science, 54*, 73-91.
[159]Okahata, Yoshio, Noguchi, Hioshi, & Seki, Takahiro. (1986). Thermoselective permeation from a polymer-grafted capsule membrane. *Macromolecules, 19*(2), 493-494.
[160]Taylor, Lloyd D, & Cerankowski, LD. (1975). Preparation of films ex- ovarian carcinoma cells by pluronic p85 block copolymer, hibiting a balanced temperature dependence to permeation bioconj. Chem. 7 (1996) 209–216. By aqueous solutions: A study of lower consolute behavior,[142] gs kwon, t. Okano, soluble self-assembled block co. *J. Polym. Sci. Part A: Polym. Chem, 13*, 2551-2570.
[161]Bergbreiter, David E, Case, Brenda L, Liu, Yun-Shan, & Caraway, John W. (1998). Poly (n-isopropylacrylamide) soluble polymer supports in catalysis and synthesis. *Macromolecules, 31*(18), 6053-6062.
[162]Daughton, Christian G. (1988). Quantitation of acrylamide (and polyacrylamide): Critical review of methods for trace determination/formulation analysis and future-research recommendations. Final report: Daughton (Christian G.), Orinda, CA (USA).
[163]Guaraldi, Giovanni, Orlando, Gabriella, De, FD, De, L, Rottino, Antonio, & De, SG. (2005). Comparison of three different interventions for the correction of hiv-associated facial lipoatrophy: A prospective study. *Antiviral therapy, 10*(6), 753.
[164]Lee, CR, Grodzinsky, AJ, & Spector, M. (2001). The effects of cross-linking of collagen-glycosaminoglycan scaffolds on compressive stiffness, chondrocyte-mediated contraction, proliferation and biosynthesis. *Biomaterials, 22*(23), 3145-3154.
[165]Park, Si-Nae, Park, Jong-Chul, Kim, Hea Ok, Song, Min Jung, & Suh, Hwal. (2002). Characterization of porous collagen/hyaluronic acid scaffold modified by 1-ethyl-3-(3-dimethylaminopropyl) carbodiimide cross-linking. *Biomaterials, 23*(4), 1205-1212.
[166]Schoof, Heike, Apel, Jörn, Heschel, Ingo, & Rau, Günter. (2001). Control of pore structure and size in freeze-dried collagen sponges. *Journal of biomedical materials research, 58*(4), 352-357.
[167]Tan, Wei, Krishnaraj, Raj, & Desai, Tejal A. (2001). Evaluation of nanostructured composite collagen-chitosan matrices for tissue engineering. *Tissue engineering, 7*(2), 203-210.
[168]Chen, Guoping, Ushida, Takashi, & Tateishi, Tetsuya. (2001). Development of biodegradable porous scaffolds for tissue engineering. *Materials Science and Engineering: C, 17*(1), 63-69.

[169]Huang, Lei, Nagapudi, Karthik, P. Apkarian, Robert, & Chaikof, Elliot L. (2001). Engineered collagen–peo nanofibers and fabrics. *Journal of biomaterials science, Polymer edition, 12*(9), 979-993.
[170]Staudinger, H, & Husemann, E. (1935). Über hochpolymere verbindungen, 118. Mitteil.: Viscositäts-untersuchungen an organischen sphäro-und linear-kolloiden. *Berichte der deutschen chemischen Gesellschaft (A and B Series), 68*(9), 1691-1697.
[171]Pelton, RH, & Chibante, P. (1986). Preparation of aqueous latices with< i> n</i>-isopropylacrylamide. *Colloids and Surfaces, 20*(3), 247-256.
[172]Pelton, RH, Pelton, HM, Morphesis, A, & Rowell, RL. (1989). Particle sizes and electrophoretic mobilities of poly (n-isopropylacrylamide) latex. *Langmuir, 5*(3), 816-818.
[173]McPhee, Wayne, Tam, Kam Chiu, & Pelton, Robert. (1993). Poly (< i> n</i>-isopropylacrylamide) latices prepared with sodium dodecyl sulfate. *Journal of colloid and interface science, 156*(1), 24-30.
[174]Wu, X, Pelton, RH, Hamielec, AE, Woods, DR, & McPhee, W. (1994). The kinetics of poly (n-isopropylacrylamide) microgel latex formation. *Colloid and polymer science, 272*(4), 467-477.
[175]Vo, C Duan, Kuckling, D, Adler, H-JP, & Schönhoff, M. (2002). Preparation of thermosensitive nanogels by photo-cross-linking. *Colloid and Polymer Science, 280*(5), 400-409.
[176]Pelton, Robert. (2000). Temperature-sensitive aqueous microgels. *Advances in colloid and interface science, 85*(1), 1-33.
[177]Murray, Mary, Rana, Friduddin, Haq, Ihtshamul, Cook, Janice, Chowdhry, Babur Z, & Snowden, Martin J. (1994). Colloidal microgel systems: Phase transition properties in aqueous solution of poly (n-isopropylacrylamide). *J. Chem. Soc., Chem. Commun.*(15), 1803-1804.
[178]Snowden, Martin J, Chowdhry, Babur Z, Vincent, Brian, & Morris, Gayle E. (1996). Colloidal copolymer microgels of n-isopropylacrylamide and acrylic acid: Ph, ionic strength and temperature effects. *J. Chem. Soc., Faraday Trans., 92*(24), 5013-5016.
[179]Duracher, D, Elaissari, A, & Pichot, C. (1999). Characterization of cross-linked poly (n-isopropylmethacrylamide) microgel latexes. *Colloid and Polymer Science, 277*(10), 905-913.
[180]Jones, Clinton D, & Lyon, L Andrew. (2000). Synthesis and characterization of multiresponsive core-shell microgels. *Macromolecules, 33*(22), 8301-8306.
[181]Doria-Serrano, MC, Ruiz-Trevino, FA, Rios-Arciga, C, Hernandez-Esparza, M, & Santiago, P. (2001). Physical characteristics of poly (vinyl alcohol) and calcium alginate hydrogels for the immobilization of activated sludge. *Biomacromolecules, 2*(2), 568-574.
[182]Ulanski, Piotr, Janik, Ireneusz, Kadlubowski, Slawomir, Kozicki, Marek, Kujawa, Piotr, Pietrzak, Miroslaw, Stasica, Przemyslaw, & Rosiak, Janusz M. (2002).

Polymeric biomaterials synthesized by radiation techniques–current studies at iarc, poland. *Polymers for Advanced Technologies, 13*(10-12), 951-959.
[183]Braun, O, Selb, J, & Candau, F. (2001). Synthesis in microemulsion and characterization of stimuli-responsive polyelectrolytes and polyampholytes based on< i> n</i>-isopropylacrylamide. *Polymer, 42*(21), 8499-8510.
[184]Renken, Andreas, & Hunkeler, David. (1999). Effect of the surfactant blend composition on the properties of polymerizing acrylamide-based inverse-emulsions: Characterization by small-angle neutron scattering and quasi-elastic light scattering. *Polymer, 40*(12), 3545-3554.
[185]Acosta, Edgar J, Nguyen, Thu, Witthayapanyanon, Anuradee, Harwell, Jeffrey H, & Sabatini, David A. (2005). Linker-based bio-compatible microemulsions. *Environmental science & technology, 39*(5), 1275-1282.
[186]Ichimura, Kunihiro, & Watanabe, Shoji. (1982). Preparation and characteristics of photocross-linkable poly (vinyl alcohol). *Journal of Polymer Science: Polymer Chemistry Edition, 20*(6), 1419-1432.
[187]Ichimura, Kunihiro, & Komatsu, Toshio. (1987). Novel method for preparation of photocrosslinkable poly (vinyl alcohol). *Journal of Polymer Science Part A: Polymer Chemistry, 25*(6), 1475-1480.
[188]Nakayama, Yasuhide, & Matsuda, Takehisa. (1992). Preparation and characteristics of photocrosslinkable hydrophilic polymer having cinnamate moiety. *Journal of Polymer Science Part A: Polymer Chemistry, 30*(11), 2451-2457.
[189]Cockburn, Eleanor S, Davidson, R Stephen, & Pratt, Julie E. (1996). The photocrosslinking of styrylpyridinium salts via a [2+ 2]-cycloaddition reaction. *Journal of Photochemistry and Photobiology A: Chemistry, 94*(1), 83-88.
[190]Coqueret, Xavier. (1999). Photoreactivity of polymers with dimerizable side-groups: Kinetic analysis for probing morphology and molecular organization. *Macromolecular Chemistry and Physics, 200*(7), 1567-1579.
[191]Kuckling, Dirk, Adler, Hans-Jürgen P, Arndt, Karl-Friedrich, Hoffmann, Jan, Plötner, Matthias, & Wolff, Thomas. (1999). Photocrosslinking of thin films of temperature-sensitive polymers. *Polymers for advanced technologies, 10*(6), 345-352.
[192]Ivanova, Irina G, Kuckling, Dirk, Adler, Hans-Jürgen P, Wolff, Thomas, & Arndt, Karl-Friedrich. (2000). Preparation and properties of thin films of photocrosslinkable hydrophilic polymers. *Designed Monomers and Polymers, 3*(4), 447-462.
[193]Hoffmann, Jan, Plötner, Matthias, Kuckling, Dirk, & Fischer, Wolf-Joachim. (1999). Photopatterning of thermally sensitive hydrogels useful for microactuators. *Sensors and Actuators A: Physical, 77*(2), 139-144.
[194]Arndt, Karl-Friedrich, Kuckling, Dirk, & Richter, Andreas. (2000). Application of sensitive hydrogels in flow control. *Polymers for Advanced Technologies, 11*(8-12), 496-505.
[195]Guan, Ying, & Zhang, Yongjun. (2011). Pnipam microgels for biomedical applications: From dispersed particles to 3d assemblies. *Soft Matter, 7*(14),

6375-6384.
[196]Li, Chengming, Madsen, Jeppe, Armes, Steven P, & Lewis, Andrew L. (2006). A new class of biochemically degradable, stimulus-responsive triblock copolymer gelators. *Angewandte Chemie International Edition, 45*(21), 3510-3513.
[197]Das, Mallika, Mardyani, Sawitri, Chan, WCW, & Kumacheva, E. (2006). Biofunctionalized ph-responsive microgels for cancer cell targeting: Rational design. *Advanced Materials, 18*(1), 80-83.
[198]Kim, Jongseong, Nayak, Satish, & Lyon, L Andrew. (2005). Bioresponsive hydrogel microlenses. *Journal of the American Chemical Society, 127*(26), 9588-9592.
[199]Kim, Soyeon, Chung, Eugene H, Gilbert, Michele, & Healy, Kevin E. (2005). Synthetic mmp-13 degradable ecms based on poly (n-isopropylacrylamide-co-acrylic acid) semi-interpenetrating polymer networks. I. Degradation and cell migration. *Journal of Biomedical Materials Research Part A, 75*(1), 73-88.
[200]Chen, Ko-Shao, Tsai, Jui-Che, Chou, Chih-Wei, Yang, Mu-Rong, & Yang, Jen-Ming. (2002). Effects of additives on the photo-induced grafting polymerization of< i> n</i>-isopropylacrylamide gel onto pet film and pp nonwoven fabric surface. *Materials Science and Engineering: C, 20*(1), 203-208.
[201]Zhong, Chao, Wu, Jun, Reinhart-King, CA, & Chu, CC. (2010). Synthesis, characterization and cytotoxicity of photo-crosslinked maleic chitosan–polyethylene glycol diacrylate hybrid hydrogels. *Acta biomaterialia, 6*(10), 3908-3918.
[202]Zhao, Changwen, Zhuang, Xiuli, He, Pan, Xiao, Chunsheng, He, Chaoliang, Sun, Jingru, Chen, Xuesi, & Jing, Xiabin. (2009). Synthesis of biodegradable thermo-and ph-responsive hydrogels for controlled drug release. *Polymer, 50*(18), 4308-4316.
[203]Casadio, Ylenia S, Brown, David H, Chirila, Traian V, Kraatz, Heinz-Bernhard, & Baker, Murray V. (2010). Biodegradation of poly (2-hydroxyethyl methacrylate)(phema) and poly {(2-hydroxyethyl methacrylate)-co-[poly (ethylene glycol) methyl ether methacrylate]} hydrogels containing peptide-based cross-linking agents. *Biomacromolecules, 11*(11), 2949-2959.
[204]Sahoo, Sujata, Chung, Cindy, Khetan, Sudhir, & Burdick, Jason A. (2008). Hydrolytically degradable hyaluronic acid hydrogels with controlled temporal structures. *Biomacromolecules, 9*(4), 1088-1092.
[205]Rowley, Jon A, & Mooney, David J. (2002). Alginate type and rgdrgdr density control myoblast phenotype. *Journal of biomedical materials research, 60*(2), 217-223.
[206]Kong, Hyun Joon, Boontheekul, Tanyarut, & Mooney, David J. (2006). Quantifying the relation between adhesion ligand–receptor bond formation and cell phenotype. *Proceedings of the National Academy of Sciences, 103*(49), 18534-18539.
[207]Emilitri, Elisa, Ranucci, Elisabetta, & Ferruti, Paolo. (2005). New poly (amidoamine) s containing disulfide linkages in their main chain. *Journal of Polymer Science Part A: Polymer Chemistry, 43*(7), 1404-1416.

[208]Guilak, Farshid, Cohen, Daniel M, Estes, Bradley T, Gimble, Jeffrey M, Liedtke, Wolfgang, & Chen, Christopher S. (2009). Control of stem cell fate by physical interactions with the extracellular matrix. *Cell stem cell, 5*(1), 17-26.
[209]Bershadsky, Alexander D, Balaban, Nathalie Q, & Geiger, Benjamin. (2003). Adhesion-dependent cell mechanosensitivity. *Annual review of cell and developmental biology, 19*(1), 677-695.
[210]Peppas, Nicholas A. (1987). *Hydrogels in medicine and pharmacy* (Vol. 3): CRC press Boca Raton, FL.
[211]Jhon, Mu Shik, & Andrade, J D_. (1973). Water and hydrogels. *Journal of biomedical materials research, 7*(6), 509-522.
[212]Ferruti, P, Ranucci, E, Sartore, L, Bignotti, F, Marchisio, MA, Bianciardi, P, & Veronese, FM. (1994). Recent results on functional polymers and macromonomers of interest as biomaterials or for biomaterial modification. *Biomaterials, 15*(15), 1235-1241.
[213]Ferruti, Paolo, Bianchi, Sabrina, Ranucci, Elisabetta, Chiellini, Federica, & Piras, Anna Maria. (2005). Novel agmatine-containing poly (amidoamine) hydrogels as scaffolds for tissue engineering. *Biomacromolecules, 6*(4), 2229-2235.
[214]Discher, Dennis E, Janmey, Paul, & Wang, Yu-li. (2005). Tissue cells feel and respond to the stiffness of their substrate. *Science, 310*(5751), 1139-1143.
[215]Jiang, Jinqiang, Qi, Bo, Lepage, Martin, & Zhao, Yue. (2007). Polymer micelles stabilization on demand through reversible photo-cross-linking. *Macromolecules, 40*(4), 790-792.
[216]Kim, Richard H, Shapiro, Howard S, Li, Jack J, Wrana, Jeffrey L, & Sodek, Jaro. (1994). Characterization of the human bone sialoprotein (bsp) gene and its promoter sequence. *Matrix Biology, 14*(1), 31-40.
[217]Babin, Jérôme, Pelletier, Maxime, Lepage, Martin, Allard, Jean-François, Morris, Denis, & Zhao, Yue. (2009). A new two-photon-sensitive block copolymer nanocarrier. *Angewandte Chemie International Edition, 48*(18), 3329-3332.
[218]Chun, ChangJu, Lim, Hye Jin, Hong, Ki-Yun, Park, Keun-Hong, & Song, Soo-Chang. (2009). The use of injectable, thermosensitive poly (organophosphazene)–rgd conjugates for the enhancement of mesenchymal stem cell osteogenic differentiation. *Biomaterials, 30*(31), 6295-6308.
[219]Wang, Kathryn X, & Denhardt, David T. (2008). Osteopontin: Role in immune regulation and stress responses. *Cytokine & growth factor reviews, 19*(5), 333-345.

Appendix

Reducible and photosensitive polyamidoamine-magnetic iron oxide nanoparticles for doxorubicin delivery

1. Introduction

As one of the major class of nanoscale materials, magnetic nanoparticles (MNPs) play an important role in current clinical diagnostic and therapeutic techniques. MNPs are able to function both at the cellular and molecular levels in biological interactions because of their special physical properties. For the MNPs can be the best choice not only for resonance imaging (MRI) contrast agents[1], but also for carriers for targeted drug delivery [2,3]. Early research in this field can be tracked back to several decades, currently research mostly focus on the applications in the detection, diagnosis, and drug carriers, for example, cancer [4], cardiovascular disease[5], and neurological disease [6]. Furthermore, much more advantages were found in using MNPs in clinical studies of cancer therapy [3,7] and human medicine [8,9]by attacking solid tumors through targeted retention of particles.

However, these nanoparticles are easy to gather due to their hydrophobic coating. In order to improve their dispersity and water solubility in biological environment, some surface modifications should be applied to them. For example, stabilize the nanoparticles in a biological suspension with a pH around 7.4 and a high salt

concentration; provide functional groups at the surface for further derivatization [11].

Coumarins are a class of molecules including several hundred derivatives. These molecules are naturally present in many plants and have also been synthesized via different routes [10,11]. They are used in various applications, including fragrances, medicines, drug delivery, and liquid crystalline polymers. Their photosensitivity was discovered one century ago [12].

Coumarin-containing polymers have also been well studied and widely applied in many fields, including biochemical, organic–inorganic hybrid materials, liquid crystalline materials, electro-optical materials, and light harvesting/energy transferring materials [13-20]. In addition, their photo-cleavage behavior and reversible photo crosslinking property have been widely investigated for the application of photo reversible materials [21-24]. The [2+2] cycloaddition of a couple of coumarin moieties leads to a cyclobutane ring under the irradiation of UVA wave band (320nm-400nm). (Scheme.1) While after irradiation of UVC lights (200–280 nm), the coumarin photodimers can be cleaved and regenerate the original coumarin moieties. Thus, polymers containing coumarin structural parts exhibit fast photo-responsibility and effective photo-reversible property with alternative irradiation of UV light at different wavelengths.

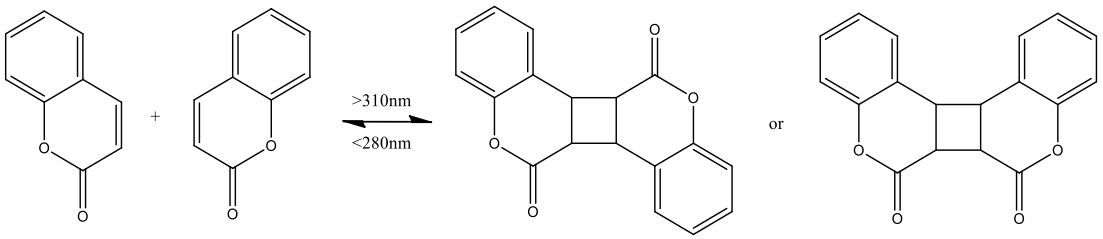

Scheme.1. Reversible photodimerization and photocleavage reactions of coumarin upon irradiation under wavelength greater than 310 nm and less than 280nm.

Biocompatibility is one of the most essential require for materials to applied as biomaterials, which means such materials will not induce severe host response in a specific application. However, in the past two decades, development also focus on the synthetic biodegradable polymers for biomedical applications. The driving force is the emergence of novel biomedical technologies, for example, tissue engineering, regenerative medicine, gene therapy, controlled drug delivery and bionanotechnology, all of which require biodegradable platform materials to build on [25].

Reducing glutathione (GSH) is one of the most abundant reducing molecule existing in intracellular compartments and extracellular environment [26-29]. Hence, the disulfide bonds, can be stable both under physiological conditions in the circulation and in extracellular tissues. A low concentration of GSH can be degraded by cells due to the high reductive environment [30].

Herein, we designed and synthesized a novel reducible polyamidoamine (rPAA) copolymer based on poly (ethylene glycol) (PEG), N, N’-bis (acryloyl) cystamine

(CBA) containing disulfide bonds in the backbone and coumarin methacrylate (CMA) contain photosensitive group. A series of reducible and photosensitive polyamidoamine-magnetic iron oxide nanoparticles were prepared, which can provide efficient drug loading, reduction-responsive and optical controlled drug release, and imaging capability. The extracellular release of DOX from these particles was studied. (Fig.1A)

2. Experimental part

2.1. Materials and instruments

All chemicals were purchased from Aldrich Chemical Co. (St. Louis, MO, US) and used without further purification unless otherwise noted. Methoxy PEG amine (mPEG-Amine) was purchased from JenKem Technology USA Inc. (Allen, TX, US). NMR studies were carried out using a Bruker AMX 300 NMR spectrophotometer.

2.2. Synthesis and characterization of copolymers

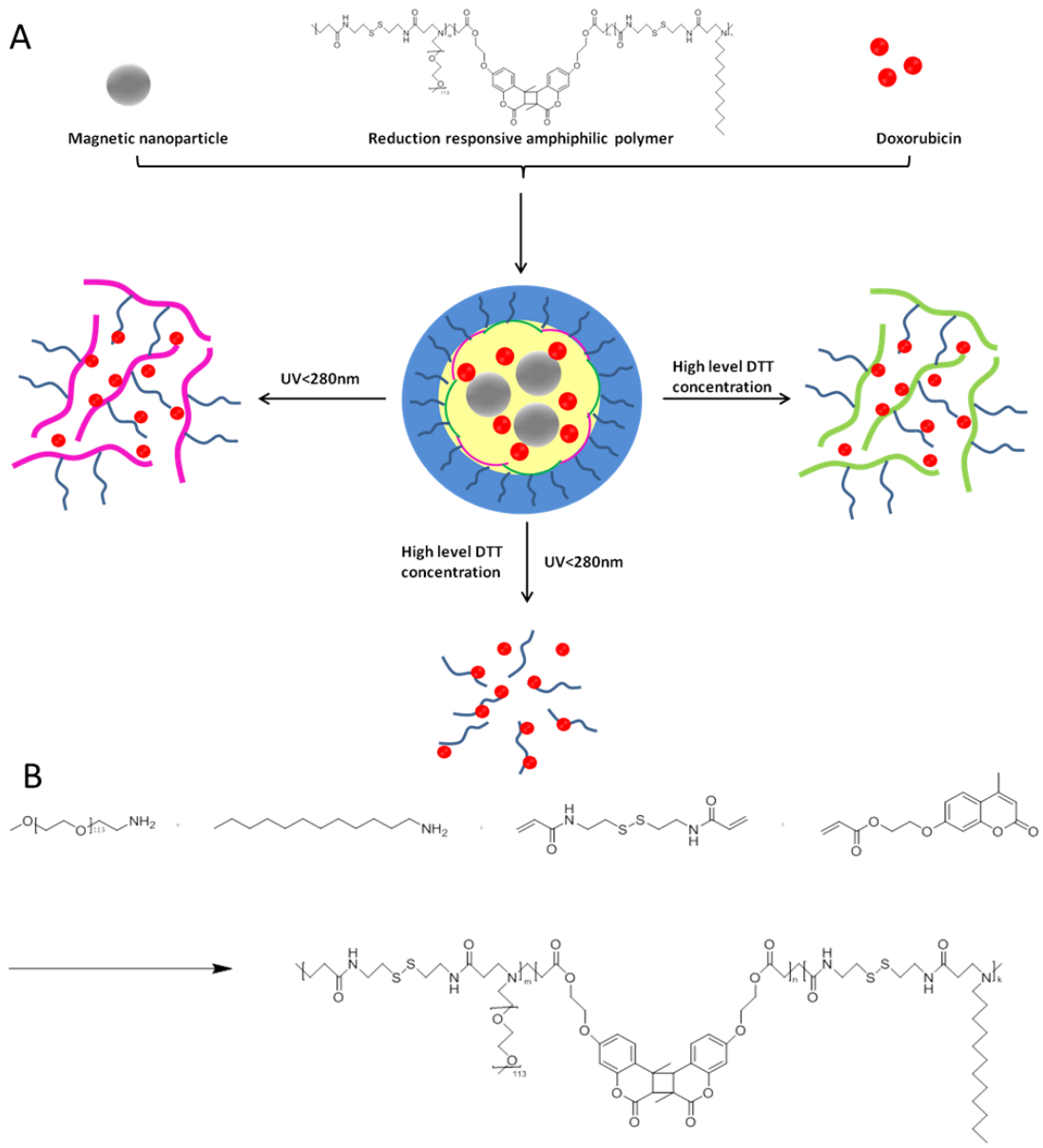

Fig. 1. A. The schematic illustration of the architecture of doxorubicin loaded reducible copolymer coated superparamagnetic iron oxide nanoparticles; B. The synthesis route of reducible polyamidoamine graft poly (ethylene glycol)/ coumarin methacrylate copolymers (rPAA).

The copolymers denoted as rPAA-CMA-PEG, was synthesized according to the routine shown in Fig. 1B. Cystamine bisacrylamide (CBA, 0.95 mmol), dodecylamine (DD,

0.9 mmol) and PEG (5 K)-amine (0.1 mmol) coumarin methacrylate (CMA, 0.05 mmol) were added in a two-neck bottle. The mixture was stirred for 72h at room temperature. And the mixture was dissolved by chloroform and was precipitated in the large excess amount of diethyl ether for twice and dried in vacuum. 1H NMR was recorded as show in Fig.2.

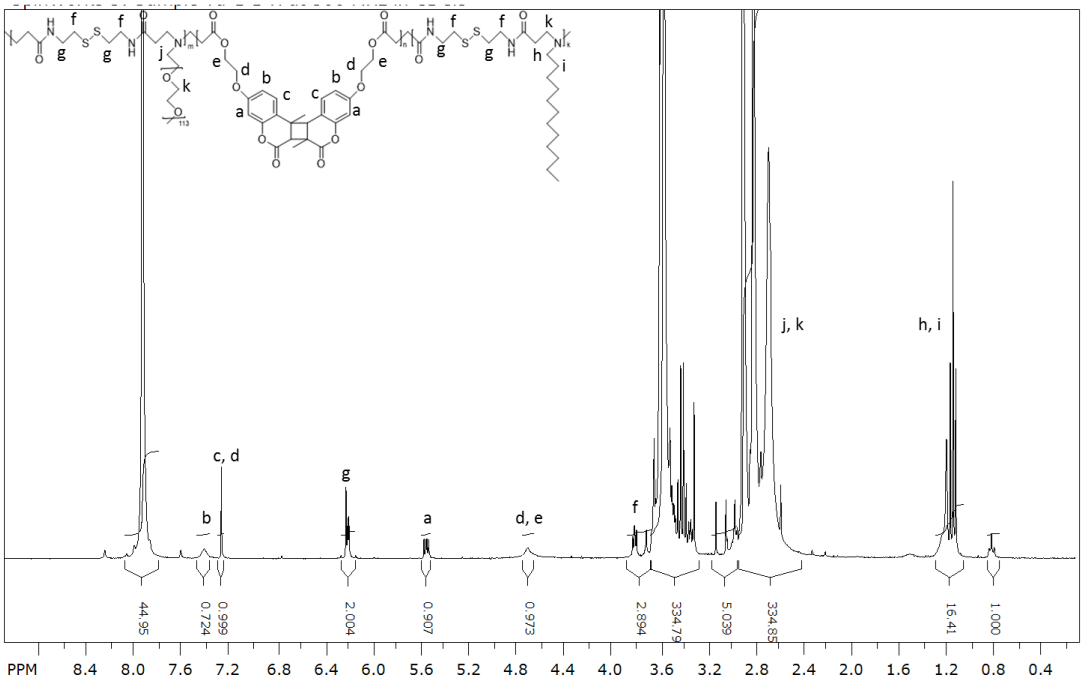

Fig.2. 1H NMR spectra of rPAA-CMA-PEG copolymer.

2.3. Synthesis of superparamagnetic iron oxide nanoparticles (MNPs)

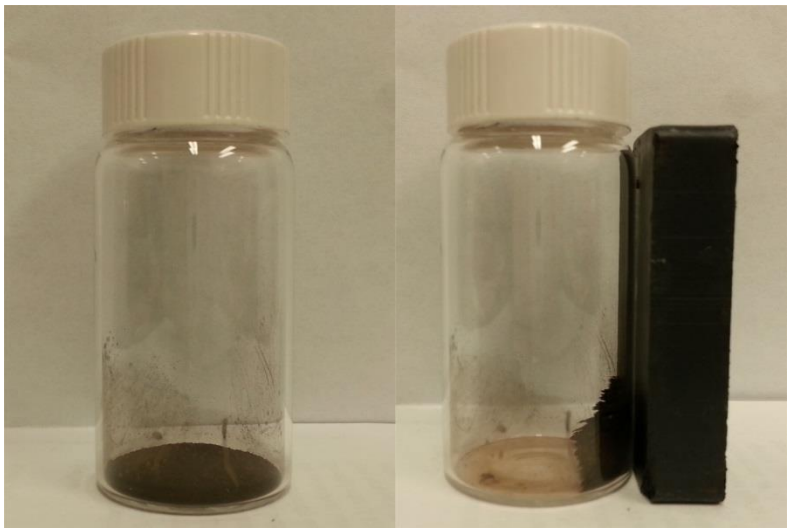

Fig.3. photo image of superparamagnetic iron oxide nanoparticles (MNPs)

The MNPs were synthesized as follows: $FeCl_3$ (about 0.0046 mol) and $Fe(NO_3)_2 \cdot 9H_2O$ (about 0.0023 mol) were dissolved in deionized water (15 mL) in a 25 mL three-necked flask and heated to the required temperature (45 °C). The solution was bubbled with nitrogen gas to prevent unwanted oxidation. Then ammonium hydroxide (2 mL, 25%) was added quickly in to the iron solution under vigorous stirring (800 rpm). After 1 h, the resulting Fe_3O_4 MNPs (black precipitate) were collected from the solution by magnetic separation and washed several times with deionized water and ethanol, then dried under vacuum conditions at 60 °C for 12 h. (Fig.3)

2.4. Preparation method of rPAA@MNPs

MNPs (1 mg) and rPAA-CMA-PEG (10 mg) were dissolved in 1ml Dichloromethane, Then 10 ml of distilled water was added to the above solution with vigorous sonication and the resulting colloid was stirred vigorously for 24 h to evaporate DCM. After that, the colloid was separated by centrifugation and the obtained rPAA@MNPs was washed

three times with distilled water to remove the unbound copolymer.

2.5. Drug loading and release profile

The DOX solution (3 mg/ml) was added to 1 ml of the above rPAA@MNPs solution in tetrahydrofuran, followed by slow addition of 10 ml phosphate buffer (20 mmol mL1, pH= 7.4). And the solution was shaken for 24 h to allow the DOX loaded into the nanoparticles. Then, the drug-loaded core-shell magnetic nanoparticles were separated from free DOX solution using a magnet.

2.6. In vitro DOX release from DOX/rPAA@MNPs

The reduction and optical control dependent DOX release measurements was conducted as below: dispersed DOX/rPAA@MNPs was added to a dialysis membrane tube (molecular weight cut-off =8000), then the tube was incubated in 10 ml phosphate buffer saline (PBS) at the concentration of Dithiothreitol (DTT) at 1 mmol or 10 mmol at 37 °C in a water bath with shaking rate at 80 rpm. At predetermined time, 5 ml incubated solution was taken out and 5 ml fresh PBS was added to refill the incubation solution to 10 ml. DOX release profiles was recorded by UV-vis absorbance of the solutions at 480 nm.

3. Results and discussion

3.1. In vitro doxorubicin release of DOX/rPAA@MNPs

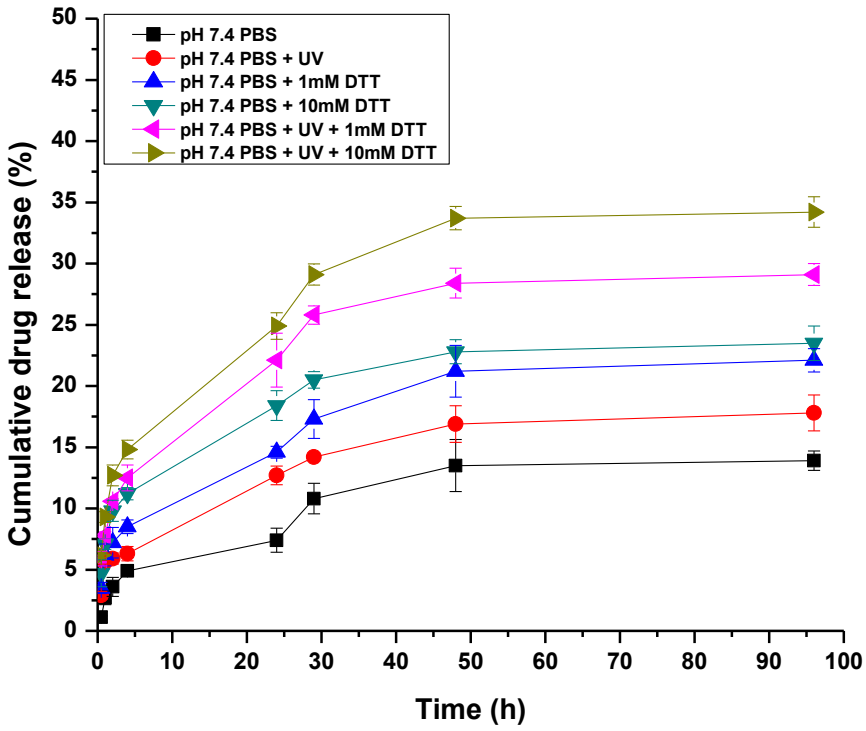

Fig. 4. The in vitro doxorubicin release of DOX/rPAA@MNPs in different concentration of DTT and UV treatment.

To evaluate the drug release efficiency of DOX/rPAA@MNPs, the nanoparticles were incubated in phosphate buffers with different concentrations of DTT and different optical controls to induce the degradation of rPAA copolymers, further to enhance the release of drugs. The drug release experiments were performed at DTT concentration of 0, 1 and 10 mM at 37 °C and two conditons of UV treatment (on/off). The concentrations were selected to mimic the reducing concentrations in circulation and cytoplasm. As shown in Fig. 4, the results showed that less than 5% of DOX was

released without DTT and UV irradiation in the first 5 h, and less than 15% of DOX was released after 48 h. Approximately 20% DOX loaded within the DOX/rPAA@MNPs was released in 48 h at 1 mM DTT or single UV irradiation. When the DTT concentration was elevated to 10 mM in addition with UV treatment, a fast release of DOX from the particles was detected, where more than 15% DOX was released in the first 5 h and over 30% DOX was released in 48 h. Drug steadily release until 96 hours.

Reference

[1]Corot, Claire, Robert, Philippe, Idée, Jean-Marc, & Port, Marc. (2006). Recent advances in iron oxide nanocrystal technology for medical imaging. *Advanced drug delivery reviews, 58*(14), 1471-1504.
[2]Pankhurst, Quentin A, Connolly, J, Jones, SK, & Dobson, J. (2003). Applications of magnetic nanoparticles in biomedicine. *Journal of physics D: Applied physics, 36*(13), R167.
[3]Dobson, Jon. (2006). Magnetic nanoparticles for drug delivery. *Drug development research, 67*(1), 55-60.
[4]Ferrari, Mauro. (2005). Cancer nanotechnology: Opportunities and challenges. *Nature Reviews Cancer, 5*(3), 161-171.
[5]Wickline, Samuel A, Neubauer, Anne M, Winter, Patrick M, Caruthers, Shelton D, & Lanza, Gregory M. (2007). Molecular imaging and therapy of atherosclerosis with targeted nanoparticles. *Journal of Magnetic Resonance Imaging, 25*(4), 667-680.
[6]Corot, Claire, Petry, Klaus G, Trivedi, Rikin, Saleh, Andreas, Jonkmanns, Cornelia, Le Bas, Jean-François, Blezer, Erwin, Rausch, Martin, Brochet, Bruno, & Foster-Gareau, Paula. (2004). Macrophage imaging in central nervous system and in carotid atherosclerotic plaque using ultrasmall superparamagnetic iron oxide in magnetic resonance imaging. *Investigative radiology, 39*(10), 619-625.
[7]Alexiou, Christoph, Arnold, Wolfgang, Klein, Roswitha J, Parak, Fritz G, Hulin, Peter, Bergemann, Christian, Erhardt, Wolfgang, Wagenpfeil, Stefan, & Luebbe, Andreas S. (2000). Locoregional cancer treatment with magnetic drug targeting. *Cancer research, 60*(23), 6641-6648.
[8]Zhang, JQ, Zhang, ZR, Yang, H, Tan, QY, Qin, SR, & Qiu, XL. (2005). Lyophilized paclitaxel magnetoliposomes as a potential drug delivery system for breast carcinoma via parenteral administration: In vitro and in vivo studies. *Pharmaceutical research,*

22(4), 573-583.
[9]Islam, Md Shariful. (2012). Development and evaluation of magnetic, photocatalytic and photothermal nanoparticles and their application to cancer therapy.
[10]Bigi, Franca, Chesini, Luca, Maggi, Raimondo, & Sartori, Giovanni. (1999). Montmorillonite ksf as an inorganic, water stable, and reusable catalyst for the knoevenagel synthesis of coumarin-3-carboxylic acids. *The Journal of organic chemistry, 64*(3), 1033-1035.
[11]Maggi, Raimondo, Bigi, Franca, Carloni, Silvia, Mazzacani, Alessandro, & Sartori, Giovanni. (2001). Uncatalysed reactions in water: Part 2. Part 1: Ref. 1. Preparation of 3-carboxycoumarins. *Green chemistry, 3*(4), 173-174.
[12]Albini, Angelo, & Fagnoni, Maurizio. (2004). Green chemistry and photochemistry were born at the same time. *Green Chemistry, 6*(1), 1-6.
[13]Graf, C, Schärtl, W, & Hugenberg, N. (2000). Photoinduced cluster formation of coumarin-labeled organosilicon micronetworks. *Advanced Materials, 12*(18), 1353-1356.
[14]Mal, Nawal Kishor, Fujiwara, Masahiro, & Tanaka, Yuko. (2003). Photocontrolled reversible release of guest molecules from coumarin-modified mesoporous silica. *Nature, 421*(6921), 350-353.
[15]Hara, Kohjiro, Wang, Zhong-Sheng, Sato, Tadatake, Furube, Akihiro, Katoh, Ryuzi, Sugihara, Hideki, Dan-oh, Yasufumi, Kasada, Chiaki, Shinpo, Akira, & Suga, Sadaharu. (2005). Oligothiophene-containing coumarin dyes for efficient dye-sensitized solar cells. *The Journal of Physical Chemistry B, 109*(32), 15476-15482.
[16]Brun, Marie-Priscille, Bischoff, Laurent, & Garbay, Christiane. (2004). A very short route to enantiomerically pure coumarin-bearing fluorescent amino acids. *Angewandte Chemie International Edition, 43*(26), 3432-3436.
[17]Zhao, Lihua, Vaupel, Matthias, Loy, Douglas A, & Shea, Kenneth J. (2008). Photoresponsive hybrid materials: Synthesis and characterization of coumarin-dimer-bridged polysilsesquioxanes. *Chemistry of Materials, 20*(5), 1870-1876.
[18]Liedtke, Alicia, O'Neill, Mary, Wertmöller, Anke, Kitney, Stuart P, & Kelly, Stephen M. (2008). White-light oleds using liquid crystal polymer networks. *Chemistry of Materials, 20*(11), 3579-3586.
[19]Chen, Ming, Ghiggino, Kenneth P, Launikonis, Anton, Mau, Albert WH, Rizzardo, Ezio, Sasse, Wolfgang HF, Thang, San H, & Wilson, Gerard J. (2003). Raft synthesis of linear and star-shaped light harvesting polymers using di-and hexafunctional ruthenium polypyridine reagents. *Journal of Materials Chemistry, 13*(11), 2696-2700.
[20]Trajkovska, Anita, Kim, Chunki, Marshall, Kenneth L, Mourey, Thomas H, & Chen, Shaw H. (2006). Photoalignment of a nematic liquid crystal fluid and glassy-nematic oligofluorenes on coumarin-containing polymer films. *Macromolecules, 39*(20), 6983-6989.
[21]Shi, Junbin, Ouyang, Jun, Li, Qintao, Wang, Leyu, Wu, Jun, Zhong, Wen, & Xing,

Malcolm MQ. (2012). Cell-compatible hydrogels based on a multifunctional crosslinker with tunable stiffness for tissue engineering. *Journal of Materials Chemistry, 22*(45), 23952-23962.
[22]Ekenseair, Adam K, Boere, Kristel WM, Tzouanas, Stephanie N, Vo, Tiffany N, Kasper, F Kurtis, & Mikos, Antonios G. (2012). Synthesis and characterization of thermally and chemically gelling injectable hydrogels for tissue engineering. *Biomacromolecules, 13*(6), 1908-1915.
[23]Urban, Marek W. (2012). Dynamic materials: The chemistry of self-healing. *Nature chemistry, 4*(2), 80-82.
[24]Imato, Keiichi, Nishihara, Masamichi, Kanehara, Takeshi, Amamoto, Yoshifumi, Takahara, Atsushi, & Otsuka, Hideyuki. (2012). Self-healing of chemical gels cross-linked by diarylbibenzofuranone-based trigger-free dynamic covalent bonds at room temperature. *Angewandte Chemie International Edition, 51*(5), 1138-1142.
[25]Lu, DR, Xiao, CM, & Xu, SJ. (2009). Starch-based completely biodegradable polymer materials. *Express Polymer Letters, 3*(6), 366-375.
[26]Hwang, CJSA, Sinskey, Anthony J, & Lodish, Harvey F. (1992). Oxidized redox state of glutathione in the endoplasmic reticulum. *Science, 257*(5076), 1496-1502.
[27]Kong, XF, Wu, GY, Liao, YP, Hou, ZP, Liu, HJ, Yin, FG, Li, TJ, Huang, RL, Zhang, YM, & Deng, D. (2007). Effects of chinese herbal ultra-fine powder as a dietary additive on growth performance, serum metabolites and intestinal health in early-weaned piglets. *Livestock Science, 108*(1), 272-275.
[28]Raina, S, & Missiakas, D. (1997). Making and breaking disulfide bonds. *Annual Reviews in Microbiology, 51*(1), 179-202.
[29]Widder, Julian D, Fraccarollo, Daniela, Galuppo, Paolo, Hansen, Jason M, Jones, Dean P, Ertl, Georg, & Bauersachs, Johann. (2009). Attenuation of angiotensin ii–induced vascular dysfunction and hypertension by overexpression of thioredoxin 2. *Hypertension, 54*(2), 338-344.
[30]Saito, Go, Swanson, Joel A, & Lee, Kyung-Dall. (2003). Drug delivery strategy utilizing conjugation via reversible disulfide linkages: Role and site of cellular reducing activities. *Advanced drug delivery reviews, 55*(2), 199-215.